The author appreciates the generosity of

DR. SENNEWALD
medizintechnik gmbh

ERASMUS UNIVERSITEIT ROTTERDAM

Erasmus MC
Department of Surgery

Lipoid

greiner bio-one

Halberstadt
MR APPLICATION AND IMAGING

The research for this thesis was performed within the framework of the Erasmus Postgraduate School Molecular Medicine.

Molecular Medicine
Postgraduate School

Mild Hyperthermia and Thermosensitive Liposomes for Chemotherapy

Li Li

ISBN: 978-94-6182-235-2

Printed by Off Page, Amsterdam

Layout & Cover design by Li Li

Mild Hyperthermia and Thermosensitive Liposomes for Chemotherapy

Milde hyperthermie en thermosensitieve liposomen voor chemotherapie

THESIS
to obtain the degree of Doctor from Erasmus University Rotterdam
by command of the rector magnificus
Prof.dr. H.G. Schmidt
and according to the decision of the Doctorate Board

The public defense is held on Thursday, March 28, 2013
at 3.30 pm
by

Li Li
born in Fushun, Liaoning, P.R. China

Doctoral committee

Promotor	Prof.dr. A.M.M. Eggermont
Other members	Prof.dr. R.J. Griffin Prof.dr. G. Storm Prof.dr. G.C. van Rhoon
Co-promotor	Dr. G.A. Koning

In memory of my grandparents.

怀念姥爷，姥姥。

"If a man can... make a better mousetrap, the world will make a beaten path to his door."
Ralph Waldo Emerson

Forward

Mark Dewhirst, D.V.M., Ph.D.

This thesis contains 7 chapters that summarize an immense body of work centered on the demonstration of utility of a long circulating low temperature sensitive doxorubicin containing liposome (Dox-TSL). The work in total clearly demonstrates the utility of this approach and suggests that it may have superior qualities to thermally sensitive liposome that has a shorter circulation time [1]. Altogether, the ability to harness triggered drug release holds great promise for a number of clinical applications, where enhanced drug delivery may make the difference between treatment success and treatment failure. The advantage of being able to control the spatial distribution of drug delivery has important implications for increasing efficacy as well as decreasing normal tissue toxicity.

The enhanced permeability and retention (EPR) effect has provided rationale for nanoparticle delivery, since the first description of this phenomenon by Maeda [2-3]. However, the promise of the EPR effect to improve nanoparticle drug delivery has met with modest success in the clinic. The flagship liposomal drug, Doxil™, was approved for use on the basis of less cardiotoxicity compared with free drug, as opposed to improved anti-tumor effect [4].

In parallel with the development of Doxil™, there was the increasing appreciation for the fact that hyperthermia augmented liposomal drug delivery to tumors. This effect was first reported by Yatvin [5], and verified by a number of additional authors, as summarized in a comprehensive review by Kong and Dewhirst[6]. Although there appeared to be consistent, but variable improvement of liposomal drug delivery by hyperthermia, the underlying mechanism for this effect was not understood. Adding to the confusion in the field was the development of thermally sensitive liposomes. For these formulations, it was not possible to ascertain whether augmented drug delivery was a consequence of heat mediated-liposomal drug release or enhanced liposome extravasation, or both. It is clear that the answer to these questions is complex – likely influenced by liposome formulation and size, temperature of heating and tumor type.

Gaber et al. were the first to study liposome extravasation vs. content release, using the original thermosensitive liposome formulation of Yatvin (DPPC, HSPC, CHOL, PEGPE, at a molar ratio of 100:50:30:6) with the addition of polyethylene glycol (PEGPE) to extend the circulation time [7]. In this work,

they used the skin-fold window chamber model in Fischer 344 rats to evaluate these two features of drug delivery, using doxorubicin to monitor content release and a fluorescently labeled lipid to monitor delivery of liposomes. The R3230Ac mammary carcinoma was used as the tumor model. This formulation exhibits rather slow kinetics of drug release, hence accumulation of drug in this tumor model was a product of both enhanced drug delivery and drug release at both 42 and 45°C.

Kong et al. were the first to systematically evaluate the effects of hyperthermia on liposomal drug delivery and release, using the SKOV3 ovarian carcinoma model, grown in the skin fold window chamber. This tumor was chosen because it was impermeable to 100nm liposomes when studied in normothermic conditions (34°C). In contrast to the elegant work of Dr. Li in this thesis, these mice were housed in environmental chambers at an ambient temperature of 34°C, so the lack of vascular permeability at 34°C represents the control condition. Important features of this work included the following observations: 1) The rate of liposomal extravasation was linearly dependent upon temperature in the range between 40 and 42°C, 2) The enhancement in permeability persisted out to 6 hours post treatment and reestablishment of permeability was not attainable if reheating was used 8hr after an initial heating [8]. The results of this work suggested that rearrangements of the cytoskeleton were responsible for increased endothelial cell gap size with heating. The supposition that the cytoskeleton was involved relates to the fact that denaturation of protein is a major target of cell damage from hyperthermia [9]. Arrhenius analysis of the rate of heat inactivation for proteins vs. temperature shows that the rate doubles for every degree rise in temperature. In the work of Kong, the liposomal extravasation rate doubled for each degree of temperature rise consistent with the supposition that protein denaturation was responsible for the increase in pore size. Further evidence for this hypothesis came from the acquired resistance to reopening of pores with a second heat treatment. This latter observation suggested that the increase in pore size was likely due to opening of endothelial cell gaps, which are maintained by cellular cytoskeleton. The resistance to reopening was likely the result of thermotolerance, which would create resistance to cytoskeletal rearrangements [10], 3) 42°C heating increased vascular pore sizes to as large as 400nm, since thermal augmentation of liposomal extravasation occurred up to that size [11].

Although the work of Kong was thorough with respect to studying various parameters that might influence thermally mediated liposomal extravasation, there were several limitations to the work. First, all of the studies were done in one tumor line. Information on variability of these thermal effects will broaden our knowledge base about the general applicability of this approach. Second, the studies were performed with less than ideal optics and were done at relatively high power using epifluorescence. Because of

this, it was not possible to assess intratumoral heterogeneity, nor assess the magnitude enhanced extravasation at depth. Dr. Li's third chapter presents a comprehensive step forward in our understanding of how to exploit the use of hyperthermia to augment drug delivery to tumors. The utilization of transgenic mice that express green fluorescence protein in endothelial cells, combined with high resolution confocal microscopy to visualize drug delivery has revealed important information about the uniformity of the effects of heat on liposomal extravasation and the extent of variation between tumor types. Her results also reveal that the enhanced extravasation after heating may be prolonged in some tumors, beyond the 6 hour window originally reported by Kong [8]. In fact, it is likely that such effects occur in spontaneous tumors as well. Matteuci examined radiolabelled liposome accumulation in companion cats with vaccine associated fibrosarcomas [12]. Here, enhanced extravasation was observed for up to 16 hours after application of local hyperthermia in several individuals.

The variability in the enhancement of liposome extravasation between and within tumors raises the rationale for using imaging to monitor drug delivery. With respect to delivery of liposomes, one of the most promising methods is to use technicium-99-m radiolabelled liposomes. The method to radiolabel liposomes with this tracer is quite straightforward and subsequent imaging can be accomplished with SPECT imaging, to yield volume distributions. Kleiter et al, reported that co-administration of radiolabelled liposomes along with Doxil can accurately reflect the doxorubicin concentration in tissues at 18 hour after administration of hyperthermia [13].

In her fourth chapter, Dr. Li presents provocative data related to a sterically stabilized thermosensitive liposome. In this chapter, she compares the in vitro drug release characteristics of the sterically stabilized thermosensitive liposome (Dox-TSL) to the Dox-LTSL of Needham. She also examined the delivery of doxorubicin to tumors, using high resolution intravital microscopy. As has been reported by Manzoor using Dox-LTSL, hyperthermia causes intravascular drug release and increased drug penetration into tumor, with specific accumulation in tumor and endothelial cell nuclei [14]. Growth delay data, comparing the Dox-TSL to Dox-LTSL revealed improved anti-tumor effect for both compared with controls. Dox-TSL revealed a trend toward being more effective than Dox-LTSL; a statistical comparison was not reported, however.

In the fifth chapter, Dr. Li explores the relative efficacy of a two-step drug delivery approach that combines the thermally enhanced EPR effect with heat mediated drug release. Two different Dox-TSL formulations were compared: fast release (Dox-fTSL, rapid drug release within 5 min) and slow release (Dox-sTSL) release over an hour of heating. To do the two step approach, the tumor is heated twice; the first time this is done to increase

EPR and liposomes are not administered until after first heat is concluded. The second heat is delivered several hours later, to rapidly release the drug from extravasated liposomes. The long circulation time of the Dox-TSL makes this approach feasible. Although the two step approach seems attractive in theory, the anti-tumor effect of Dox-TSL administered during hyperthermia yielded better antitumor effect. It would be interesting nonetheless to consider giving a second heat a day or two later, even with the Dox-fTSL, because one presumes that liposomes with unreleased drug would continue to accumulate in the tumor even after heat is concluded. By waiting a day or two after hyperthermia treatment is concluded, any effects of thermotolerance, which will decrease efficacy of doxorubicin [15], would have decayed. Dr. Li looked at this possibility, but only at 4 hour after heating. Peak thermotolerance levels occur during heating at 41°C for 60 min, decay by 50% by 4 hour, and return to baseline levels within 24h in theHA-1 cell line [16]. Thus, there is merit in considering a second heat treatment a day later, if the temperatures within the tumor can be maintained around 41°C. Dr. Li recommends the two step approach to "limit normal tissue toxicity" from rapid drug release in normal tissues during heating. Theoretically, this might be an issue, but in phase I trials in dogs [17] and humans [18] in which the Dox-LTSL formulation has been tested, there has not been evidence for normal tissue toxicity that could be attributable to doxorubicin.

By comparison, a two step approach cannot be used with Dox-LTSL. As is pointed out by Dr. Li, the original thermosensitive formulation developed by Needham exhibits some drug release at normothermia; it has a circulation half-life of about 60 min in humans [19, 18]. Thus, this liposome is not amenable to taking advantage of the heat-enhanced EPR effect. In fact, the short half-life of this drug can challenge its clinical application. To take maximal advantage of Dox-LTSL, it is ideal to initiate heating first and then give drug when the tumor has already reached thermal steady state. This requirement is challenging in the clinic, where the chemotherapy suite may often be physically located separately from the hyperthermia facilities. Additionally, the short circulation time restricts the application to heating of one region. If one desired to treat more than one lesion in the same patient, it would be quite challenging, because by the time the first heat is completed, circulating drug levels will have diminished to subtherapeutic levels. The advantages of the Dox-TSL are obvious, when compared with Dox-LTSL, even without considering the two step approach.

The sixth chapter deals with the concept of pulsed heating, which might be encountered if one elected to use this Dox-TSL in combination with high intensity focused ultrasound. Here, Dr. Li shows that pulsed heating (5cycles of 5 min at 42C with 10 min at normothermia) yields drug levels nearly equivalent to continuous low temperature heating and similar anti-tumor effects in a human melanoma xenograft. This observation will be of interest to

the growing number of investigators interested in combining thermosensitive liposomes with HIFU [20-24].

In summary, this body of work sets the stage for the next steps in development of Dox-TSL. I look forward to seeing it develop into a legitimate therapeutic approach for a variety of human cancers.

Citations

[1] D. Needham, G. Anyarambhatla, G. Kong, M.W. Dewhirst, A new temperature-sensitive liposome for use with mild hyperthermia: characterization and testing in a human tumor xenograft model, Cancer Res, 60 (2000) 1197-1201.
[2] H. Maeda, J. Wu, T. Sawa, Y. Matsumura, K. Hori, Tumor vascular permeability and the EPR effect in macromolecular therapeutics: a review, Journal of Controlled Release, 65 (2000) 271-284.
[3] H. Maeda, The enhanced permeability and retention (EPR) effect in tumor vasculature: The key role of tumor-selective macromolecular drug targeting, in: G. Weber (Ed.) Advances in Enzyme Regulation, Vol 41, 2001, pp. 189-207.
[4] T. Tejada-Berges, C.O. Granai, M. Gordinier, W. Gajewski, Caelyx/Doxil for the treatment of metastatic ovarian and breast cancer, Expert review of anticancer therapy, 2 (2002) 143-150.
[5] M.B. Yatvin, H. Muhlensiepen, W. Porschen, J.N. Weinstein, L.E. Feinendegen, , Cancer Research, 41 (1981) 1602-1607.
[6] G. Kong, M.W. Dewhirst, Hyperthermia and liposomes, International Journal of Hyperthermia, 15 (1999) 345-370.
[7] M.H. Gaber, N.Z. Wu, K. Hong, S.K. Huang, M.W. Dewhirst, D. Papahadjopoulos, Thermosensitive liposomes: extravasation and release of contents in tumor microvascular networks, International journal of radiation oncology, biology, physics, 36 (1996) 1177-1187.
[8] G. Kong, R.D. Braun, M.W. Dewhirst, Characterization of the effect of hyperthermia on nanoparticle extravasation from tumor vasculature, Cancer Research, 61 (2001) 3027-3032.
[9] J.R. Lepock, H.E. Frey, K.P. Ritchie, protein denaturation in intact hepatocytes and isolated cellular organelles during heat-shock, Journal of Cell Biology, 122 (1993) 1267-1276.
[10] F.A.C. Wiegant, P.M.P.V.E. Henegouwen, G. Vandongen, W.A.M. Linnemans, Stress-Induced Thermotolerance of the Cytoskeleton of Mouse Neuroblastoma N2a Cells and Rat Reuber H35 Hepatoma-Cells, Cancer Research, 47 (1987) 1674-1680.
[11] G. Kong, R.D. Braun, M.W. Dewhirst, Hyperthermia enables tumor-specific nanoparticle delivery: Effect of particle size, Cancer Research, 60 (2000) 4440-4445.
[12] M.L. Matteucci, G. Anyarambhatla, G. Rosner, C. Azuma, P.E. Fisher, M.W. Dewhirst, D. Needham, D.E. Thrall, Hyperthermia increases accumulation

of technetium-99m-labeled liposomes in feline sarcomas, Clin Cancer Res, 6 (2000) 3748-3755.
[13] M.M. Kleiter, D.H. Yu, L.A. Mohammadian, N. Niehaus, I. Spasojevic, L. Sanders, B.L. Viglianti, P.S. Yarmolenko, M. Hauck, N.A. Petry, T.Z. Wong, M.W. Dewhirst, D.E. Thrall, A tracer dose of technetium-99m-labeled liposomes can estimate the effect of hyperthermia on intratumoral Doxil extravasation, Clin Cancer Res, 12 (2006) 6800-6807.
[14] A.A. Manzoor, L.H. Lindner, C.D. Landon, J.Y. Park, A.J. Simnick, M.R. Dreher, S. Das, G. Hanna, W. Park, A. Chilkoti, G.A. Koning, T.L.M. ten Hagen, D. Needham, M.W. Dewhirst, Overcoming Limitations in Nanoparticle Drug Delivery: Triggered, Intravascular Release to Improve Drug Penetration into Tumors, Cancer Research, 72 (2012) 5566-5575.
[15] E.H. Richards, T.A. Begum, J.R.W. Masters, Thermotolerance and sensitivity of human cancer cells to cisplatin and doxorubicin, Int J Oncol, 8 (1996) 1265-1271.
[16] G.C. Li, G.M. Hahn, A proposed operational model of thermotolerance based on effects of nutrients and the initial treatment temperature, Cancer Res, 40 (1980) 4501-4508.
[17] M.L. Hauck, S.M. LaRue, W.P. Petros, J.M. Poulson, D. Yu, I. Spasojevic, A.F. Pruitt, A. Klein, B. Case, D.E. Thrall, D. Needham, M.W. Dewhirst, Phase I trial of doxorubicin-containing low temperature sensitive liposomes in spontaneous canine tumors, Clin Cancer Res, 12 (2006) 4004-4010.
[18] R.T. Poon, N. Borys, Lyso-thermosensitive liposomal doxorubicin: an adjuvant to increase the cure rate of radiofrequency ablation in liver cancer, Future oncology, 7 (2011) 937-945.
[19] R.T. Poon, N. Borys, Lyso-thermosensitive liposomal doxorubicin: a novel approach to enhance efficacy of thermal ablation of liver cancer, Expert opinion on pharmacotherapy, 10 (2009) 333-343.
[20] M. de Smet, E. Heijman, S. Langereis, N.M. Hijnen, H. Grull, Magnetic resonance imaging of high intensity focused ultrasound mediated drug delivery from temperature-sensitive liposomes: an in vivo proof-of-concept study, Journal of controlled release : official journal of the Controlled Release Society, 150 (2011) 102-110.
[21] R. Staruch, R. Chopra, K. Hynynen, Localised drug release using MRI-controlled focused ultrasound hyperthermia, International journal of hyperthermia : the official journal of European Society for Hyperthermic Oncology, North American Hyperthermia Group, 27 (2011) 156-171.
[22] H. Grull, S. Langereis, Hyperthermia-triggered drug delivery from temperature-sensitive liposomes using MRI-guided high intensity focused ultrasound, Journal of controlled release : official journal of the Controlled Release Society, 161 (2012) 317-327.
[23] A. Partanen, P.S. Yarmolenko, A. Viitala, S. Appanaboyina, D. Haemmerich, A. Ranjan, G. Jacobs, D. Woods, J. Enholm, B.J. Wood, M.R. Dreher, Mild hyperthermia with magnetic resonance-guided high-intensity focused ultrasound for applications in drug delivery, International journal

of hyperthermia : the official journal of European Society for Hyperthermic Oncology, North American Hyperthermia Group, 28 (2012) 320-336.
[24] C. Lorenzato, A. Cernicanu, M.E. Meyre, M. Germain, A. Pottier, L. Levy, B.D. de Senneville, C. Bos, C. Moonen, P. Smirnov, MRI contrast variation of thermosensitive magnetoliposomes triggered by focused ultrasound: a tool for image-guided local drug delivery, Contrast media & molecular imaging, 8 (2013) 185-192.

List of abbreviations

BG	background
CD31	platelet endothelial cell adhesion molecule
CEM43	cumulative equivalent minutes at 43°C
CF	carboxyfluorescein
TEM	transmission electron microscopy
DMEM	Dulbecco's modified eagle medium
Dox	doxorubicin
DPPC	1,2-dipalmitoyl-*sn*-glycero-3-phosphocholine
DSPC	1,2-distearoyl-*sn*-glycero-3-phosphocholine
DSPE-PEG_{2000}	1,2-distearoyl-*sn*-glycero-3-phosphoethanolamine-*N*-PEG_{2000}
Em.	emission
EPR	enhanced permeability and retention
Ex.	excitation
FCS	fetal calf serum
Fig.	figure
GFP	green fluorescence protein
HC	heat cycling
H&E	hematoxylin and eosin
HIFU	high intensity focused ultrasound
HPLC	high performance liquid chromatography
HT	hyperthermia
IC_{50}	the half maximal inhibitory concentration
IR	infrared
i.v.	intravenous
LLC	Lewis lung carcinoma
LTSL	lysolipid-based thermosensitive liposomes
MRI	magnetic resonance imaging
MSPC	monostearoylphosphatidylcholine
NEF	normalized extravascular fluorescence
NT	normothermia
PBS	phosphate buffered saline
PDI	polydispersity index
PLD	pegylated liposomal doxorubicin
Rho-PE	sulforhodamine B-dioleoyl-phosphatidylethanolamine
RPMI	Roswell Park Memorial Institute
s.c.	subcutaneous
SD	standard deviation
SEM	standard error of the mean
TBR	tumor-to-background ratio
T_m	melting temperature
TNF-α	tumor necrosis factor-alpha
TSL	thermosensitive liposomes

Table of Contents

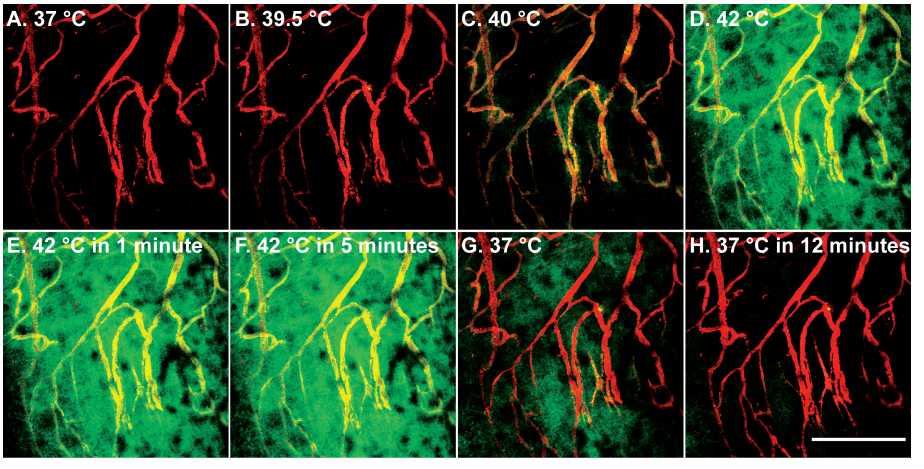

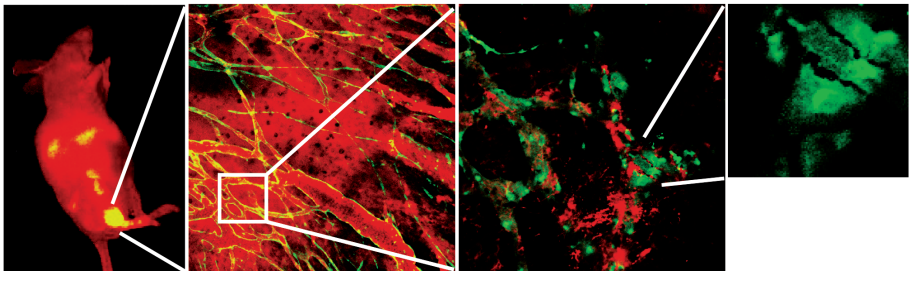

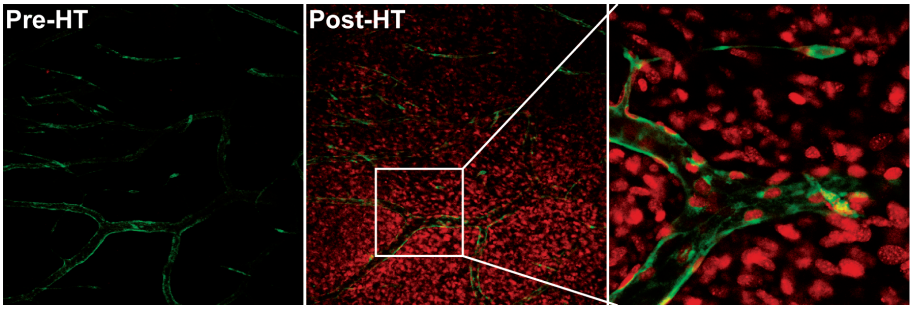

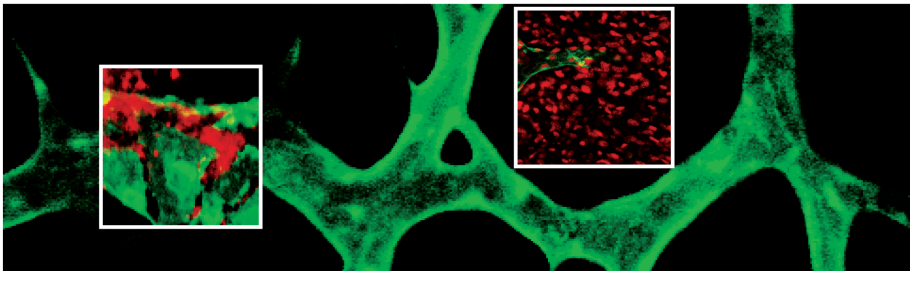

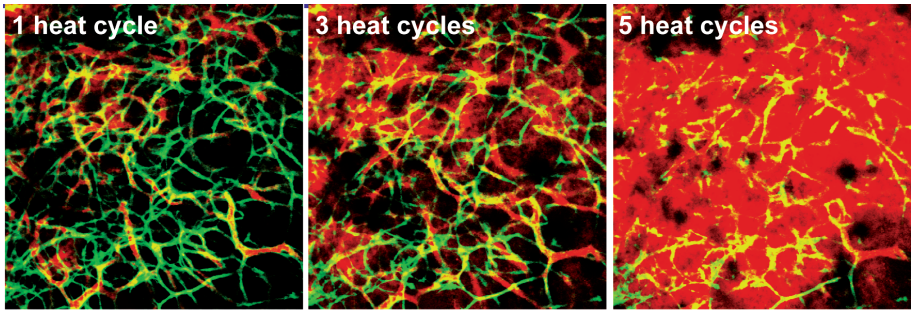

Chapter 1

1

Introduction

1

Chemotherapy in cancer

Conventional chemotherapy relies on cytotoxic compounds to suppress cancer development. These compounds non-selectively attack proliferating cells in tumors, but also at other sites in the body, leading to toxicity in healthy organs and tissues. The systemic toxicity is related to the aspecificity of the cytotoxic compounds, their large volume of distribution, short circulation half-lives that all require high dosing to obtain therapeutic levels at tumors. For example, doxorubicin (Dox) is an anthracycline antibiotic, which is widely used in cancer treatments [1]. Although Dox can effectively kill cancer cells by intercalating with DNA to inhibit cell proliferation, it is limited in clinical use because of its severe cardiotoxicity and myelosuppression, which are the dose limiting toxicities. Dox cardiotoxicity may manifest acute in the form of tachycardia or arrythmias and as delayed cardiomyopathy including congestive heart failure, during or after the course of treatment. In addition, Dox may cause nausea and vomiting and can affect other tissues such as bone marrow, causing e.g. myelosuppression and may due to its carcinogenic nature also induce secondary hematological cancers.

Liposomal chemotherapy

Liposomes are potent biocompatible nanocarriers, widely used to deliver cytotoxic compounds, genetic materials, and contrast agents for therapies and imaging. A draw-back of the initially proposed liposomal carriers was the relatively fast clearance. In order to prevent liposomes from being recognized and taken up by the reticuloendothelial system (RES), 1,2-distearoyl-*sn*-glycero-3-phosphoethanolamine-*N*-polyethylene glycol$_{2000}$ (DSPE-PEG$_{2000}$) is commonly grafted on the lipid membrane to prolong liposome retention in circulation [2]. A well known and most widely used chemotherapeutic liposomal Dox formulation is Caelyx® (in Europe) also known as Doxil® (in USA), which is a pegylated liposomal Dox (PLD). The formulation reduces the systemic side-effects of Dox by encapsulating the drug into long circulating liposomes, which strongly prolongs the circulation half-life of Dox [3-5]. Moreover, PLD can also extravasate through leaky tumor vasculature to locally accumulate in tumors [6]. However, PLD causes a new dose limiting side-effect, i.e. hand-foot syndrome related to the passive targeting of the nanocarriers to the skin especially at hands and feet, where Dox is slowly released causing toxicity. PLD improves treatment outcome in Kaposi sarcoma, and head and neck tumors [7-8]. However, PLD shows limited efficacy in sarcoma and breast cancer [3, 5]. The essential drawback of PLD is the slow Dox release and lack of tumor specific targeting, which impedes its therapeutic efficacy [9-11]. Studies on improving liposomal chemotherapy involve manipulation of tumor microenvironment and design of novel nanovesicles with improved drug delivery potential.

Liposomal drug delivery mechanism involves extravasation through permeable tumor vasculature and deposition of liposomal drugs into the interstitial space in tumors [12-14]. Upon liposome extravasation through the permeable tumor vasculature, liposomes may penetrate further in the interstitial space. However, due to liposome size and the compact nature of the interstitial matrix in tumors, liposome penetration depth in the extravascular extracellular space (EES) is limited [15-16]. It is noteworthy to emphasize that the heterogeneity of tumor vascular density, functionality and permeability are not the only limitations, but more importantly the majority of tumor vasculature is not permeable to liposomes under physiological conditions [17-18, 9, 11]. Manipulation of tumor vasculature provides essential paths to improve anticancer drug delivery [19-22]. For example, approaches on normalizing tumor vasculature through targeting vascular endothelial growth factor (VEGF) or its receptors improve delivery of chemotherapeutic drugs administered in free form [23-25]. Alternatively, abnormalization of tumor vasculature by increasing vascular permeability upon administration of compounds such as TNF-α and histamine can also enhance the effect of chemotherapeutic compounds [26-29, 21]. Normalization of tumor vasculature did not improve drug delivery with nanoparticle entrapped drug [30], whereas abnormalization using TNF-α strongly improved liposomal drug delivery [31, 11].

Local mild hyperthermia

Mild HT may function as a physical alternative to the use of biological modifiers to increase tumor vasculature permeability. Regarding improved delivery of liposomal drugs, mild HT can increase permeability of tumor vasculature, thus increase intratumoral liposomal drug accumulation [32-35]. Moreover, mild HT increases tissue perfusion and extravascular fluid flow in the heated volume, therefore may facilitate liposomal drug penetration in solid tumors [36-37]. Additionally, vasculature endurance towards HT is suggested to be lower in tumor tissue compared to normal tissues, rendering increased specificity of liposomal drug delivery to tumors [38]. HT increases perfusion and tissue oxygenation, elevates interstitial microconvection and fluid flow, inhibits DNA repair, as well as sensitizes cancer cells towards chemotherapeutic compounds [36, 39-41]. Therefore, local mild HT at solid tumors can contribute to improved liposomal chemotherapy via several mechanisms.

Mild HT of 39-43°C is clinically applied as an adjuvant to chemotherapy and radiotherapy to improve the therapeutic outcome and used to treat various tumors, e.g. melanoma, sarcoma, breast cancer, cervix cancer, and head and neck cancer [42-43]. Van der Zee et al. reported that HT improved the clinical outcome of standard radiotherapy for locally advanced bladder, cervix and rectum tumors [42]. The first randomized phase III clinical trial on combination of chemotherapy and HT proved that regional HT increased the

benefit of chemotherapy in high grade soft-tissue sarcoma [43]. Clinical mild HT is routinely scheduled for 1 hour after reaching a steady hyperthermic temperature to maximize the synergistic effect [42, 44]. During clinical application, catheter installed thermometers or more recently magnetic resonance imaging (MRI) thermometry, are employed to monitor tissue temperature in time. Although reaching mild hyperthermic temperatures in a tumor depends on tumor size, location, perfusion, treatment planning and imaging, the available equipment nowadays allows for increasingly precise heating of a defined tissue volume up to 43°C using external microwave or high intensity focused ultrasound (HIFU) [45-47].

Thermosensitive liposomes

Design of liposomes has been focused on improving functionality or increasing targeting. To do so, novel lipids have been introduced to optimize liposome characteristics [48]. Targeting of liposomes is improved for instance by attaching e.g. cationic charges or antibodies on the liposome membrane to recognize tumor-specific sites [49-52]. Another alternative approach to improve liposomal chemotherapy delivery emphasizes on triggered drug release from liposomes accumulated in tumors. In this thesis, thermosensitive liposomes (TSL) and local mild hyperthermia (HT) are employed as means to further advance liposomal chemotherapy. TSL are nanovesicles composed of a temperature sensitive phospholipid-based membrane, which features a gel-to-liquid crystalline phase transition at its membrane melting temperature (T_m) tailored around temperatures achievable by mild (HT) [53]. In the core of TSL, hydrophilic compounds can be entrapped; while in the membrane of TSL, hydrophobic molecules can be embedded. At T_m, trans to gauche conformational changes increase the mobility of phospholipids, rendering the fluidized TSL membrane more permeable towards water and solutes [54]. Therefore, hydrophilic compounds can be released from the TSL. When a single-chain phospholipid, lysolecithin, is incorporated in the TSL membrane, rapid release of contents is further enhanced through formation and evolution of porous defects when the temperature is approaching T_m [55-57]. Tagami, et al. introduced Brij surfactants to replace lysolecithin and DSPE-PEG_{2000}, and maintained stability and release kinetics at similar levels to lysolecithin-based TSL [58]. Alternatively, Lindner et al. reported inclusion of a novel phospholipid, 1,2-dipalmitoyl-*sn*-glycoero-3-phosphoglyceroglycerol, which in replacement of DSPE-PEG_{2000} was able to ensure long circulation of TSL as well as contribute to enhanced drug release around the T_m of the TSL membrane [59]. Optimization of TSL formulation, in terms of drug encapsulation efficiency, stability at physiological temperature and release kinetics at mild HT will undoubtedly further enhance the unique features of TSL for an advanced TSL-mediated drug delivery to disease sites.

Aim of the thesis

The aim of the work described in this thesis is to improve intratumoral liposomal drug accumulation, by applying local mild HT at tumors to induce hyperpermeable tumor vasculature for liposomal drug extravasation and increased fluid flow to further facilitate liposomal drug penetration in the EES. After the maximal accumulation of liposomal drugs in tumors, drugs are actively released from liposomes to disclose their bioavailability. In order to achieve an active triggered drug release from the liposomes, TSL with T_m at mild HT are used as drug carriers. The use of mild HT focuses on two targets, tumor vasculature and the membrane of TSL. The correlations between mild HT and TSL stability and release kinetics, and between mild HT and tumor vasculature permeability are matters of the study. TSL formulation for rapid Dox release is preferred for intravascular release upon mild HT, while TSL formulation for slow Dox release is desirable for extravascular release upon two-step mild HT (see Diagram for two-step planning, interstitial drug release (a) vs. intravascular drug release (b)) [60-62].

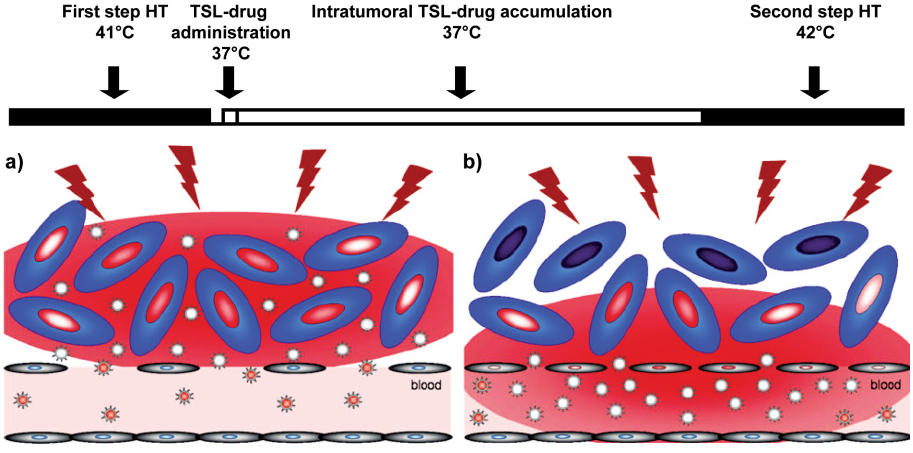

Diagram

Diagram. Schedule of mild HT in a two-step manner. Illustration of interstitial drug release (a) vs. intravascular drug release (b).

Topics of the thesis

To begin such a project, a TSL formulation that is stable at physiological temperature in circulation is required. **Chapter 2** describes a TSL formulation composed of classic temperature sensitive phospholipids, omitting the lyso-lecithin for ultrafast release, but with an optimized DSPE-PEG_{2000} concentration for stability at physiological temperature and fast release at mild HT. These optimized TSL ensure a prolonged content retention at physiological temperature when exposed to serum proteins, and also feature *in vitro* and

in vivo rapid content release at mild HT. **Chapter 3** investigates the effect of mild HT on tumor vasculature permeability for liposome extravasation and intratumoral penetration. Multiple thermal doses are compared for levels of liposome density in the EES, penetration depth in murine and xenograft tumor models, covering four major models in cancer research. The heterogeneity of tumor vasculature permeability is compared and quantified among tumor models and locations of individual tumors, and demonstrated by computer modeling. Liposome extravasation and penetration processes are illustrated through intravital confocal microscopy, and intratumoral liposome accumulation is visualized by whole body optical imaging. **Chapter 4** focuses on *in vitro* and *in vivo* profiling of Dox encapsulated in optimized TSL. Dox-TSL *in vitro* stability and release kinetics in serum, and *in vivo* tumor growth control and survival after a single treatment of intravascular Dox release are compared to Dox encapsulated in lyso-lipid based TSL (Dox-LTSL), which is currently in clinical trials [63]. **Chapter 5** proposes a novel two-step mild HT approach. The first-step local mild HT is for inducing permeable tumor vasculature, after which liposomal drugs are systemically administered at physiological temperature. Liposomal drugs are allowed to circulate for two hours, to gradually accumulate in the EES in tumors through permeable tumor vasculature. Then, the second-step local mild HT is applied to trigger extravascular Dox release from extravasated Dox-TSL. In this thesis, tumor growth control and survival after the two-step mild HT approach is compared to intravascular release approach. **Chapter 6** studies the effect of heat cycling on tumor vasculature permeability and content release kinetics of TSL. Heat cycling mimics the clinical application of HIFU-based heating of large tumors. While HIFU is scanning through tumors, every fraction of a tumor is experiencing tissue heating and cooling alternately, resulting in a rather heterogeneous heat delivery. Through each heat cycle, contents are released from TSL and tumor vasculature accumulates heat stress. Heat cycling is studied for tumor vasculature permeability induced by heat stress, and for content release from TSL triggered by mild HT. The therapeutic efficacy of heat cycling is investigated and compared to continuous mild HT. **Chapter 7** discusses the results of the studies and reviews the current status of mild HT mediated drug delivery using TSL.

References:

[1] D.J. Slamon, B. Leyland-Jones, S. Shak, H. Fuchs, V. Paton, A. Bajamonde, T. Fleming, W. Eiermann, J. Wolter, M. Pegram, J. Baselga, L. Norton, Use of chemotherapy plus a monoclonal antibody against HER2 for metastatic breast cancer that overexpresses HER2, N. Engl. J. Med., 344 (2001) 783-792.
[2] T.M. Allen, C. Hansen, F. Martin, C. Redemann, A. Yauyoung, Liposomes Containing Synthetic Lipid Derivatives of Poly(Ethylene Glycol) Show Prolonged Circulation Half-Lives Invivo, Biochimica Et Biophysica Acta, 1066 (1991) 29-36.
[3] I. Judson, J.A. Radford, M. Harris, J.Y. Blay, Q. van Hoesel, A. le Cesne, A.T. van Oosterom, M.J. Clemons, C. Kamby, C. Hermans, J. Whittaker, E.D. di Paola, J. Verweij, S. Nielsen, Randomised phase II trial of pegylated liposomal doxorubicin (DOXIL (R)/CAELYX (R)) versus doxorubicin in the treatment of advanced or metastatic soft tissue sarcoma: a study by the EORTC Soft Tissue and Bone Sarcoma Group, European Journal of Cancer, 37 (2001) 870-877.
[4] A. Gabizon, H. Shmeeda, Y. Barenholz, Pharmacokinetics of pegylated liposomal doxorubicin - Review of animal and human studies, Clin Pharmacokinet, 42 (2003) 419-436.
[5] M.E.R. O'Brien, N. Wigler, M. Inbar, R. Rosso, E. Grischke, A. Santoro, R. Catane, D.G. Kieback, P. Tomczak, S.P. Ackland, F. Orlandi, L. Mellars, L. Alland, C. Tendler, C.B.C.S. Grp, Reduced cardiotoxicity and comparable efficacy in a phase III trial of pegylated liposomal doxorubicin HCl (CAELYX (TM)/Doxil (R)) versus conventional doxorubicin for first-line treatment of metastatic breast cancer, Annals of Oncology, 15 (2004) 440-449.
[6] F. Yuan, M. Leunig, S.K. Huang, D.A. Berk, D. Papahadjopoulos, R.K. Jain, Microvascular permeability and interstitial penetration of sterically stabilized (stealth) liposomes in a human tumor xenograft., Cancer Research, 54 (1994) 3352-3356.
[7] D.W. Northfelt, B.J. Dezube, J.A. Thommes, B.J. Miller, M.A. Fischl, A. Friedman-Kien, L.D. Kaplan, C. Du Mond, R.D. Mamelok, D.H. Henry, Pegylated-liposomal doxorubicin versus doxorubicin, bleomycin, and vincristine in the treatment of AIDS-related Kaposi's sarcoma: Results of a randomized phase III clinical trial, Journal of Clinical Oncology, 16 (1998) 2445-2451.
[8] K.J. Harrington, C. Lewanski, A.D. Northcote, J. Whittaker, A.M. Peters, R.G. Vile, J.S. Stewart, Phase II study of pegylated liposomal doxorubicin (Caelyx) as induction chemotherapy for patients with squamous cell cancer of the head and neck, Eur J Cancer, 37 (2001) 2015-2022.
[9] K.J. Harrington, S. Mohammadtaghi, P.S. Uster, D. Glass, A.M. Peters, R.G. Vile, J.S. Stewart, Effective targeting of solid tumors in patients with locally advanced cancers by radiolabeled pegylated liposomes, Clin Cancer Res, 7 (2001) 243-254.
[10] K.M. Laginha, S. Verwoert, G.J. Charrois, T.M. Allen, Determination of doxorubicin levels in whole tumor and tumor nuclei in murine breast cancer

tumors, Clin Cancer Res, 11 (2005) 6944-6949.
[11] A.L.B. Seynhaeve, S. Hoving, D. Schipper, C.E. Vermeulen, G.A. de Wiel-Ambagtsheer, S.T. van Tiel, A.M.M. Eggermont, T.L.M. ten Hagen, Tumor necrosis factor alpha mediates homogeneous distribution of liposomes in murine melanoma that contributes to a better tumor response, Cancer Research, 67 (2007) 9455-9462.
[12] M.H. Gaber, N.Z. Wu, K. Hong, S.K. Huang, M.W. Dewhirst, D. Papahadjopoulos, Thermosensitive liposomes: extravasation and release of contents in tumor microvascular networks, Int J Radiat Oncol Biol Phys, 36 (1996) 1177-1187.
[13] H. Maeda, J. Wu, T. Sawa, Y. Matsumura, K. Hori, Tumor vascular permeability and the EPR effect in macromolecular therapeutics: a review, Journal of Controlled Release, 65 (2000) 271-284.
[14] R.K. Jain, T. Stylianopoulos, Delivering nanomedicine to solid tumors, Nature Reviews Clinical Oncology, 7 (2010) 653-664.
[15] P. Vaupel, F. Kallinowski, P. Okunieff, Blood Flow, Oxygen and Nutrient Supply, and Metabolic Microenvironment of Human Tumors: A Review, Cancer Research, 49 (1989) 6449-6465.
[16] F. Yuan, M. Leunig, S.K. Huang, D.A. Berk, D. Papahadjopoulos, R.K. Jain, Microvascular permeability and interstitial penetration of sterically stabilized (stealth) liposomes in a human tumor xenograft., Cancer Research, 54 (1994) 3352-3356.
[17] H.F. Dvorak, J.A. Nagy, J.T. Dvorak, A.M. Dvorak, Identification and characterization of the blood vessels of solid tumors that are leaky to circulating macromolecules., American Journal of Pathology, 133 (1988) 95-109.
[18] H.F. Dvorak, L.F. Brown, M. Detmar, A.M. Dvorak, Vascular permeability factor/vascular endothelial growth factor, microvascular hyperpermeability, and angiogenesis., American Journal of Pathology, 146 (1995) 1029-1039.
[19] J.M. Brown, A.J. Giaccia, The unique physiology of solid tumors: Opportunities (and problems) for cancer therapy, Cancer Research, 58 (1998) 1408-1416.
[20] P. Carmeliet, R.K. Jain, Angiogenesis in cancer and other diseases, Nature, 407 (2000) 249-257.
[21] T.L.M. ten Hagen, A.L.B. Seynhaeve, A.M.M. Eggermont, Tumor necrosis factor-mediated interactions between inflammatory response and tumor vascular bed, Immunological Reviews, 222 (2008) 299-315.
[22] J. Fang, H. Nakamura, H. Maeda, The EPR effect: Unique features of tumor blood vessels for drug delivery, factors involved, and limitations and augmentation of the effect, Adv Drug Deliv Rev, 63 (2011) 136-151.
[23] R.T. Tong, Y. Boucher, S.V. Kozin, F. Winkler, D.J. Hicklin, R.K. Jain, Vascular normalization by vascular endothelial growth factor receptor 2 blockade induces a pressure gradient across the vasculature and improves drug penetration in tumors, Cancer Research, 64 (2004) 3731-3736.
[24] R.K. Jain, Normalization of tumor vasculature: An emerging concept in antiangiogenic therapy, Science, 307 (2005) 58-62.

[25] R.K. Jain, D.G. Duda, J.W. Clark, J.S. Loeffler, Lessons from phase III clinical trials on anti-VEGF therapy for cancer, Nature Clinical Practice Oncology, 3 (2006) 24-40.
[26] F. Brunstein, S. Hoving, A.L.B. Seynhaeve, S.T. van Tiel, G. Guetens, E.A. de Bruijn, A.M.M. Eggermont, T.L.M. ten Hagen, Synergistic antitumor activity of histamine plus melphalan in isolated limb perfusion: Preclinical studies, Journal of the National Cancer Institute, 96 (2004) 1603-1610.
[27] F. Brunstein, J. Rens, S.T. van Tiel, A.M.M. Eggermont, T.L.M. ten Hagen, Histamine, a vasoactive agent with vascular disrupting potential, improves tumour response by enhancing local drug delivery, British Journal of Cancer, 95 (2006) 1663-1669.
[28] D.J. Grunhagen, J.H.W. de Wilt, T.L.M. ten Hagen, A.M.M. Eggermont, Technology Insight: utility of TNF-alpha-based isolated limb perfusion to avoid amputation of irresectable tumors of the extremities, Nature Clinical Practice Oncology, 3 (2006) 94-103.
[29] T.L.M. ten Hagen, A.M.M. Eggermont, Changing the pathophysiology of solid tumours: The potential of TNF and other vasoactive agents, International Journal of Hyperthermia, 22 (2006) 241-246.
[30] T.D. Tailor, G. Hanna, P.S. Yarmolenko, M.R. Dreher, A.S. Betof, A.B. Nixon, I. Spasojevic, M.W. Dewhirst, Effect of Pazopanib on Tumor Microenvironment and Liposome Delivery, Molecular Cancer Therapeutics, 9 (2010) 1798-1808.
[31] T.L.M. Ten Hagen, A.H. Van Der Veen, P. Nooijen, S.T. Van Tiel, A.L.B. Seynhaeve, A.M.M. Eggermont, Low-dose tumor necrosis factor-alpha augments antitumor activity of stealth liposomal doxorubicin (Doxil (R)) in soft tissue sarcoma-bearing rats, International Journal of Cancer, 87 (2000) 829-837.
[32] S.K. Huang, P.R. Stauffer, K.L. Hong, J.W.H. Guo, T.L. Phillips, A. Huang, D. Papahadjopoulos, Liposomes and hyperthermia in mice: increased tumor uptake and therapeutic efficacy of doxorubicin in sterically stabilized liposomes., Cancer Research, 54 (1994) 2186-2191.
[33] G. Kong, M.W. Dewhirst, Hyperthermia and liposomes, Int J Hyperthermia, 15 (1999) 345-370.
[34] G. Kong, R.D. Braun, M.W. Dewhirst, Hyperthermia enables tumor-specific nanoparticle delivery: effect of particle size, Cancer Res, 60 (2000) 4440-4445.
[35] G. Kong, R.D. Braun, M.W. Dewhirst, Characterization of the effect of hyperthermia on nanoparticle extravasation from tumor vasculature, Cancer Res, 61 (2001) 3027-3032.
[36] C.W. Song, Effect of local hyperthermia on blood flow and microenvironment: a review, Cancer Res, 44 (1984) 4721s-4730s.
[37] C.W. Song, H.J. Park, C.K. Lee, R. Griffin, Implications of increased tumor blood flow and oxygenation caused by mild temperature hyperthermia in tumor treatment, International Journal of Hyperthermia, 21 (2005) 761-767.
[38] F.D. Yuan, M.; Fukumura, D.; Leunig, M.; Berk, D. A.; Torchilin, V. P.; Jain, R. K. , Vascular Permeability in a Human Tumor Xenograft: Molecular Size

Dependence and Cutoff Size, Cancer Research, 55 (1995) 3752-3756.
[39] W.C. Dewey, Arrhenius relationships from the molecule and cell to the clinic, International Journal of Hyperthermia, 10 (1994) 457-483.
[40] H.H. Kampinga, E. Dikomey, Hyperthermic radiosensitization: mode of action and clinical relevance, Int. J. Radiat. Biol., 77 (2001) 399-408.
[41] P.M. Krawczyk, B. Eppink, J. Essers, J. Stap, H. Rodermond, H. Odijk, A. Zelensky, C. van Bree, L.J. Stalpers, M.R. Buist, T. Soullie, J. Rens, H.J.M. Verhagen, M.J. O'Connor, N.A.P. Franken, T.L.M. ten Hagen, R. Kanaar, J.A. Aten, Mild hyperthermia inhibits homologous recombination, induces BRCA2 degradation, and sensitizes cancer cells to poly (ADP-ribose) polymerase-1 inhibition, Proceedings of the National Academy of Sciences of the United States of America, 108 (2011) 9851-9856.
[42] J. van der Zee, D.G. Gonzalez, G.C. van Rhoon, J.D.P. van Dijk, W.L.J. van Putten, A.A.M. Hart, G. Dutch Deep Hyperthermia, Comparison of radiotherapy alone with radiotherapy plus hyperthermia in locally advanced pelvic tumours: a prospective, randomised, multicentre trial, Lancet, 355 (2000) 1119-1125.
[43] R.D. Issels, L.H. Lindner, J. Verweij, P. Wust, P. Reichardt, B.C. Schem, S. Abdel-Rahman, S. Daugaard, C. Salat, C.M. Wendtner, Z. Vujaskovic, R. Wessalowski, K.W. Jauch, H.R. Durr, F. Ploner, A. Baur-Melnyk, U. Mansmann, W. Hiddemann, J.Y. Blay, P. Hohenberger, E.-S.E. European Org, Neo-adjuvant chemotherapy alone or with regional hyperthermia for localised high-risk soft-tissue sarcoma: a randomised phase 3 multicentre study, Lancet Oncology, 11 (2010) 561-570.
[44] P. Wust, B. Hildebrandt, G. Sreenivasa, B. Rau, J. Gellermann, H. Riess, R. Felix, P.M. Schlag, Hyperthermia in combined treatment of cancer, Lancet Oncol, 3 (2002) 487-497.
[45] C.R. Hill, G.R. terHaar, Review article: High intensity focused ultrasound-potential for cancer treatment, British Journal of Radiology, 68 (1995) 1296-1303.
[46] M.S. Anscher, T.V. Samulski, R. Dodge, L.R. Prosnitz, M.W. Dewhirst, Combined external beam irradiation and external regional hyperthermia for locally advanced adenocarcinoma of the prostate, International Journal of Radiation Oncology Biology Physics, 37 (1997) 1059-1065.
[47] B.D. de Senneville, C. Mougenot, C.T.W. Moonen, Real-time adaptive methods for treatment of mobile organs by MRI-controlled high-intensity focused ultrasound, Magnetic Resonance in Medicine, 57 (2007) 319-330.
[48] M. van Lummel, W.J. van Blitterswijk, S.R. Vink, R.J. Veldman, M.A. van der Valk, D. Schipper, B.M. Dicheva, A.M. Eggermont, T.L. ten Hagen, M. Verheij, G.A. Koning, Enriching lipid nanovesicles with short-chain glucosylceramide improves doxorubicin delivery and efficacy in solid tumors, FASEB J, 25 (2011) 280-289.
[49] T.M. Allen, E. Brandeis, C.B. Hansen, G.Y. Kao, S. Zalipsky, A new strategy for attachment of antibodies to sterically stabilized liposomes resulting in efficient targeting to cancer-cells, Biochimica Et Biophysica Acta-

Biomembranes, 1237 (1995) 99-108.
[50] D.B. Kirpotin, D.C. Drummond, Y. Shao, M.R. Shalaby, K.L. Hong, U.B. Nielsen, J.D. Marks, C.C. Benz, J.W. Park, Antibody targeting of long-circulating lipidic nanoparticles does not increase tumor localization but does increase internalization in animal models, Cancer Research, 66 (2006) 6732-6740.
[51] F. Pastorino, C. Brignole, D. Di Paolo, B. Nico, A. Pezzolo, D. Marimpietri, G. Pagnan, F. Piccardi, N. Cilli, R. Longhi, D. Ribatti, A. Corti, T.M. Allen, M. Ponzoni, Targeting liposomal chemotherapy via both tumor cell-specific and tumor vasculature-specific ligands potentiates therapeutic efficacy, Cancer Research, 66 (2006) 10073-10082.
[52] B.M. Dicheva, T.L. Hagen, L. Li, D. Schipper, A.L. Seynhaeve, G.C. Rhoon, A.M. Eggermont, L.H. Lindner, G.A. Koning, Cationic Thermosensitive Liposomes: A Novel Dual Targeted Heat-Triggered Drug Delivery Approach for Endothelial and Tumor Cells, Nano Lett, (2012). ePub ahead of print DOI: 10/1021/nl3014154.
[53] W.J. Yatvin MB, Dennis WH, Blumenthal R, Design of liposomes for enhanced local release of drugs by hyperthermia, Science, 202 (1978) 1290-1293.
[54] T.Y. Tsong, Kinetics of the crystalline-liquid crystalline phase transition of dimyristoyl L-alpha-lecithin bilayers, Proc Natl Acad Sci U S A, 71 (1974) 2684-2688.
[55] J.K. Mills, D. Needham, The materials engineering of temperature-sensitive liposomes, Methods Enzymol, 387 (2004) 82-113.
[56] J.K. Mills, D. Needham, Lysolipid incorporation in dipalmitoylphosphatidylcholine bilayer membranes enhances the ion permeability and drug release rates at the membrane phase transition, Biochimica Et Biophysica Acta-Biomembranes, 1716 (2005) 77-96.
[57] P.S. Yarmolenko, Y. Zhao, C. Landon, I. Spasojevic, F. Yuan, D. Needham, B.L. Viglianti, M.W. Dewhirst, Comparative effects of thermosensitive doxorubicin-containing liposomes and hyperthermia in human and murine tumours, Int J Hyperthermia, 26 (2010) 485-498.
[58] T. Tagami, M.J. Ernsting, S.D. Li, Optimization of a novel and improved thermosensitive liposome formulated with DPPC and a Brij surfactant using a robust in vitro system, Journal of Controlled Release, 154 (2011) 290-297.
[59] L.H. Lindner, M.E. Eichhorn, H. Eibl, N. Teichert, M. Schmitt-Sody, R.D. Issels, M. Dellian, Novel temperature-sensitive liposomes with prolonged circulation time, Clinical Cancer Research, 10 (2004) 2168-2178.
[60] G.A. Koning, Li, L., Ten Hagen, T.L.M., Thermosensitive liposomes for the delivery of cancer therapeutics, Therapeutic Delivery, 1 (2010) 707-711.
[61] G.A. Koning, A.M.M. Eggermont, L.H. Lindner, T.L.M. ten Hagen, Hyperthermia and Thermosensitive Liposomes for Improved Delivery of Chemotherapeutic Drugs to Solid Tumors, Pharmaceutical Research, 27 (2010) 1750-1754.
[62] A.A. Manzoor, L.H. Lindner, C.D. Landon, J.-Y. Park, A.J. Simnick, M.R.

Dreher, S. Das, G. Hanna, W. Park, A. Chilkoti, G.A. Koning, T.L.M. ten Hagen, D. Needham, M.W. Dewhirst, Overcoming limitations in nanoparticle drug delivery: triggered, intravascular release to improve drug penetration into tumors, Cancer Research, 72 (2012) 5566-5575.
[63] R.T. Poon, N. Borys, Lyso-thermosensitive liposomal doxorubicin: a novel approach to enhance efficacy of thermal ablation of liver cancer, Expert Opin Pharmacother, 10 (2009) 333-343.

Chapter 2

Triggered content release from optimized stealth thermosensitive liposomes using mild hyperthermia

Li Li, Timo L.M. ten Hagen, Debby Schipper, Tom M. Wijnberg, Gerard van Rhoon, Alexander M.M. Eggermont, Lars H. Lindner, Gerben A. Koning

PMID: 20074595.

Abstract

Liposomes are potent nanocarriers to deliver chemotherapeutic drugs to tumors. However, the inefficient drug release hinders their application. Thermosensitive liposomes (TSL) can release drugs upon heat. This study aims to identify the optimum 1,2-distearoyl-*sn*-glycero-3-phosphoethanolamine-*N*-PEG_{2000} (DSPE-PEG_{2000}) concentration in stealth TSL to improve content release efficiency under mild hyperthermia (HT). TSL were prepared with DSPE-PEG_{2000} from 1 to 10 mol%, around 80 nm in size. Quenched carboxyfluorescein (CF) in aqueous phase represented encapsulated drugs. *In vitro* temperature/time-dependent CF release and TSL stability in serum were quantified by fluorometry. *In vivo* CF release in dorsal skin flap window chamber models implanted with human BLM melanoma was captured by confocal microscopy. *In vitro* heat triggered CF release increased with increasing DSPE-PEG_{2000} density. However, 6 mol% and higher DSPE-PEG_{2000} caused CF leakage at physiological temperature. TSL with 5 mol% DSPE-PEG_{2000} were stable at 37°C, while released 60% CF in one minute and almost 100% CF in one hour at 42°C. *In vivo* optical intravital imaging showed immediate massive CF release above 41°C. In conclusion, incorporation of 5 mol% DSPE-PEG_{2000} optimized stealth TSL content release triggered by HT.

Keywords:

Thermosensitive liposomes, hyperthermia, poly(ethylene glycol), drug delivery, triggered release, tumor, intravital microscopy.

1. Introduction

The major obstacle of current available chemotherapy is the inability to deliver adequate concentration of drugs to tumors, but causes considerable systemic toxicity which limits their applicable dose. Most chemotherapeutic drugs are delivered intravenously and rapidly cleared from circulation, e.g. doxorubicin (Dox) has a five to ten minutes half-life in plasma [1]. Therefore, only a fraction of the administered dose can reach tumors. Long-circulating drug-carrying nanoparticles, e.g. pegylated liposomal Dox (Doxil or Caelyx), reduce toxicity and augment intratumoral delivery compared to free drugs [2-5]. Despite the prolonged circulation time and increased tumor accumulation [2, 6], slow and passive drug release from these liposomes hinders an optimal antitumor effect. Thus, it is critical to actively trigger liposomal drug release. Therefore, thermosensitive liposomes (TSL) [7] and local hyperthermia (HT) are used. This approach relies on features of tumor microvasculature and TSL. Relative leakiness of partial tumor vessels can cause extravasation of small liposomes (i.e. < 400 nm) [8-12]. Permeability of tumor microvasculature can be further enhanced by heat [13], causing more liposomes to accumulate intratumorally [14].

Intratumoral liposome accumulation does not guarantee drug bioavailability. The entrapped drugs need to be released from the liposomes to reach tumor cells for a therapeutic effect. TSL are phospholipid-based vesicles with a large capacity to encapsulate drugs and to release them upon heat. This release depends on temperature and lipid composition of TSL [15]. When a TSL lipid membrane undergoes a gel-to-liquid crystalline phase transition, it becomes more permeable towards water and solutes, because trans to gauche conformational changes increase the mobility of phospholipids [16]. In this way, the entrapped hydrophilic drugs can be released.

For phospholipids with saturated hydrocarbon chains, lengths of fatty acid chains primarily determine the T_m, the main gel-to-liquid crystalline phase transition temperature of lipid membranes. For stealth non-thermosensitive liposomes [17, 18], the concentration of grafted 1,2-distearoyl-*sn*-glycero-3-phosphoethanolamine-*N*-PEG_{2000} (DSPE-PEG_{2000}) in lipid membrane influences membrane permeability [19]. Surface-grafted polymers can disturb membrane integrity by inducing steric repulsion between opposing polymers, e.g. DSPE-PEG_{2000} and DSPE-PEG_{5000} [20]. Molecular structures of PEG-polymers can be distinguished as interdigitated mushroom, mushroom and brush regimes [21]. Polymer regimes are determined by distance between grafting sites, and by polymer sizes [21]. Kenworthy et al. suggested that 4 mol% DPPE-PEG_{2000} induced maximum membrane permeability [21, 22].

For stealth non-thermosensitive liposomes in general, 1 – 5 mol% DSPE-PEG_{2000} is commonly grafted on lipid membranes for prolonged circulation

time, and 5 mol% DSPE-PEG_{2000} is the sufficient and optimal concentration [17]. In addition, DSPE-PEG_{2000} also prevents liposome aggregation in plasma [23]. Formulations containing up to 10 mol% DSPE-PEG_{2000} have been described [20, 22, 24], though PEG-lipids tend to form micellar structures at higher concentrations [25], and disk-like micelle formation can be enhanced by extrusion repeatedly crossing T_m [26]. Therefore, all TSL formulations in this study were extruded above their T_m to avoid PEG-micelle formation.

Stealth TSL typically adopt conventional DSPE-PEG_{2000} concentrations between 1 and 5 mol% in stealth non-thermosensitive liposomes to prolong half-lives in plasma for drug delivery [17, 18, 27]. However, the ideal DSPE-PEG_{2000} concentration for TSL content release has not yet been determined. This study provides a valuable guide on the use of DSPE-PEG_{2000} in TSL by identifying the optimum DSPE-PEG_{2000} concentration with regard to intrinsic stability, *in vitro* and *in vivo* content release properties, to improve content release of stealth TSL triggered by mild HT.

2. Materials and methods

2.1 Chemicals

The phospholipids 1,2-dihexadecanoyl-*sn*-glycero-3-phosphocholine (DPPC), 1,2-distearoyl-*sn*-glycero-3-phosphocholine (DSPC), 1,2-distearoyl-*sn*-glycero-3-phosphoethanolamine-*N*-PEG_{2000} (DSPE-PEG_{2000}) were provided by Lipoid (Ludwigshafen, Germany), and phosphatidylethanolamine-dioleoyl-sulforhodamine B (Rho-PE) was purchased from Avanti Polar Lipid Inc. Carboxyfluorescein (CF) purified by recrystallization [28]. Other chemicals were obtained from Sigma Aldrich (Netherlands) unless otherwise specified.

2.2 Preparation of TSL

TSL were composed of DPPC/DSPC/DSPE-PEG_{2000} in a molar ratio of 80:(20-x):x (x = 1, 3, 4, 5, 6, 10). TSL < 100 nm in diameter were prepared by lipid film hydration and extrusion method at 60°C (thermobarrel extruder, Northern Lipids, Vancouver, Canada) [29]. Quenched CF (100 mM) at pH 7.2 was encapsulated in the aqueous phase, and 0.1 mol% Rho-PE was incorporated in the liposome bilayer. Unencapsulated CF was removed by gel filtration through PD-10 columns (GE Healthcare, Buckinghamshire, UK). Size and polydispersity index (PDI) were determined by dynamic light scattering using a Zetasizer Nano ZS (Malvern Instruments, Worcestershire, UK). Lipid concentration was measured by phosphate assay [30].

2.3 Differential scanning calorimetry

T_m was measured by a Capillary Cell MicroCalorimeter (MicroCal VP-DSC)

[31].

2.4 Stability and encapsulation capability

TSL *in vitro* membrane stability in serum was tested by exposure to 90% serum for one hour. CF leakage was detected by fluorometry [28]. Encapsulation was determined by TSL exposure to detergent to receive maximal CF fluorescence. A TSL suspension (1 mM [lipid]) and pre-heated fetal calf serum (FCS) (37°C) were mixed at 1:9 (v/v). The mixture was then incubated at 37°C for one hour in a thermal-shaker (Eppendorf Thermomixer) at 300 rpm. After incubation, samples were diluted in 10 mM Tris/NaCl 0.9% at pH 8.0 at 1:50 (v/v) (I_t), and measured by fluorometry at Ex. 493 nm / Em. 513 nm (Hitachi F-4500 Fluorescence Spectrophotometer). Samples without incubation were measured as negative controls (I_0). Samples in the replacement of FCS to detergent (2% Triton X-100 in H_2O) were incubated at 55°C for 30 minutes at 1400 rpm and measured as positive controls (I_∞). Positive controls were adjusted to contain identical amounts of FCS. CF release was calculated as CF (%) = $(I_t - I_0)/(I_\infty - I_0)$ x100 [28]. TSL stability was determined as Stability (%) = 100 – CF (%). TSL stability at 4 and 25°C was determined in the same way. TSL encapsulation was calculated as Encapsulation ratio (CF/lipid) = [CF]/[lipid].

2.5 Temperature-dependent CF release

Temperature influence on *in vitro* TSL content release rate in 90% FCS was determined. Samples were measured after five minutes incubation at desired temperatures from 37 to 45°C and CF release (%) was calculated as above (2.4).

2.6 Time-dependent CF release

In vitro TSL content release over time was monitored online by fluorometry. The optimal temperature achieved from temperature-dependent CF release experiments was adopted for time-dependent CF release experiments. A TSL suspension (1 mM [lipid]) and pre-heated FCS were mixed 1:150 (v/v) under stirring. CF release was measured online for one hour (Ex. 493 nm / Em. 513 nm). Then samples were added with 10% Triton X-100 151:1 (v/v) as positive control. Samples without heating were measured as negative controls. CF release (%) was calculated as above (2.4).

2.7 Animal models

NMRI nu/nu mice were purchased from Charles River and housed at 20 – 22°C, humidity of 50 – 60%, and 12 hour light-dark cycles. Sterile rodent food and acidified vitamin C-fortified water were given *ad libitum*. Eight-week old mice, weighing 20 – 25 g were used. All animal studies were done in accordance

with protocols approved by the committee on Animal Research of Erasmus MC, Rotterdam, the Netherlands.

2.8 In vivo tumor models and content release

BLM cells were cultured in DMEM medium (Lonza, Belgium) containing 10% (v/v) FCS, and incubated at 37°C in a humidified environment of 95% air and 5% CO_2. 10^6 tumor cells were injected subcutaneously in flanks of mice, and bulk tumors of 10 mm in diameter were used.

In vivo CF release was observed by intravital fluorescence microscopy on dorsal skin flap window chamber models in mice implanted with human BLM melanoma [32, 33]. Models were used for experiments within two weeks, when tumor size reached 4 – 6 mm in diameter. Mice were anesthetized with isofluorane (Nicholas Piramal, London, UK) and placed on a thermal stage at 37°C during experiments. Homogenous local HT was provided by an external circular resistive electric heating coil attached to glass at the back side of the window chamber. Thermocouples (point-welded thin manganese and constantane wires, H. Drijfhout & Zoon's edelmetaalbedrijven, Amsterdam) were inserted in window chambers to monitor tissue temperature. Two μmol lipids of TSL with 5 mol% DSPE-PEG_{2000} with Rho-PE and CF labeling were injected intravenously through the tail vein.

Regions of interest were selected by confocal microscopy (Zeiss LSM 510 META). Background images were captured before TSL injection. Imaging was started within 10 minutes post-injection. CF release was monitored online by a 488 nm argon laser and Rho-PE was detected by a 543 nm Helium-Neon laser. Window chamber tissue was heated up to 42°C and remained for five minutes before cooling down to 37°C and maintained for 10 minutes. Images of transmission channel and fluorescent channels (x 10 objective lens, 284 μm pinhole) were recorded intermittently at each temperature point from 39 to 42°C, and at 1, 2, 3, 4, 5 minutes after tissue temperature reached 42°C, and end points of experiments after tissue temperature was down to 37°C. Images of 512 x 512 pixels were analyzed with a Zeiss image program (LSM, Germany). CF release was quantified as Area (mm^2) x Average Intensity at 150 – 255 threshold by Image J (Wayne Rasband, National Institutes of Health, USA). As additions to the same experimental models, images (x 10 objective lens) were also taken every 18 seconds throughout experiments and converted to videos by Image J.

2.9 Statistical analysis

All *in vitro* data were represented as mean ± standard error of the mean (SEM) of triplicate samples from three independent experiments. *In vitro* TSL CF release were compared through temperature-dependent CF release study,

and analyzed by nonparametric Mann-Whitney test.

3. Results

3.1 Characterization of the TSL

In vitro characteristics of the TSL are summed up in Table 1. TSL encapsulation ratio of CF/lipid (mole/mole) of the different formulations was comparable except for TSL with 10 mol% DSPE-PEG_{2000}, which was significantly lower than any other formulation (p value ≤ 0.05). TSL with 1 – 5 mol% DSPE-PEG_{2000} in 90% serum retained over 96% CF and TSL with 6 mol% DSPE-PEG_{2000} retained 91% CF, while TSL with 10 mol% DSPE-PEG_{2000} were the least stable to retain 83% CF after one hour incubation at 37°C. Size of the TSL was around 80 nm, PDI < 0.1. T_m of the TSL was identical at 43°C (supplementary Fig. 1). TSL lacking DSPE-PEG_{2000} (0 mol%) were instable after preparation (data not shown), and therefore could not be tested.

Table 1: TSL characteristics

PEG (%)	Encapsulation ratio[a] (mole/mole of CF/lipid)	Stability[a] (%) at 37 °C in 90 % FCS in one hour	Size[a] (nm)	PDI[a]	T_m (°C)
1	0.11 ± 0.01	98 ± 1	84 ± 5	0.05 ± 0.01	43
3	0.09 ± 0.01	96 ± 2	80 ± 5	0.07 ± 0.03	43
4	0.07 ± 0.00	97 ± 1	75 ± 1	0.07 ± 0.02	43
5	0.08 ± 0.00	98 ± 1	77 ± 1	0.06 ± 0.01	43
6	0.07 ± 0.01	91 ± 3	77 ± 1	0.05 ± 0.01	43
10	0.02 ± 0.01*	83 ± 4	81 ± 0	0.05 ± 0.00	43

* Nonparametric Mann-Whitney test, p value ≤ 0.05, [a] mean ± SEM, N = 3.

3.2 Temperature-dependent CF release

Temperature-dependent CF release of the TSL was measured after 5 minutes incubation in 90% serum and is represented in Fig. 1. TSL with different PEG-densities were all stable up to 38°C, with CF leakage < 2%. TSL slowly started to release CF at 39°C, except for TSL with 10 mol% DSPE-PEG_{2000}, which already released more than 15% CF in five minutes. TSL with 1 – 5 mol% DSPE-PEG_{2000} reached their highest CF release levels at 42°C, while TSL with 6 and 10 mol% DSPE-PEG_{2000} shifted their highest release levels to 43°C though not significant compare to 42°C (6 mol% DSPE-PEG_{2000}, p value = 0.827; 10 mol% DSPE-PEG_{2000}, p value = 0.275). For all TSL, CF release levels decreased gradually from 43 to 45°C. In general CF release increased with increasing PEG-density. TSL with 5 mol% DSPE-PEG_{2000} showed the highest release level amongst stable TSL with 1 – 5 mol% DSPE-PEG_{2000} (p value ≤ 0.05). The difference in release levels between TSL with 5 and 6 mol% DSPE-PEG_{2000} was negligible at up to 42°C. There was no CF leakage from any TSL at 4 or 25°C (data not shown).

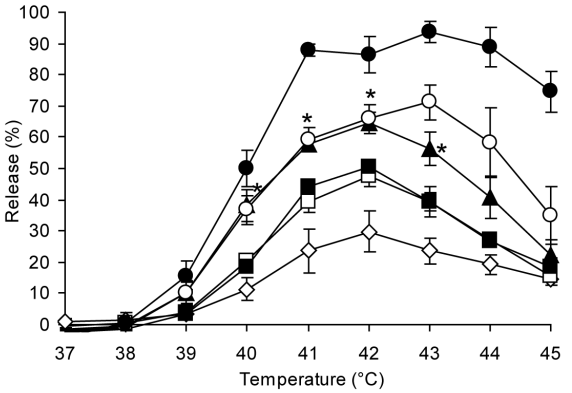

Fig. 1: *In vitro* CF release from TSL with different PEG-densities, 1 mol% (◊), 3 mol% (□), 4 mol% (■), 5 mol% (▲), 6 mol% (◘), and 10 mol% (●), measured after five minutes incubation at indicated temperatures in 90% serum. TSL with 1 – 5 mol% DSPE-PEG_{2000} were stable up to 38°C and show maximal release at 42°C. TSL with 5 mol% DSPE-PEG_{2000} showed significantly higher release level than stable TSL containing 1 – 4 mol% DSPE-PEG_{2000} at 40 – 43°C. * Nonparametric Mann-Whitney test, $p \leq 0.05$, N = 3.

3.3 Time-dependent CF release

In vivo time-dependent CF release at 42°C in 99.7% serum was monitored online for one hour (Fig. 2 A). TSL with 5 mol% DSPE-PEG_{2000} released CF faster than TSL with lower PEG-densities, and boosted CF release over 3-fold of the level of TSL with 1 mol% DSPE-PEG_{2000}. More than 60% CF was effectively released from TSL with 5 mol% DSPE-PEG_{2000} in the first minute (Fig. 2 B). Almost 100% CF was released in one hour (Fig. 2 A and Table 2). CF release levels were comparable amongst TSL with 5, 6, and 10 mol% DSPE-PEG_{2000}. Comparing Fig. 1 and 2 B, CF release of TSL after five minutes incubation was higher in time-dependent than in temperature-dependent CF release experiments, likely due to increased FCS concentration (90 to 99.7%). Serum protein components are involved in membrane instability.

Table 2: TSL characteristics on CF release

PEG (%)	Release[a] (%)	
	One minute	One hour
1	19 ± 7	72 ± 8
3	42 ± 5	88 ± 6
4	47 ± 5	97 ± 3
5	62 ± 9	98 ± 2
6	60 ± 5	99 ± 1
10	71 ± 5	99 ± 1

[a] mean ± SEM, N = 3.

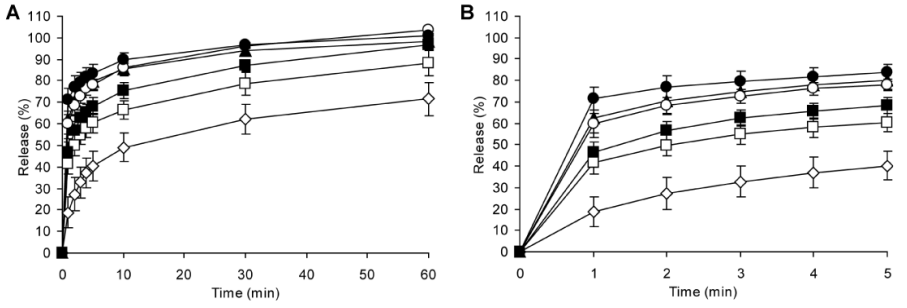

Fig. 2 A: *In vitro* CF release in time from TSL with different PEG-densities, 1 mol% (◊), 3 mol% (□), 4 mol% (■), 5 mol% (▲), 6 mol% (⭘), and 10 mol% (●), measured at indicated time after placing TSL at 42°C in 99.7% serum. Rapid release occurred in the first few minutes. TSL with 5 mol% DSPE-PEG_{2000} released comparable amount of CF to TSL with 6 or 10 mol% DSPE-PEG_{2000} and reached their maximal release in one hour (N = 3). B: Kinetics of *in vitro* CF release from TSL with different PEG-densities in the first five minutes measured at indicated time after placing TSL in 99.7% serum at 42°C. Rapid CF release occurred in the first minute, N = 3.

3.4 In vivo CF release

In vivo CF release of TSL was studied by intravital optical imaging using dorsal skin fold window chamber models implanted with human BLM melanoma (Fig. 3 and supplementary video). Functioning tumor vessels were visualized by Rho-PE labeled TSL with 5 mol% DSPE-PEG_{2000}, and no CF leakage was observed up to 39.5°C (Fig. 3 B). TSL slowly released CF at 40°C (Fig. 3 C), and massively released CF within seconds when tissue temperature was reaching 42°C. Free CF diffused into interstitial space (Fig. 3 D – F and supplementary video), but CF release was shut down immediately when tissue temperature was decreasing to 37°C (Fig. 3 G). Free CF was quickly washed out from tumor tissue, with almost no remaining within 12 minutes at 37°C (Fig. 3 H). Tissue temperatures were recorded online (Fig. 4) and the letters correspond to Fig. 3 images. Tissue temperature increased from 37°C to 42°C in 15 minutes, remained at 42°C for five minutes, and then decreased to 37°C in five minutes. Quantified CF release was negligible up to 40°C (Fig. 5), while elevated steeply to almost two-fold (180×10^6 vs. 100×10^6) (Area (mm^2) x Average Intensity) in five minutes at 42°C. Decreasing temperature shut down CF release back to baseline.

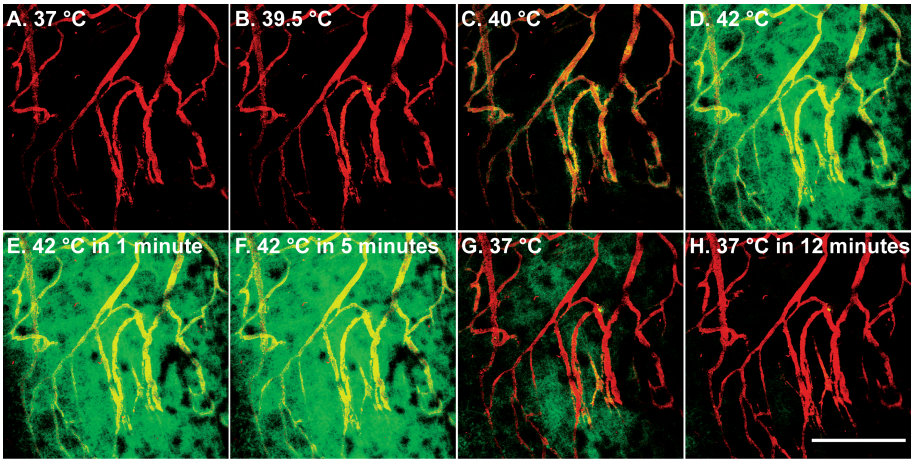

Fig. 3: *In vivo* CF release from TSL with CF in aqueous phase and Rho-PE labeled lipid membrane. Images are presented as merged green (CF) and red (Rho-PE) fluorescence (x 10 objective lens, N = 3) A, T_{tissue} = 37°C post-injection; B, T_{tissue} = 39.5°C; C, T_{tissue} = 40°C; D, T_{tissue} = 42°C; E, T_{tissue} = 42°C in one minute; F, T_{tissue} = 42°C in five minutes; G, T_{tissue} = 37°C; H, T_{tissue} = 37°C in 12 minutes. Bar, 500 μm.

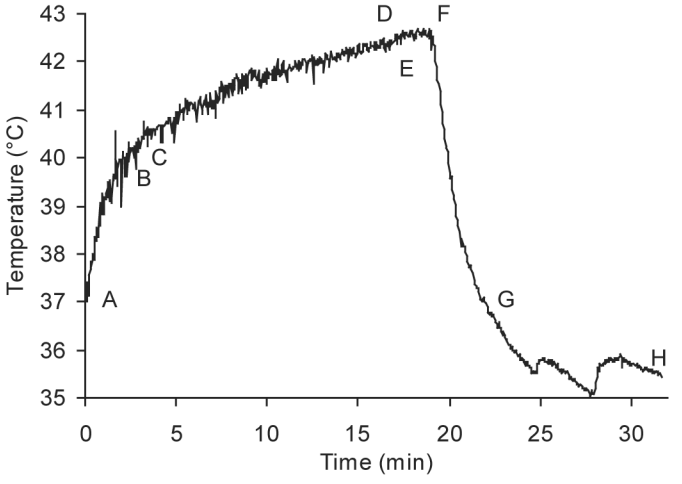

Fig. 4: Online monitoring of tissue temperature. A – H correspond with the images in Fig 3.

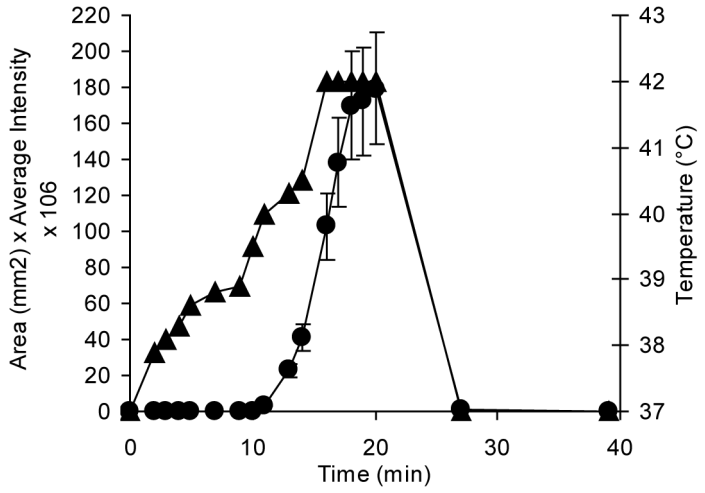

Fig. 5: Quantification of *in vivo* CF release in Fig. 3. Primary Y-axis represents Area (mm^2) x Average Intensity x 10^6 (●) as mean ± SD. Secondary Y-axis represents corresponding tissue temperatures (▲).

4. Discussion

Stealth TSL with 5 mol% DSPE-PEG_{2000} were optimal, considering stability at 4, 25, 37°C and release kinetics at mild HT. Stealth TSL with 1 – 5 mol% DSPE-PEG_{2000} were stable (< 4% CF leakage) at 37°C in 90% serum, while TSL with 6 and 10 mol% DSPE-PEG_{2000} leaked out 9 and 17% CF, after one hour incubation. High DSPE-PEG_{2000} density, especially 10 mol%, collapsed the membrane integrity, causing content leakage at relatively low temperatures. Based on *in vitro* stability study of stealth TSL (Table 1), 1 – 5 mol% DSPE-PEG_{2000} can sufficiently stabilize lipid membrane in 90% serum at physiological temperature, known as the major effect of DSPE-PEG_{2000} [17, 18]. Noticeable CF release started at 40°C in both *in vitro* and *in vivo* experiments. Remarkable *in vitro* CF release occurred between 42 and 43°C, which is consistent with their T_m. Increase of DSPE-PEG_{2000} density from 1 to 4 mol% diminishes the distance between grafting sites for mushroom regime, while increase of DSPE-PEG_{2000} density from 4 to 5 mol% forces the mushroom-to-brush transition. We speculate the structural heterogeneity of DSPE-PEG_{2000} destabilizes lipid membrane at around T_m, causing increased content release. More importantly, DSPE-PEG_{2000}-density strikingly modified the permeability of lipid membranes against temperature for hydrophilic content release. By contrast, T_m of the TSL remained intact (Table 1). Five mol% DSPE-PEG_{2000} noteworthily enhanced TSL release kinetics, compared to lower densities (Fig. 1). Above T_m, membrane phospholipids likely reached a more homogeneous liquid crystaline phase, causing decreased CF release. At 42°C, TSL with 5

mol% DSPE-PEG_{2000} released over 60% CF in one minute, and almost 100% in one hour. Destabilization of the lipid membrane with 10 mol% DSPE-PEG_{2000} caused significant release at 37°C, and it may play a more important role than change of membrane modality for content release. Additionally, TSL with 10 mol% DSPE-PEG_{2000} showed 3-fold lower encapsulation compared to 5 mol% DSPE-PEG_{2000}. Therefore, our study concludes that the optimum DSPE-PEG_{2000} concentration to use in stealth TSL is 5 mol%. Retention of CF, which is commonly used as a fluorescent test molecule for low molecular weight hydrophilic drugs, may not be predictive of drug molecules. For each new TSL-drug formulation stability and release kinetics need to be determined.

Encouragingly, lysolipid-based Dox-containing low TSL (Dox-LTSL) in combination with local HT have showed promising efficacy [34] and are currently in clinical trials [35]. Dox-LTSL is composed of DPPC/MPPC/DSPE-PEG_{2000} in a molar ratio of 90:10:4, meaning 3.8 mol% DSPE-PEG_{2000}. Although the content release mechanism of lysolecithin-containing TSL may differ from lysolecithin-free TSL, higher DSPE-PEG_{2000} density (i.e. 5 mol%) in the lipid membrane can still facilitate Dox-LTSL drug release by forcing phospholipid monolayers apart [36] to create more space for proton exchange across the membrane, causing the pH gradient to collapse, which in return eases doxorubicin cross-membrane penetration. On the other hand, traditional TSL is composed of DPPC/HSPC/cholesterol/DSPE-PEG_{2000} in a molar ratio of 100:50:30:6, meaning 3.2 mol% DSPE-PEG_{2000}. These Dox-encapsulated cholesterol-containing TSL released ~ 60% Dox *in vitro* in 50% plasma in 30 minutes [37]. Gaber, et al. [37] also concluded from their study that cholesterol shielded TSL thermosensitivity, while DSPE-PEG_{2000} not only protected TSL in plasma but also revealed their thermosensitivity. Therefore, it appears to be undoubtedly beneficial to increase DSPE-PEG_{2000} concentration in cholesterol-containing TSL to 5 mol%.

According to literature, we standardized TSL size to be smaller than 100 nm, to ultimately enhance intratumoral liposomal drug accumulation by liposome extravasation through tumor microvasculature [38]. Several groups demonstrated that 100 nm liposomes extravasate much easier than 200 or 400 nm liposomes [12, 32, 38]. Moreover, small liposomes can diffuse better throughout tumor tissue to avoid limited perivascular accumulation. It is practical to expect greater drug encapsulation in larger TSL (e.g. 200 nm), which might lead to higher content release. Nevertheless, our 100 nm TSL showed compatible release rates, compared with 170 nm PEG-free TSL, DPPC/DSPC/DPPGOG in a molar ratio of 5:2:3 [39].

In conclusion, incorporation of 5 mol% DSPE-PEG_{2000} in the lipid membrane optimized stealth TSL content release triggered by mild HT (~ 42°C). *In vivo* tumor models confirmed these *in vitro* TSL release characteristics. These TSL will be employed with local HT to achieve both maximal intratumoral

liposomal drug accumulation and rapid triggered drug release. The superior application of stealth TSL and local HT has the potential to aid liposomal chemotherapy in clinical practice.

Acknowledgements

The authors thank Dr. Kristina Djanashvili, Dr. Daniel Schuhle, Dr. Aurelie M. A. Brizard at ChemTech, Delft University of Technology, Delft, for DSC measurements; Dr. Martin Hossann at Medical Clinic and Pre-clinic III, Ludwig-Maximilians University, Munich, and Dr. Gert van Cappellen at Erasmus MC, Rotterdam, for technical support; Stichting Vanderes, Stichting Fondsen, SEHK, Dr. Mildred Scheel Stiftung and Erasmus MC grants (Mrace) for financial support.

References

[1] P.K. Working, A.D. Dayan, Pharmacological-toxicological expert report - Caelyx(TM) - (Stealth(R) liposomal doxorubicin HCl) - Foreword. Hum. Exp. Toxicol. 15(9) (1996) 751-785.
[2] A. Gabizon, H. Shmeeda, Y. Barenholz, Pharmacokinetics of pegylated liposomal doxorubicin - Review of animal and human studies. Clin. Pharmacokinet. 42(5) (2003) 419-436.
[3] A.A. Gabizon, Selective Tumor-Localization and Improved Therapeutic Index of Anthracyclines Encapsulated in Long-Circulating Liposomes. Cancer Res. 52(4) (1992) 891-896.
[4] D.W. Northfelt, F.J. Martin, P. Working, P.A. Volberding, J. Russell, M. Newman, M.A. Amantea, L.D. Kaplan, Doxorubicin encapsulated in liposomes containing surface-found polyethylene glycol: Pharmacokinetics, tumor localization, and safety in patients with AIDS-related Kaposi's sarcoma. J. Clin. Pharmacol. 36(1) (1996) 55-63.
[5] T.L.M. Ten Hagen, A.L.B. Seynhaeve, S.T. Van Tiel, D.J. Ruiter, A.M.M. Eggermont, Pegylated liposomal tumor necrosis factor-alpha results in reduced toxicity and synergistic antitumor activity after systemic administration in combination with liposomal doxorubicin (Doxil (R)) in soft tissue sarcoma-bearing rats. Int. J. Cancer 97(1) (2002) 115-120.
[6] A. Gabizon, R. Catane, B. Uziely, B. Kaufman, T. Safra, R. Cohen, F. Martin, A. Huang, Y. Barenholz, Prolonged Circulation Time and Enhanced Accumulation in Malignant Exudates of Doxorubicin Encapsulated in Polyethylene-Glycol Coated Liposomes. Cancer Res. 54(4) (1994) 987-992.
[7] M.B. Yatvin, J.N. Weinstein, W.H. Dennis, R. Blumenthal, Design of liposomes for enhanced local release of drugs by hyperthermia. Science 202(4374) (1978) 1290-1293.
[8] E.G. Mayhew, D. Lasic, S. Babbar, F.J. Martin, Pharmacokinetics and Antitumor-Activity of Epirubicin Encapsulated in Long-Circulating Liposomes Incorporating a Polyethylene Glycol-Derivatized Phospholipid. Int. J. Cancer 51(2) (1992) 302-309.
[9] H.F. Dvorak, L.F. Brown, M. Detmar, A.M. Dvorak, Vascular-Permeability Factor Vascular Endothelial Growth-Factor, Microvascular Hyperpermeability, and Angiogenesis. Am. J. Pathol. 146(5) (1995) 1029-1039.
[10] F. Yuan, M. Dellian, D. Fukumura, M. Leunig, D.A. Berk, V.P. Torchilin, R.K. Jain, Vascular-Permeability in a Human Tumor Xenograft - Molecular-Size Dependence and Cutoff Size. Cancer Res. 55(17) (1995) 3752-3756.
[11] H. Maeda, J. Wu, T. Sawa, Y. Matsumura, K. Hori, Tumor vascular permeability and the EPR effect in macromolecular therapeutics: a review. J. Control. Release 65(1-2) (2000) 271-284.
[12] G.J.R. Charrois, T.M. Allen, Rate of biodistribution of STEALTH((R)) liposomes to tumor and skin: influence of liposome diameter and implications for toxicity and therapeutic activity. Biochim. Biophys. Acta-Biomembr. 1609(1) (2003) 102-108.

[13] M.H. Gaber, N.Z. Wu, K.L. Hong, S.K. Huang, M.W. Dewhirst, D. Papahadjopoulos, Thermosensitive liposomes: Extravasation and release of contents in tumor microvascular networks. Int. J. Radiat. Oncol. Biol. Phys. 36(5) (1996) 1177-1187.
[14] G. Kong, R.D. Braun, M.W. Dewhirst, Characterization of the effect of hyperthermia on nanoparticle extravasation from tumor vasculature. Cancer Res. 61(7) (2001) 3027-3032.
[15] G.R. Anyarambhatla, D. Needham, Enhancement of the phase transition permeability of DPPC liposomes by incorporation of MPPC: A new temperature-sensitive liposome for use with mild hyperthermia. J. Liposome Res. 9(4) (1999) 491-506.
[16] T.Y. Tsong, Kinetics of the crystalline-liquid crystalline phase transition of dimyristoyl L-alpha-lecithin bilayers. Proc. Natl. Acad. Sci. U. S. A. 71(7) (1974) 2684-2688.
[17] T.M. Allen, C. Hansen, F. Martin, C. Redemann, A. Yauyoung, Liposomes Containing Synthetic Lipid Derivatives of Poly(Ethylene Glycol) Show Prolonged Circulation Half-Lives Invivo. Biochimica Et Biophysica Acta 1066(1) (1991) 29-36.
[18] D. Papahadjopoulos, T.M. Allen, A. Gabizon, E. Mayhew, K. Matthay, S.K. Huang, K.D. Lee, M.C. Woodle, D.D. Lasic, C. Redemann, F.J. Martin, Sterically Stabilized Liposomes - Improvements in Pharmacokinetics and Antitumor Therapeutic Efficacy. Proc. Natl. Acad. Sci. U. S. A. 88(24) (1991) 11460-11464.
[19] A.R. Nicholas, M.J. Scott, N.I. Kennedy, M.N. Jones, Effect of grafted polyethylene glycol (PEG) on the size, encapsulation efficiency and permeability of vesicles. Biochim. Biophys. Acta-Biomembr. 1463(1) (2000) 167-178.
[20] A.K. Kenworthy, K. Hristova, D. Needham, T.J. McIntosh, Range and Magnitude of the Steric Pressure between Bilayers Containing Phospholipids with Covalently Attached Poly(Ethylene Glycol). Biophys. J. 68(5) (1995) 1921-1936.
[21] P.G. deGennes, Polymers at an interface: a simplified view. Adv. Colloid Interface Sci. 27 (1987) 189-209.
[22] A.K. Kenworthy, S.A. Simon, T.J. McIntosh, Structure and Phase-Behavior of Lipid Suspensions Containing Phospholipids with Covalently Attached Poly(Ethylene Glycol). Biophys. J. 68(5) (1995) 1903-1920.
[23] H. Yoshioka, Surface Modification of Hemoglobin-Containing Liposomes with Polyethylene-Glycol Prevents Liposome Aggregation in Blood-Plasma. Biomaterials 12(9) (1991) 861-864.
[24] S. Belsito, R. Bartucci, L. Sportelli, Lipid chain length effect on the phase behaviour of PCs/PEG : 2000-PEs mixtures. A spin label electron spin resonance and spectrophotometric study. Biophys. Chem. 93(1) (2001) 11-22.
[25] K. Edwards, M. Johnsson, G. Karlsson, M. Silvander, Effect of polyethyleneglycol-phospholipids on aggregate structure in preparations of small unilamellar liposomes. Biophys. J. 73(1) (1997) 258-266.

[26] L.M. Ickenstein, M.C. Arfvidsson, D. Needham, L.D. Mayer, K. Edwards, Disc formation in cholesterol-free lippsornes during phase transition. Biochim. Biophys. Acta-Biomembr. 1614(2) (2003) 135-138.
[27] T.M. Allen, Long-Circulating (Sterically Stabilized) Liposomes for Targeted Drug-Delivery. Trends Pharmacol. Sci. 15(7) (1994) 215-220.

[28] M. Hossann, M. Wiggenhorn, A. Schwerdt, K. Wachholz, N. Teichert, H. Eibl, R.D. Issels, L.H. Lindner, In vitro stability and content release properties of phosphatidylglyceroglycerol containing thermosensitive liposomes. Biochim. Biophys. Acta-Biomembr. 1768(10) (2007) 2491-2499.
[29] D.D. Lasic, in: D. D. Lasic (Ed.), Liposomes from physics to applications, Elsevier Science, Amsterdam, 1993, pp. 63-107.
[30] G. Rouser, S. Fkeischer, A. Yamamoto, Two dimensional thin layer chromatographic separation of polar lipids and determination of phospholipids by phosphorus analysis of spots. Lipids 5(5) (1970) 494-496.
[31] S. Mabrey, J.M. Sturtevant, Investigation of phase transitions of lipids and lipid mixtures by high sensitivity differential scanning calorimetry. Proc. Natl. Acad. Sci. U. S. A. 73(11) (1976) 3862-3866.
[32] A.L.B. Seynhaeve, S. Hoving, D. Schipper, C.E. Vermeulen, G.A. de Wiel-Ambagtsheer, S.T. van Tiel, A.M.M. Eggermont, T.L.M. ten Hagen, Tumor necrosis factor alpha mediates homogeneous distribution of liposomes in murine melanoma that contributes to a better tumor response. Cancer Res. 67(19) (2007) 9455-9462.
[33] H.D. Papenfuss, J.F. Gross, M. Intaglietta, F.A. Treese, A transparent access chamber for the rat dorsal skin fold. Microvasc. Res. 18(3) (1979) 311-318.
[34] D. Needham, G. Anyarambhatla, G. Kong, M.W. Dewhirst, A new temperature-sensitive liposome for use with mild hyperthermia: Characterization and testing in a human tumor xenograft model. Cancer Res. 60(5) (2000) 1197-1201.
[35] M.L. Hauck, S.M. Larue, W.P. Petros, J.M. Poulson, D.H. Yu, I. Spasojevic, A.F. Pruitt, A. Klein, B. Case, D.E. Thrall, D. Needham, M.W. Dewhirst, Phase I trial of doxorubicin-containing low temperature sensitive liposomes in spontaneous canine tumors. Clinical Cancer Research 12(13) (2006) 4004-4010.
[36] A.N. Nikolova, M.N. Jones, Phospholipid free thin liquid films with grafted poly(ethylene glycol)-2000: formation, interaction forces and phase states. Biochim. Biophys. Acta-Biomembr. 1372(2) (1998) 237-243.
[37] M.H. Gaber, K.L. Hong, S.K. Huang, D. Papahadjopoulos, Thermosensitive Sterically Stabilized Liposomes - Formulation and in-Vitro Studies on Mechanism of Doxorubicin Release by Bovine Serum and Human Plasma. Pharmaceutical Research 12(10) (1995) 1407-1416.
[38] G. Kong, R.D. Braun, M.W. Dewhirst, Hyperthermia enables tumor-specific nanoparticle delivery: Effect of particle size. Cancer Res. 60(16) (2000) 4440-4445.
[39] L.H. Lindner, M.E. Eichhorn, H. Eibl, N. Teichert, M. Schmitt-Sody,

Chapter 3

Improved intratumoral nanoparticle extravasation and penetration by mild hyperthermia

Li Li, Timo L.M. ten Hagen, Michiel Bolkestein, Astrid Gasselhuber, Jeremy Yatvin, Gerard C. van Rhoon, Alexander M.M. Eggermont, Dieter Haemmerich, Gerben A. Koning

DOI: 10.1016/j.jconrel.2013.01.026.

Abstract

Accumulation of nanoparticles in solid tumors depends on their extravasation. However, vascular permeability is very heterogeneous within a tumor and among different tumor types, hampering efficient delivery. Local hyperthermia at a tumor can improve nanoparticle delivery by increasing tumor vasculature permeability, perfusion and interstitial fluid flow. The aim of this study is to investigate hyperthermia conditions required to improve tumor vasculature permeability, subsequent liposome extravasation and interstitial penetration in 4 tumor models. Tumors are implanted in dorsal skin flap window chambers and observed for liposome (~85 nm) accumulation by intravital confocal microscopy. Local hyperthermia at 41°C for 30 minutes initiates liposome extravasation through permeable tumor vasculature in all 4 tumor models. A further increase in nanoparticle extravasation occurs while continuing heating to 1 hour, which is a clinically relevant duration. After hyperthermia, tumor vasculature remains permeable for 8 hours. We visualize gaps in the endothelial lining of up to 10 μm induced by HT. Liposomes extravasate through these gaps and penetrate into the interstitial space to at least 27.5 μm in radius from vessel walls. Whole body optical imaging confirms HT induced extravasation while liposome extravasation was absent at normothermia. In conclusion, thermal dose of 41°C for 1 hour is effective to induce long-lasting permeable tumor vasculature for liposome extravasation and interstitial penetration. These findings hold promise for improved intratumoral drug delivery upon application of local mild hyperthermia prior to administration of nanoparticle-based drug delivery systems.

Keywords:

Liposome extravasation, mild hyperthermia, hyperpermeable tumorvasculature, nanoparticle drug delivery, intravital confocal microscopy, whole body optical imaging.

1. Introduction

Conventional chemotherapy relies on systemic delivery of cytotoxic drugs. However, intratumoral drug concentration is low, while toxicity to healthy tissues is dose-limiting. Tumor vasculature manipulation provides a mode to improve anticancer drug delivery [1-3].

Nanoparticle-based chemotherapeutic drug delivery reduces systemic toxicity of the encapsulated drug, improves drug retention in circulation, and increases intratumoral drug concentration [4-8]. The drug delivery mechanism involves nanoparticle extravasation through permeable tumor vasculature and deposition of drugs into the interstitial space in tumors [9-10]. However, due to nanoparticle size, limited interstitial fluid flow and the compact nature of the interstitial matrix in tumors, nanoparticle penetration in the extravascular extracellular space (EES) is limited [11-12]. Only a fraction of the tumor vessels are permeable inflicting a poor and rather heterogeneous delivery of nanoparticles [13, 10]. Both heterogeneous extravasation and limited intratumoral nanoparticle penetration leave room for further improvement of nanoparticle-based drug delivery.

Normalization of tumor vasculature does not improve liposomal drug delivery, while abnormalization using TNF-α strongly improved liposome-based drug delivery [14-16]. Mild hyperthermia (HT) may function as a physical alternative to increase tumor vasculature permeability. Mild HT is used in combination with chemotherapy or radiotherapy [17-18]. The first randomized phase III clinical trial proving that regional hyperthermia increased the benefit of chemotherapy in high grade soft-tissue sarcoma has been reported by Issels' group [19]. Regarding improved delivery of nanoparticles, the HT-induced hyperpermeability of tumor vasculature can increase nanoparticle extravasation [20-22]. Kong et al. pioneered the use of mild HT on nanoparticle extravasation [21-22]. Local mild HT increased the pore size in tumor vasculature, decreased steric and hydrodynamic hindrances, therefore elevating the intratumoral interstitial fluid flow and pressure to facilitate extravascular nanoparticle (~125 nm in diameter) penetration [23]. Additionally, vasculature endurance towards heat is lower in tumor tissues compared to normal tissues, rendering increased specificity of nanoparticle delivery in tumors [24].

We investigated the HT conditions required to improve the intratumoral delivery of liposomes as the first step towards improved drug delivery. We also made use of optimized thermosensitive liposomes (TSL), which enable a triggered drug release upon mild HT [25]. The ultimate purpose is to apply thermosensitive liposomes in combination with mild HT in a two-step manner (see diagram). HT to induce liposome extravasation will be applied as the first step. We show that the observed enhanced permeability and retention

(EPR) of liposomes upon HT benefits drug delivery, but it has to be taken into account that entrapment of the drug in, and release from the liposomes are crucial steps, which co-determine final accumulation of the active compound at the target site. The second HT step is to force release of the encapsulated drug, making it bioavailable.

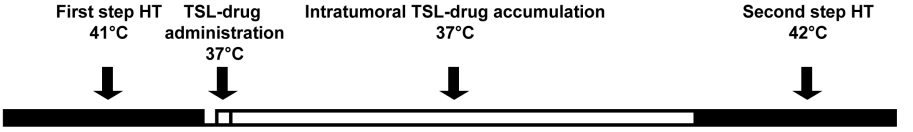

Diagram. Schedule of mild HT in a two-step manner.

2. Materials and methods

2.1. Lipids and chemical reagents

The phospholipids 1,2-dipalmityol-*sn*-glycero-3-phosphocholine (DPPC), 1,2-distearoyl-*sn*-glycero-3-phosphocholine (DSPC), 1,2-distearoyl-*sn*-glycero-3-phosphoethanolamine-*N*-PEG_{2000} (DSPE-PEG_{2000}) were from Lipoid GmbH (Ludwigshafen, Germany). 3-(2-pyridyl)-dithiopropionyl-PEG-DSPE (PDP-PEG-DSPE) and 1,2-dioleoyl-*sn*-glycero-3-phosphoethanolamine-N-(lissamine rhodamine B sulfonyl) (Rho-PE) were purchased from Avanti Polar Lipid Inc. IRDye 800CW Maleimide infrared dye was from LI-COR Biosciences. Dulbecco's modified eagle media (DMEM media) and fetal calf serum (FCS) were obtained from Sigma Aldrich (Netherlands) unless otherwise specified.

2.2. Liposomes

Liposomes were composed of DPPC/DSPC/DSPE-PEG_{2000} in a molar ratio of 80:15:5 [25]. Liposomes were labeled with 0.1 mol% Rho-PE in the lipid membrane [25]. For the optical imaging study of liposome localization in s.c. tumors in mice, liposomes were prepared with 1% PDP-PEG-DSPE to conjugate the IRDye 800CW Maleimide (molar ratio of 1:0.5). Size and polydispersity index (PDI) of samples at 10 – 50 μM [lipid] were determined by dynamic light scattering using a Zetasizer Nano ZS (Malvern Instruments, Worcestershire, UK). Lipid concentration was measured by phosphate assay [26]. Liposome stock of 40 mM [lipid] at size of ~85 nm in diameter with PDI < 0.1 were used for all experiments.

2.3. In vivo tumor models and animal models

Murine B16 melanoma, BFS-1 sarcoma, Lewis Lung Carcinoma (LLC) and human BLM melanoma cells were cultured (Greiner Bio-One, the Netherlands) in DMEM medium (Lonza, Belgium) containing 10% (v/v) FCS, and incubated

at 37°C in a humidified environment of 95% air and 5% CO_2. C57BL/6 mice were used for murine B16 melanoma, BFS-1 sarcoma, and LLC carcinoma models. NMRI *nu/nu* mice were used for human BLM melanoma model. All mice were purchased from Charles River and housed at 20-22°C, humidity of 50-60%, and 12 hour light-dark cycles. Sterile rodent food and acidified vitamin C-fortified water were given *ad libitum*. Eight-week old mice at weight of 20-25 g were used. C57BL/6 mice with constitutive vascular endothelial cell expression of an eNOS-Tag-GFP (green fluorescent protein) fusion protein were developed by Dr. R. de Crom and R. van Haperen, Department of Cell Biology, Erasmus MC, Rotterdam, the Netherlands, bred in-house. All animal studies were done in accordance to protocols approved by the committee on Animal Research of Erasmus MC, Rotterdam, the Netherlands. General methods to prepare a dorsal skin flap window chamber model is to inject tumor cells (10^6) subcutaneously in flanks of mice, and bulk tumors of 1 cm in diameter are used for transplantation. A small viable tumor piece (~1 mm^3) is removed from the bulk tumor and transplanted in the fascia of a dorsal skin flap placed in a window chamber in mice [25]. After tumor transplantation, mice carrying window chambers are housed individually at 30°C and 60% humidity. For whole body optical imaging, a tumor piece (~3 mm^3) of human BLM melanoma was transplanted subcutaneously in the hind leg of NMRI *nu/nu* mice. Mice were used for experiments, when tumors reached ~5 mm in diameter in dorsal skin flap window chamber models and ~7 mm in diameter in s.c. models.

2.4. Intravital confocal microscopy

2.4.1. General experimental setup

In vivo liposome extravasation was studied by intravital fluorescence microscopy. Models were used in two weeks when tumor size reached ~5 mm in diameter. Mice were anesthetized with isofluorane (Nicholas Piramal, London, UK) and placed on a thermal mattress at 37°C during experiments. An external circular resistive heating coil was attached to the glass at the back side of the window chamber to provide homogenous local HT [25]. Thermocouples (point-welded thin manganese and constantan wires, Thessco®, Amsterdam) were imbedded in window chambers to monitor tissue temperature online. Liposomes at a dose of 6 μmol lipid labeled with fluorescent Rho-PE were injected intravenously through the tail vein. Liposomes were given prior to HT, except when duration of tumor vessel permeability after HT was determined (see session 2.4.5.). Regions of interest were selected by confocal microscopy (Zeiss LSM 510 META). Background images were captured before liposome administration. Amplifier offsets for both GFP and Rho-PE were adjusted to intensity 0 when the lasers were off for initial image calibration. Imaging was started within 20 minutes post-administration. Liposome extravasation was monitored online by a Helium-

Neon laser (543 nm), and constitutive GFP-expressing endothelial cells were visualized by an argon laser (488 nm). Fluorescent channels (BP 505-550 LP 585, Plan-Neofluar 10x/0.3 lens) were recorded in 40 μm thin single images and 120 μm thick Z-stack before and after HT. Intermittent images were taken every 5 minutes during heating, HT at 41°C and resting after HT. Images with higher magnifications (Plan-Neofluar 20x/0.5 lens, with optical slice thickness of 6 μm) were taken at the end of the experiments to image discontinuous endothelial lining in permeable tumor vasculature. Images of 1024x1024 pixels were analyzed with LSM image software (Zeiss, Germany). All images are presented at their original quality without any modification. The images on *in vivo* liposome extravasation kinetics were converted to videos by Image J (Wayne Rasband, National Institutes of Health, USA).

2.4.2. Determine optimal thermal dose

Pre-selection of an optimal thermal dose was performed in murine B16 melanoma, BFS-1 sarcoma and LLC carcinoma in C57BL/6 mice. Window chamber tissues were heated up to 41°C in 10 minutes and remained for 30 minutes (3.75 CEM43 (Cumulative Equivalent Minutes at 43°C)) or 1 hour (7.5 CEM43), followed by resting without HT (temperature decreased down to 30°C in ~15 minutes). Liposome extravasation through tumor vasculature was quantified and compared between thermal dose of 41°C for 30 minutes and 41°C for 1 hour. Thermal dose which induced more liposome extravasation was selected for the following experiments.

2.4.3. A pilot-study on delta T (temperature) on intratumoral liposome accumulation

Tumors in dorsal skin flap window chamber models in mice have a baseline temperature of ~30°C, while s.c. tumors in mice mostly have a physiological temperature of 37°C. In order to evaluate whether an absolute temperature or temperature elevation from baseline causes vasculature hyperpermeability, we determined permeability at 37°C which would be an increase of 7°C over the baseline (~30°C).

2.4.4. Compare liposome extravasation in different tumors

Murine B16 melanoma, BFS-1 sarcoma and LLC carcinoma in C57BL/6 mice, and human BLM melanoma in NMRI *nu/nu* mice, were selected to measure liposome intensity and penetration depth during defined time courses at thermal dose of 41°C for 1 hour. Seven to 12 locations within a tumor were recorded throughout the experiments to compare liposome extravasation levels.

2.4.5. Determine the duration of liposome-permeable vessels after HT

Liposome administration was performed at pre HT, or 4, 8, 24 hours post-HT in murine B16 melanoma to study the duration of permeable tumor vessels after a thermal dose of 41°C for 1 hour.

2.5. In vivo whole body optical imaging of liposome localization in s.c. tumors

In order to find out the correlation between liposome extravasation and systemic clearance, we followed intratumoral liposome accumulation over time in s.c. tumors under whole body imaging. Mice were transplanted with s.c. human BLM melanoma in their right hind leg. Mice were anesthetized, and the tumor bearing hind legs were covered in aquasonic ultrasound gel (Parker Laboratories, Inc.) to ensure efficient heat transfer to the tumor surface, surrounding tissues and muscles were protected by a syringe. The hind legs were maintained inside of the syringes and fixed onto a rack to ensure a steady position in a water-bath during the HT treatment. Tumor temperature was monitored by a thermocouple probe, which was placed on the tumor and attached to an electrical thermometer. The tumor temperature was maintained at 41°C for 1 hour (it took ~10 minutes to increase the tumor temperature to 41°C). After HT, mice rested at room temperature (25°C) for 10 minutes, after which 1 μmol of IRDye 800CW Maleimide-TSL was injected through a tail vein. Mice were anesthetized before imaging with the IVIS Spectrum (threshold set at min. $1.5x10^7$ and max. $4x10^8$ radiant efficiency) (Caliper Life Sciences, Perkin Elmer) at 0, 1, 2, 4, 24 and 48 hours post-injection. Background images were taken pre-HT and pre-injection. The fluorescence images were retrieved (Ex. 500 nm (background) and 745 nm and Em. 800 nm) and analyzed using Living Image 4.2 software (Caliper Life Sciences). To determine the tumor-to-background ratio (TBR), the tumor was set as a region of interest and compared to an equal size region of interest placed on an area with background values within the mouse.

2.6. Quantitative image analysis

In vivo liposome extravasation through tumor vasculature upon local mild HT was quantified by image processing methods below in software Matlab, MeVisLab and ImageJ. Motion compensation was performed by geometrical transformation between images in each time series. Intravascular regions were identified from images taken immediately following injection of liposomes, and initial intravascular fluorescence liposome intensity was used for normalization of extravascular intensity. Change in normalized extravascular fluorescence over time was calculated to quantify extravasation. Vessel distance maps were then generated by Euclidean distance transfer, and average liposomal fluorescence intensity calculated depending on distance to closest vessel [13]. Due to the typical vessel distance in the range of < 100 μm, penetration analysis up to 55 μm (half-way between vessels) was

performed. Liposome penetration during HT was visualized by surface plots. Extravascular fluorescence liposome intensity was normalized via dividing by initial average intravascular intensity after administration of liposomes pre-HT. The total percentage of tumor vascular surface (in the field of view) which responded to the thermal dose of 41°C for 1 hour and became permeable after the HT was identified and calculated for each tumor type. When extravascular intensity adjacent to a vessel was same or above average intravascular intensity (mean over all intravascular regions), the tumor vascular surface was considered permeable.

Liposome extravasation post-HT at 4, 8, 24 hours was quantified by ImageJ. Real time intravascular liposome intensity was subtracted to obtain extravascular liposome intensity over time.

2.7. Statistics

The quantification of intravital confocal data are represented as mean ± standard error of the mean (SEM) of 3 mice per group. The quantification of whole body optical imaging and liposome accumulation in s.c. tumors are presented as mean ± standard deviation (SD) of 3 mice per group. Extravasated liposome intensity over time amongst four tumor models are analyzed by F-test and Kruskal-Wallis test, followed for pair wise comparison by Mann-Whitney test with Bonferroni correction (p-value ≤ 0.05). The total percentage of permeable tumor vascular surface after HT and liposome intensity over time after administration at 4, 8, 24 hours post-HT were analyzed for pair wise comparison by Mann-Whitney test (p-value ≤ 0.05).

3. Results

3.1. Increased liposome extravasation after HT at 41°C for 1 hour

In order to maximize the effect of local mild HT on extravascular liposome accumulation in tumors, we first compared different thermal doses on induction of liposome extravasation and penetration depth in the interstitial space. In clinical HT treatments, temperatures of 41 - 43°C are applied. In order to avoid permanent vascular damage by HT, we used 41°C for hyperthermic tumor tissue temperature. This local mild HT increased the permeability of tumor vasculature for extravasation of small liposomes (~85 nm) in time. Based on the images prior to injection of the liposomes, vessels were identified and a vascular map generated. The quantification analysis applying the vascular map revealed time point and extend of liposome extravasation. (Fig. 1, indicated with arrow heads). Murine BFS-1 sarcoma and LLC carcinoma required 20 minutes, murine B16 melanoma and human BLM melanoma required 30 minutes exposure at 41°C to initiate liposome extravasation (Supplemental Fig. 1). Liposome intensity increased in the EES over time up

to 1 hour at 41°C in all tumor models (Supplemental Fig. 1 and Supplemental Video S1). As a control, we used normothermia (NT) (no external heating) and observed no liposome extravasation during 4-hour period (data not shown). As an additional control, we heated the dorsal skin tissues from its normal temperature which lies around 30°C in anesthetized mice to core body temperature 37°C. Obvious liposome extravasation occurred in murine LLC carcinoma, when the window chamber tissue was heated to 37°C for 1 hour (Supplemental Fig. 2).

After identifying the initiation of liposome extravasation, we compared the effect of thermal doses 41°C for 30 minutes and 41°C for 1 hour on liposome penetration depth and liposome intensity in the EES in all 4 tumor models. Longer exposure to mild HT caused more liposome extravasation and accumulation in the EES of murine B16 melanoma (30 minutes HT at 41°C + 1 hour post-HT resting without HT vs. 1 hour HT at 41°C + 30 minutes post-HT resting without HT) (Supplemental Fig. 3). Quantification demonstrated murine B16 melanoma had significantly higher extravascular liposome intensity after the thermal dose escalation (Mann-Whitney test, p-value < 0.05) (Supplemental Fig. 3 b). Yet both thermal doses increased liposome extravasation compared to NT. In general, local mild HT at 41°C for 1 hour offered sufficient extravascular liposomal accumulation, thus was employed for further experiments.

3.2. Liposome extravasation and penetration depend on tumor type

Tumor vasculature in all 4 tumor models responded strongly to mild HT at 41°C for liposome extravasation and subsequent interstitial penetration (Fig. 1). Tumor vasculature remained functional during and after HT throughout the experiments (observed at bright field). Without mild HT, liposomes remained within the tumor vasculature, and no liposome extravasation was recorded in any of the selected locations up to 2 hours post-injection (Fig. 1 a). Similarly, liposome extravasation was negligible in normal vasculature after thermal dose of 41°C for 1 hour (Supplemental Fig. 4). Liposome extravasation in murine LLC carcinoma was significantly higher compared to murine B16 melanoma, murine BFS-1 sarcoma and human BLM melanoma (F-test < 0.001, Kruskal-Wallis test p-value ≤ 0.05) (Fig. 1 b). Liposome extravasation in murine B16 melanoma was also significantly higher compared to murine BFS-1 sarcoma and human BLM melanoma (F-test < 0.001, Kruskal-Wallis test p-value ≤ 0.05) (Fig. 1 b). Among all selected locations throughout the tumors, mild HT at 41°C for 1 hour induced more than 50% of permeable tumor vascular surface in murine B16 melanoma and LLC carcinoma (Fig. 2 a). Although murine BFS-1 sarcoma and human BLM melanoma tumor vessels responded less to the same thermal dose, the permeable tumor vascular surface in murine BFS-1 sarcoma and human BLM melanoma still reached more than 25%, which represents a more than 50-fold increase compared to human BLM melanoma without HT

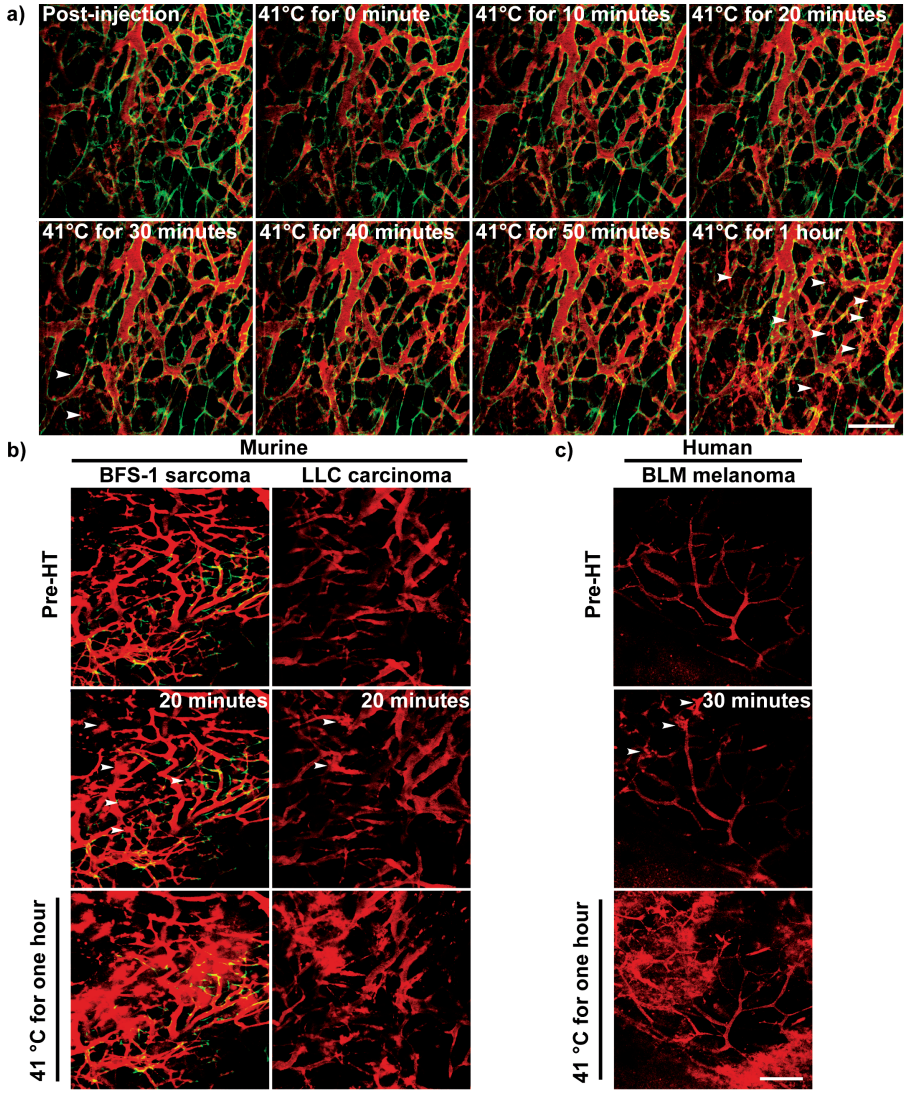

Supplemental Fig. 1. a) Liposome (red) extravasation through tumor vasculature (green) in murine B16 melanoma. Initial liposome extravasation occurred at 41°C for 30 minutes, with additional liposome extravasation at 41°C for 1 hour. b) Initiation of liposome extravasation in murine LLC carcinoma, BFS-1 sarcoma and c) human BLM melanoma during mild HT. White arrows indicate permeable tumor vasculature regions. Bar, 200 μm.

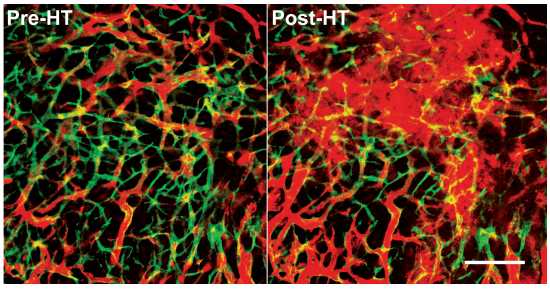

Supplemental Fig. 2. Liposome (red) extravasation through murine LLC carcinoma tumor vessels (green) after 37°C for 1 hour. Bar, 200 μm.

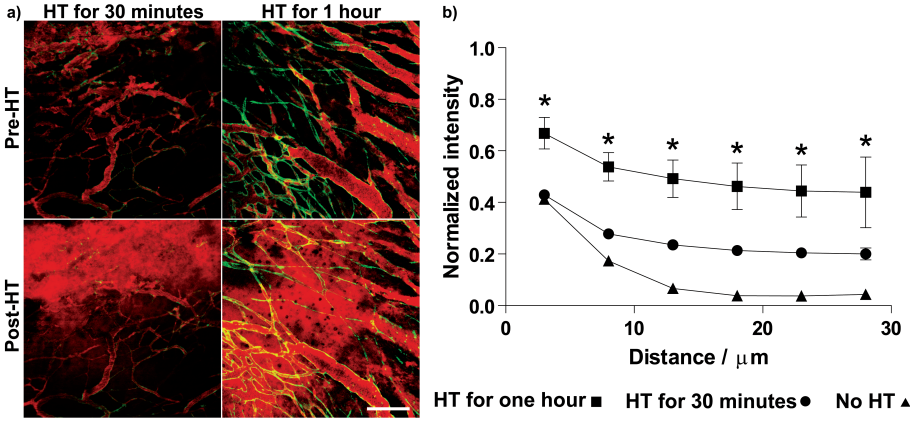

Supplemental Fig. 3. a) Thermal dose compare of 41°C for 30 minutes vs. 41°C for 1 hour on liposome (red) extravasation through murine B16 melanoma tumor vasculature (green). b) Comparison of extravascular liposome intensity and distance from vessels after mild HT at 41°C for 30 minutes (●) and 1 hour (■) in murine B16 melanoma (mean ± SEM, n=3). Murine B16 melanoma without HT (tissue temperature was at 30°C) (▲) is indicated in b) as controls. Bar, 200 μm. *Mann-Whitney test, *p*-value < 0.05.

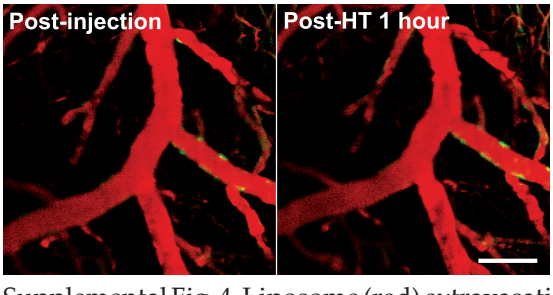

Supplemental Fig. 4. Liposome (red) extravasation through normal vasculature (green) before and after mild HT at 41°C for 1 hour. Bar, 200 μm.

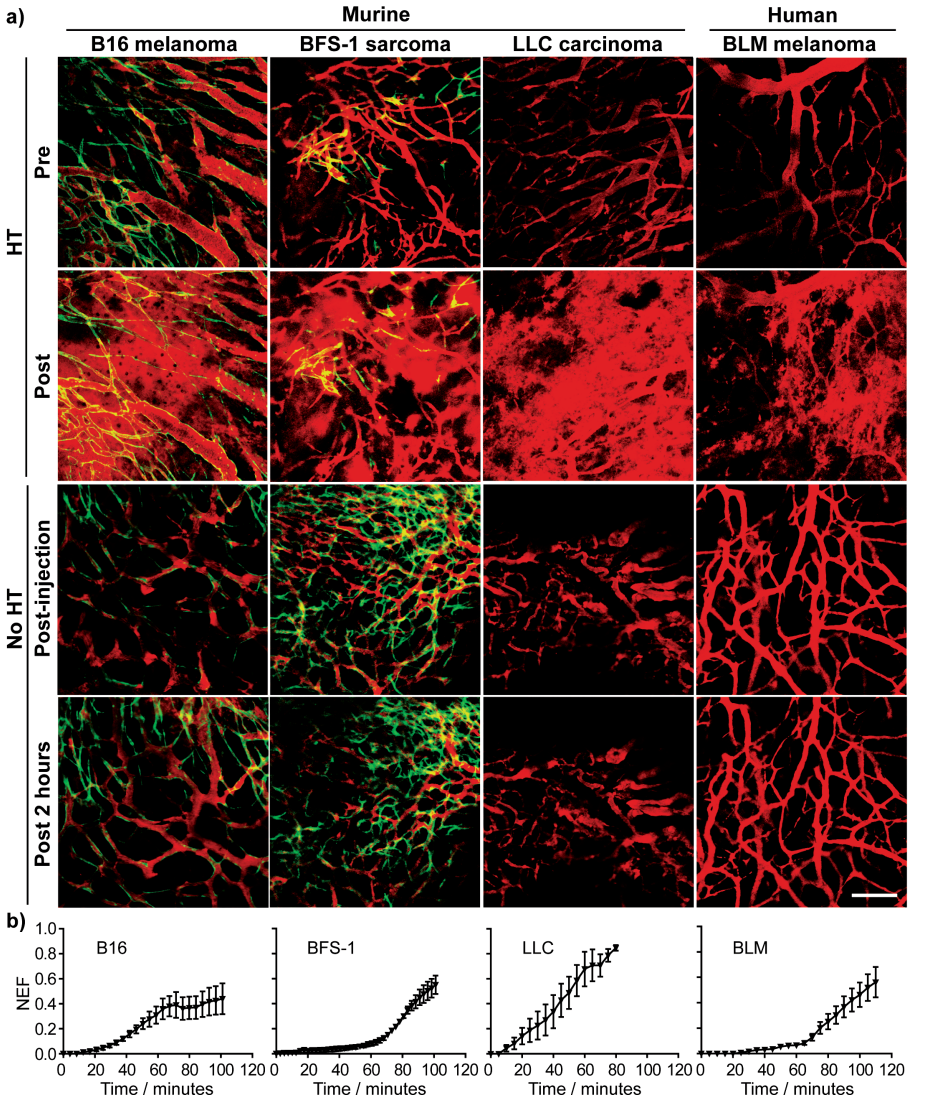

Fig. 1. a) Liposome (red) extravasation through tumor vasculature (green) with or without mild HT for 1 hour. b) Quantification of liposome extravasation through tumor vasculature in 4 tumor models under local mild HT at 41°C for 1 hour. NEF, normalized extravascular fluorescence. Bar, 200 μm.

(Fig. 2 a). In all HT treated tumors, extravascular liposome intensity increased significantly over time in not only the perivascular regions, but also deeper in the EES (up to at least 27.5 μm from the vessels), and was most pronounced in murine B16 melanoma and LLC carcinoma (Fig. 2 b). Over 1 hour at 41°C, extravascular liposome intensity in murine B16 melanoma and LLC

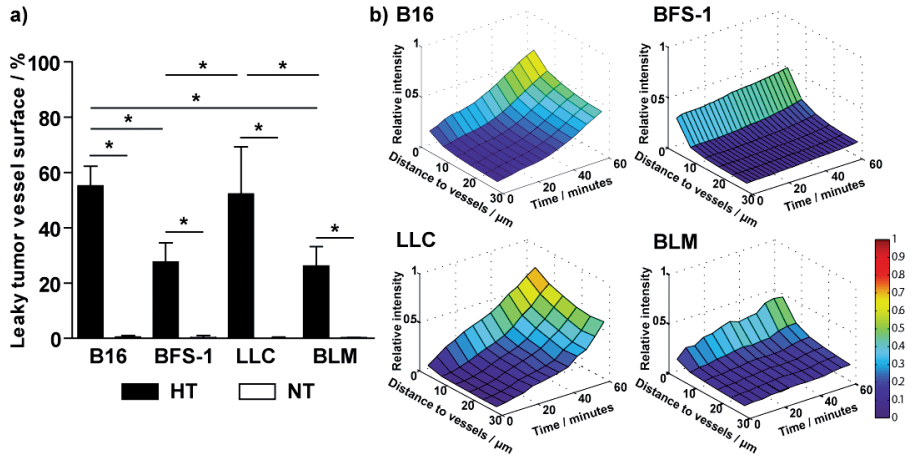

Fig. 2. a) Leaky tumor vessel surface% post-HT or post-NT is demonstrated as mean ± SEM (n=3). b) Surface plots of extravascular liposome intensity in 4 tumor models during HT at 41°C for 1 hour. *Mann-Whitney test, *p*-value ≤0.05. Initial liposome intensities at t = 0 min have values greater than 0 is an artifact.

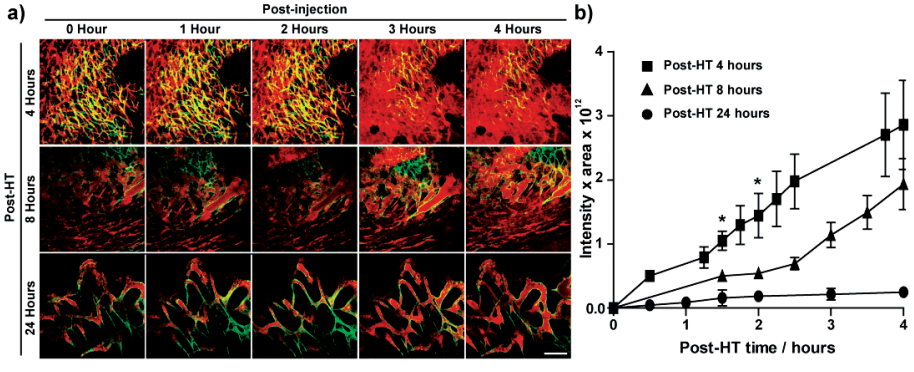

Fig. 3. a) Preservation of liposome (red) extravasation through murine B16 melanoma tumor vasculature (green) after HT at 41°C for 1 hour. Liposome administration was performed in different mice at pre-HT, or 4, 8, 24 hour post-HT. Bar, 200 µm. b) Liposome intensity post-injection at 4, 8, 24 hours post-HT for a duration of 4 hours in circulation. ■ Post-HT 4 hours, ▲Post-HT 8 hours, ● Post-HT 24 hours. *Mann-Whitney test, *p*-value ≤ 0.05.

carcinoma increased in all regions up to 27.5 µm away from the vessels, while extravascular liposome intensity in murine BFS-1 sarcoma and human BLM melanoma was mostly perivascular and dropped more strongly with increasing distance from the vasculature, with little liposome intensity at a distance further than 10 µm away from the vessels (Fig. 2 b).

3.3. Liposome permeable vessels remained for 8 hours

The duration of the tumor vasculature permeability after local mild HT at 41°C for 1 hour was studied. It was observed that once tumor vasculature responded to mild HT, liposome extravasation continued post-HT. Tumor vasculature permeability was preserved for liposome extravasation up to 8 hours post-HT, but to a lesser extent (Fig. 3). No permeable tumor vessels were observed at 24 hours post-HT and liposomes remained confined to the tumor vasculature during the subsequent 4 hours of imaging (Fig. 3). Level of extravasated liposomes differed significantly at time points 1.5 and 2 hours post-injection (Mann-Whitney test, p-value ≤ 0.05) (Fig. 3 b).

3.4. Heterogeneous tumor vasculature permeability

The intensity of extravasated liposomes was heterogeneous within the tumor and also between different tumor models (Fig. 4 a). Three dimensional reconstructions of liposome extravasation in tumor over time demonstrated that extravasation started from focal points in the vasculature and was followed by a more general extravasation and distribution in these areas (Supplemental Video S2). Similar heterogeneity of tumor vasculature permeability was also observed in murine LLC carcinoma, BFS-1 sarcoma, and human BLM melanoma (data not shown).

Before HT, tumor endothelial cells appeared as a virtually closed vascular lining (Fig. 6 b, left panel Pre-HT). Mild HT at 41°C for 1 hour caused discontinuance of tumor endothelial lining, which formed pronounced gaps with sizes up to 10 μm between endothelial cells (Fig. 4 b middle and right panel, white arrow). Liposomes escaped from circulation through these gaps between the endothelial cells (Fig. 4 b, and Supplemental Video S3). We also observed similar gaps (10 μm) in murine LLC carcinoma models (data not shown). Blood circulation at the region of interest was observed, proving that these tumor vessels remained functional after mild HT at 41°C for 1 hour, yet allowed extravasation of liposomes.

3.5. HT increased liposome accumulation in s.c. tumors

Intratumoral liposome accumulation was visible in mice at 1 hour post-HT and increased to a maximum at 4 hours post-HT (Fig. 5). Beyond 4-hour post-HT, absolute tumor fluorescence did not further increase, but the TBR kept increasing (Fig. 5 b), due to clearance of liposomes from the body in combination with prolonged retention in the tumor. Accumulation of liposomes in liver and spleen was visualized by in vivo imaging of mice in dorsal position (data not shown). Mice without local HT showed no visible intratumoral accumulation of liposomes.

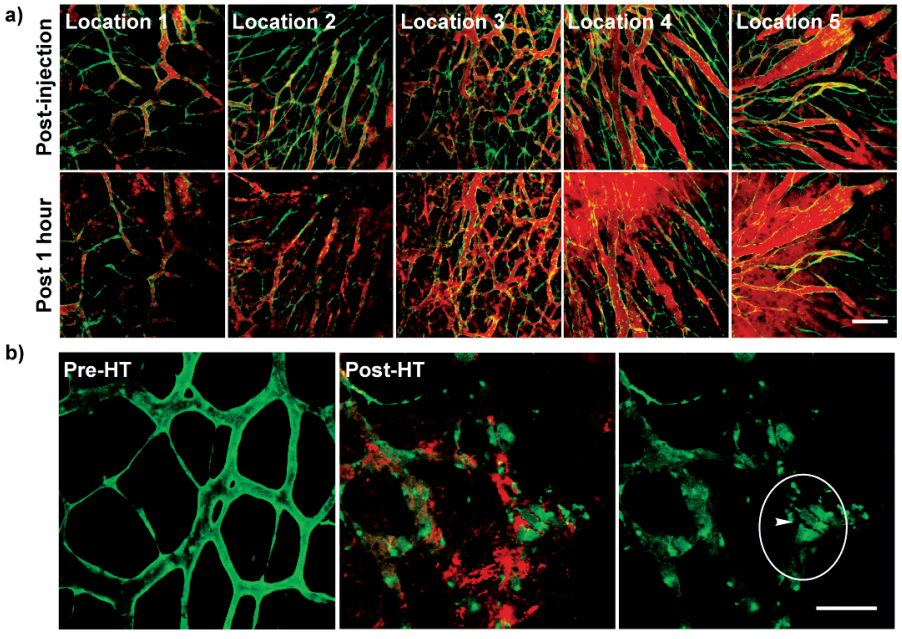

Fig. 4. a) Post-HT liposome penetration in the interstitial space at five different locations of one tumor. b) gaps between endothelial cells (green) post-HT for liposome (red) extravasation, in comparison to tumor vessels pre-HT. Bar in a), 200 μm. Bar in b), 100 μm.

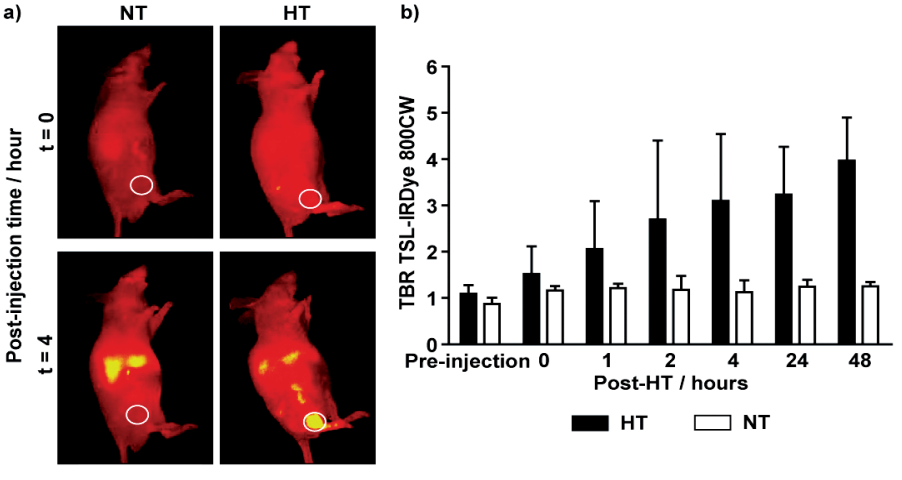

Fig. 5. a) *In vivo* whole body optical imaging of liposome accumulation in s.c. human BLM melanoma in mice, images at 0 and 4 hours post-injection with and without local HT at 41°C for 1 hour. b) Liposome accumulation tumor-to-background ratios (TBR) over time with and without local HT (mean ± SD) (n=3 for HT group, n=2 for NT group).

4. Discussion

We studied the effect of a clinical thermal dose (41°C for 1 hour) on liposome extravasation, and compared this among 4 tumor models. This thermal dose is effective to induce permeable tumor vasculature in murine B16 melanoma, BFS-1 sarcoma, LLC carcinoma and human BLM melanoma (Fig. 1). Murine B16 melanoma and human BLM melanoma can be considered orthotopically implanted in our dorsal skin fold window chamber models. The overwhelming extravascular accumulation of liposomes implies that local mild HT induced sufficient permeable tumor vasculature for liposome extravasation. We did not observe liposome accumulation in tumors under NT, nor was extravasation observed under HT in non-pathological tissues (Fig. 1 a, and Supplemental Fig. 4). These results are indicative for a tumor vasculature specific effect of HT.

We observed deep liposome penetration throughout the tumors, rather than perivascular accumulation, by intravital confocal microscopy (Fig. 2 b). Local mild HT (39 – 45°C) mediated liposome extravasation has been studied previously [21, 27, 22]. Primarily perivascular liposome accumulation was observed in human SKOV-3 ovarian carcinoma [21]. Dreher et al. reported that increasing molecular weight reduced particle extravasation and resulted in perivascular accumulation [28]. We suspect that the differences in thermal doses applied may be a cause of variation in the penetration depth. By studying these phenomena in several different tumor models, we were able to demonstrate that the fraction of heat-responsive tumor vascular surface, liposome extravasation depth and intensity in the interstitial space also greatly vary among different tumors (Fig. 2). For instance, liposome intensity in the EES in murine LLC carcinoma increased in all regions over 1 hour; while in murine BFS-1 sarcoma tumor intensity mainly increased in the perivascular region (~15 μm away from the vessels) (Fig. 2 b). We speculate that the interstitial fluid flow and/or matrix density is significantly different in these tumors. Under HT, intratumoral liposome extravasation and accumulation patterns are heterogeneous [29]. The permeability of a specific tumor vessel does not only depend on perfusion of the vessel, but also on intrinsic profile of the endothelial lining and the surrounding microenvironment [30]. This may also explain the differences between a permeable part of a tumor vessel and a non-permeable part of the same tumor vessel. Liu et al. showed increased liposome extravasation in the tumor periphery compared to the tumor center in murine 4T1 carcinoma [29]. We further demonstrated that the heterogeneity of tumor vasculature permeability can be pinpointed to any vessel regardless of its location in the tumor periphery or center (Supplemental Video 2). We extensively quantified liposome extravasation and penetration from tumor vessels in 3D, which allowed us to demonstrate for the first time, the fraction of tumor vasculature that responds to a clinically relevant thermal dose, to become permeable for intratumoral liposome accumulation. Tumor

vasculature is compact in the microenvironment, especially in the periphery of a tumor, where an advanced functional vascular network is often seen and the spacing between functional vessels can be limited [31]. In conclusion, we observed significant liposome penetration specifically in tumor tissue of up to 27.5 μm in the 4 tumor models upon HT, which is in contrast to Kong et al. who observed mainly perivascular liposome accumulation in a human ovarian carcinoma model. The differences observed amongst the tumor models suggest that the liposome extravasation and penetration processes are strongly dependent on tumor type and likely depend on structure of the interstitial matrix.

The gaps within the endothelial lining are an indication of the stress induced on the tumor vasculature by local mild HT. Due to the use of fluorescently labeled liposomes in a recombinant mouse model with constitutive GFP-expressing vasculature and high resolution confocal imaging, we were able to capture for the first time, endothelial gaps (up to 10 μm) with extravasating liposomes induced by mild HT, in tumor vessels that retained their functionality. In response to a thermal stress, vasculature within the tumor not only increased local blood flow and vasculature dilation, but also increases permeability. More crucially, tumor vasculature tends to lose fluid to the interstitial space, which profits intratumoral liposome penetration. The thermal dose of 41°C for 1 hour did not cause any permanent damage (i.e. hemorrhage) to the tumor vasculature, but temporarily altered the integrity of the endothelial network. It is likely that the heat stress induced loosening of the endothelial cells from the basement membrane [32-33].

A prior study demonstrated that local mild HT at 42°C for 1 hour increased the pore cutoff size of tumor microvasculature in human SKOV-3 ovarian carcinoma to > 400 nm, while no liposomes of any size (100, 200 or 400 nm in diameter) extravasated after 1 hour NT (34°C) [21]. We found that the threshold to initiate liposome (~85 nm) extravasation through permeable tumor vasculature in various tumor models was 41°C for 30 minutes, and that the longer HT exposure leads to increasingly larger volume of tumor tissue penetrated by liposomes (Supplemental Fig. 1 and 3). Importantly, the permeable tumor vasculature was preserved for at least 8 hours after HT, which allows continuous accumulation of long circulating liposomes after HT (Fig. 3). Our whole body imaging results indicated that HT treated tumors showed a significantly prolonged liposome retention up to 48 hours post-HT. Seynhaeve et al. demonstrated tumor vasculature abnormalization by tumor necrosis factor (TNF) α causing tumor vasculature permeability and augmented accumulation of liposomal drug (~100 nm) in murine B16 melanoma [15]. Comparably, our study illustrated mild HT induced hyperpermeability of tumor vasculature in all 4 tumor models, including deep penetration in murine B16 melanoma. To apply mild HT for improved liposomal drug delivery with success in patients, a better understanding

on the mechanism of vascular response is needed. In particular, the matters on differences between responding and non-responding tumor vasculature require further studies.

It's been reported by Gaber et al. that liposome extravasation at NT (34°C for 1 hour) is negligible, but becomes positive after HT (42 or 45°C for 1 hour) [9]. They observed no further liposome extravasation after 24 hours post-HT, which is in agreement with the tumor models we experimented in this study [9]. We observed remarkable vascular leakage up to 8 hours after mild HT, significantly longer than Kong et al. concluded that local mild HT 40 – 42°C was able to increase liposome (~100 nm) extravasation in human SKOV-3 ovarian carcinoma for 6 hours post-HT [22]. We detected that the window chamber tissue temperature was always around 30°C, as the tissue was held away from the body and the climate room was set to 30°C meaning that the tumor developed under this temperature. With regard to the definition of NT and HT, we explored the effect of local mild HT at 37°C, which is the physiological human body temperature, but actually represented an elevation of 7°C. To our surprise, thermal dose of 37°C for 1 hour also induced significant amount of liposome extravasation (Supplemental Fig. 2). Our results imply that the difference in temperature between NT under which the tumor developed and adapted to (here 30°C) and HT, is responsible for the induction of permeable tumor vessels. This finding suggests there is no absolute thermal dose for a positive liposome extravasation through permeable tumor vasculature. A relative temperature difference that can be reached in a specific tumor determines the potential intratumoral liposome accumulation. In relation to translational research, we urge that a well-defined temperature measuring and controlling system is critical for *in vivo* studies. Although this is seen in our dorsal skin flap window chamber model, further research needs to be conducted to proof the hypothesis.

5. Conclusion

We identified a minimum thermal dose to initiate liposome extravasation, compared tumor vasculature response towards different thermal doses in multiple tumor models and defined duration of permeable tumor vasculature. For the purpose of increasing anticancer therapeutic efficacy, we have optimized the first step in our liposomal chemotherapy approach. The findings from this study enable us to first maximize liposomal drug accumulation in tumors, after which a subsequent second heat treatment can trigger drug release and will deliver high concentrations of bioavailable cytotoxic compounds directly to tumors.

Acknowledgements

This work was funded by Stichting Vanderes, Stichting Fondsen, SEHK.

Supplemental Video S1.
Liposome extravasation through murine B16 melanoma tumor vasculature under mild HT at 41°C for 1 hour.

Supplemental Video S2.
Computer modeling of the heterogeneity of liposome extravasation through tumor vasculature under HT at 41°C for 1 hour.

Supplemental Video S3.
3-D rendering of endothelial gaps induced by mild HT at 41°C for 1 hour.

References:

[1] P. Carmeliet, R.K. Jain, Angiogenesis in cancer and other diseases, Nature, 407 (2000) 249-257.
[2] F. Brunstein, S. Hoving, A.L.B. Seynhaeve, S.T. van Tiel, G. Guetens, E.A. de Bruijn, A.M.M. Eggermont, T.L.M. ten Hagen, Synergistic antitumor activity of histamine plus melphalan in isolated limb perfusion: Preclinical studies, Journal of the National Cancer Institute, 96 (2004) 1603-1610.
[3] J. Fang, H. Nakamura, H. Maeda, The EPR effect: Unique features of tumor blood vessels for drug delivery, factors involved, and limitations and augmentation of the effect, Adv Drug Deliv Rev, 63 (2011) 136-151.
[4] K.J. Harrington, S. Mohammadtaghi, P.S. Uster, D. Glass, A.M. Peters, R.G. Vile, J.S. Stewart, Effective targeting of solid tumors in patients with locally advanced cancers by radiolabeled pegylated liposomes, Clin Cancer Res, 7 (2001) 243-254.
[5] A. Gabizon, H. Shmeeda, Y. Barenholz, Pharmacokinetics of pegylated liposomal Doxorubicin: review of animal and human studies, Clin Pharmacokinet, 42 (2003) 419-436.
[6] T.M. Allen, P.R. Cullis, Drug delivery systems: entering the mainstream, Science, 303 (2004) 1818-1822.
[7] M.E. O'Brien, N. Wigler, M. Inbar, R. Rosso, E. Grischke, A. Santoro, R. Catane, D.G. Kieback, P. Tomczak, S.P. Ackland, F. Orlandi, L. Mellars, L. Alland, C. Tendler, Reduced cardiotoxicity and comparable efficacy in a phase III trial of pegylated liposomal doxorubicin HCl (CAELYX/Doxil) versus conventional doxorubicin for first-line treatment of metastatic breast cancer, Ann Oncol, 15 (2004) 440-449.
[8] G.A. Koning, G.C. Krijger, Targeted multifunctional lipid-based nanocarriers for image-guided drug delivery, Anticancer Agents Med Chem, 7 (2007) 425-440.
[9] M.H. Gaber, N.Z. Wu, K. Hong, S.K. Huang, M.W. Dewhirst, D. Papahadjopoulos, Thermosensitive liposomes: extravasation and release of contents in tumor microvascular networks, Int J Radiat Oncol Biol Phys, 36 (1996) 1177-1187.
[10] R.K. Jain, T. Stylianopoulos, Delivering nanomedicine to solid tumors, Nature Reviews Clinical Oncology, 7 (2010) 653-664.
[11] F. Yuan, M. Leunig, S.K. Huang, D.A. Berk, D. Papahadjopoulos, R.K. Jain, Microvascular permeability and interstitial penetration of sterically stabilized (stealth) liposomes in a human tumor xenograft., Cancer Research, 54 (1994) 3352-3356.
[12] A. Chrastina, K.A. Massey, J.E. Schnitzer, Overcoming in vivo barriers to targeted nanodelivery, Wiley Interdisciplinary Reviews-Nanomedicine and Nanobiotechnology, 3 (2011) 421-437.
[13] H.F. Dvorak, L.F. Brown, M. Detmar, A.M. Dvorak, Vascular permeability factor/vascular endothelial growth factor, microvascular hyperpermeability, and angiogenesis., American Journal of Pathology, 146 (1995) 1029-1039.

[14] R.K. Jain, D.G. Duda, J.W. Clark, J.S. Loeffler, Lessons from phase III clinical trials on anti-VEGF therapy for cancer, Nature Clinical Practice Oncology, 3 (2006) 24-40.
[15] A.L.B. Seynhaeve, S. Hoving, D. Schipper, C.E. Vermeulen, G.A. de Wiel-Ambagtsheer, S.T. van Tiel, A.M.M. Eggermont, T.L.M. ten Hagen, Tumor necrosis factor alpha mediates homogeneous distribution of liposomes in murine melanoma that contributes to a better tumor response, Cancer Research, 67 (2007) 9455-9462.
[16] T.D. Tailor, G. Hanna, P.S. Yarmolenko, M.R. Dreher, A.S. Betof, A.B. Nixon, I. Spasojevic, M.W. Dewhirst, Effect of Pazopanib on Tumor Microenvironment and Liposome Delivery, Molecular Cancer Therapeutics, 9 (2010) 1798-1808.
[17] J. van der Zee, D.G. Gonzalez, G.C. van Rhoon, J.D.P. van Dijk, W.L.J. van Putten, A.A.M. Hart, G. Dutch Deep Hyperthermia, Comparison of radiotherapy alone with radiotherapy plus hyperthermia in locally advanced pelvic tumours: a prospective, randomised, multicentre trial, Lancet, 355 (2000) 1119-1125.
[18] P. Wust, B. Hildebrandt, G. Sreenivasa, B. Rau, J. Gellermann, H. Riess, R. Felix, P.M. Schlag, Hyperthermia in combined treatment of cancer, Lancet Oncol, 3 (2002) 487-497.
[19] R.D. Issels, L.H. Lindner, J. Verweij, P. Wust, P. Reichardt, B.C. Schem, S. Abdel-Rahman, S. Daugaard, C. Salat, C.M. Wendtner, Z. Vujaskovic, R. Wessalowski, K.W. Jauch, H.R. Durr, F. Ploner, A. Baur-Melnyk, U. Mansmann, W. Hiddemann, J.Y. Blay, P. Hohenberger, Neo-adjuvant chemotherapy alone or with regional hyperthermia for localised high-risk soft-tissue sarcoma: a randomised phase 3 multicentre study, Lancet Oncol, 11 (2010) 561-570.
[20] S.K. Huang, P.R. Stauffer, K.L. Hong, J.W.H. Guo, T.L. Phillips, A. Huang, D. Papahadjopoulos, Liposomes and hyperthermia in mice: increased tumor uptake and therapeutic efficacy of doxorubicin in sterically stabilized liposomes., Cancer Research, 54 (1994) 2186-2191.
[21] G. Kong, R.D. Braun, M.W. Dewhirst, Hyperthermia enables tumor-specific nanoparticle delivery: effect of particle size, Cancer Res, 60 (2000) 4440-4445.
[22] G. Kong, R.D. Braun, M.W. Dewhirst, Characterization of the effect of hyperthermia on nanoparticle extravasation from tumor vasculature, Cancer Res, 61 (2001) 3027-3032.
[23] V.P. Chauhan, T. Stylianopoulos, J.D. Martin, Z. Popovic, O. Chen, W.S. Kamoun, M.G. Bawendi, D. Fukumura, R.K. Jain, Normalization of tumour blood vessels improves the delivery of nanomedicines in a size-dependent manner, Nat Nanotechnol, 7 (2012) 383-388.
[24] C.W. Song, Effect of local hyperthermia on blood flow and microenvironment: a review, Cancer Res, 44 (1984) 4721s-4730s.
[25] L. Li, T.L. ten Hagen, D. Schipper, T.M. Wijnberg, G.C. van Rhoon, A.M. Eggermont, L.H. Lindner, G.A. Koning, Triggered content release from optimized stealth thermosensitive liposomes using mild hyperthermia, J Control Release, 143 (2010) 274-279.

[26] F.S. Rouser G, Yamamoto A., Two dimensional thin layer chromatographic separation of polar lipids and determination of phospholipids by phosphorus analysis of spots., Lipids, 5 (1970) 494-496.
[27] M.L. Matteucci, G. Anyarambhatla, G. Rosner, C. Azuma, P.E. Fisher, M.W. Dewhirst, D. Needham, D.E. Thrall, Hyperthermia increases accumulation of technetium-99m-labeled liposomes in feline sarcomas, Clin Cancer Res, 6 (2000) 3748-3755.
[28] M.R. Dreher, W.G. Liu, C.R. Michelich, M.W. Dewhirst, F. Yuan, A. Chilkoti, Tumor vascular permeability, accumulation, and penetration of macromolecular drug carriers, Journal of the National Cancer Institute, 98 (2006) 335-344.
[29] P. Liu, A. Zhang, Y. Xu, L.X. Xu, Study of non-uniform nanoparticle liposome extravasation in tumour, International Journal of Hyperthermia, 21 (2005) 259-270.
[30] A. Eberhard, S. Kahlert, V. Goede, B. Hemmerlein, K.H. Plate, H.G. Augustin, Heterogeneity of angiogenesis and blood vessel maturation in human tumors: implications for antiangiogenic tumor therapies, Cancer Res, 60 (2000) 1388-1393.
[31] D. Fukumura, R.K. Jain, Tumor microvasculature and microenvironment: targets for anti-angiogenesis and normalization, Microvasc Res, 74 (2007) 72-84.
[32] P. Baluk, S. Morikawa, A. Haskell, M. Mancuso, D.M. McDonald, Abnormalities of basement membrane on blood vessels and endothelial sprouts in tumors, American Journal of Pathology, 163 (2003) 1801-1815.
[33] K.D. Watson, C.Y. Lai, S. Qin, D.E. Kruse, Y.C. Lin, J.W. Seo, R.D. Cardiff, L.M. Mahakian, J. Beegle, E.S. Ingham, F.R. Curry, R.K. Reed, K.W. Ferrara, Ultrasound increases nanoparticle delivery by reducing intratumoral pressure and increasing transport in epithelial and epithelial-mesenchymal transition tumors, Cancer Res, 72 (2012) 1485-1493.

Chapter 4

Mild hyperthermia triggered doxorubicin release from optimized stealth thermosensitive liposomes improves intratumoral drug delivery and efficacy

Li Li, Timo L.M. ten Hagen, Martin Hossann, Regine Suss,
Gerard C. van Rhoon, Alexander M.M. Eggermont, Dieter Haemmerich,
Gerben A. Koning

Submitted.

Abstract

Liposome mediated anticancer drug delivery has the advantage of reducing cytotoxicity in healthy tissues. However, undesired slow drug release impedes the therapeutic efficacy of clinically applied PEG-liposomal doxorubicin (Dox). The aim of this study is to combine stealth thermosensitive liposomes (TSL) and local mild hyperthermia (HT) to increase bioavailable Dox levels in tumors. Dox was encapsulated in stealth TSL (~80 nm) with optimized PEG concentration in the membrane, and compared with lysolipid-based Dox-LTSL for *in vitro* stability, release kinetics, and *in vivo* tumor growth control. *In vitro* cytotoxicity of Dox-TSL against murine BFS-1 sarcoma, human BLM melanoma cell lines and Human Umbilical Vein Endothelial Cells (HUVEC) under normothermia (37°C) and HT (42°C) was compared with non-encapsulated Dox. *In vitro* Dox uptake in nuclei was imaged in BLM and HUVEC. *In vivo* intravascular Dox release from TSL in BFS-1 tumors under local mild HT in dorsal skin flap window chamber models was captured by intravital confocal microscopy. Intravascular Dox-TSL release kinetics, penetration depth and interstitial Dox density were subjected to quantitative image analysis. Systemic Dox-TSL administration in combination with local mild HT on subcutaneous tumor growth control was compared to Dox-LTSL plus local mild HT. Dox-TSL were stable at 37°C, while released over 95% Dox within 1 minute in 90% serum at 42°C. Dox-TSL demonstrated efficient *in vivo* intratumoral Dox release under local mild HT, followed by significant Dox uptake by tumor and tumor vascular endothelial cells. Dox-TSL plus mild HT showed improved tumor growth control over Dox-LTSL plus mild HT. Survival after a single treatment of Dox-TSL plus mild HT was 67%, while survival after Dox-LTSL plus mild HT was 22%. This combination of Dox-TSL and local mild HT offers promising clinical opportunities to improve liposomal Dox delivery to solid tumors.

Keywords:

Thermosensitive liposomes, hyperthermia, doxorubicin, triggered drug release, intravital microscopy, tumor growth control.

1. Introduction

The current available chemotherapeutic drugs used in conventional or combination chemotherapy are associated with substantial side-effects, but have often limited benefit to cancer patients [1-2]. Doxorubucin (Dox) is an anthracycline antibiotic, and widely used in the treatment of various tumors [2]. To reduce these side-effects, liposomal chemotherapy is recommended [3-4]. For instance, encapsulating Dox within liposomal nanoparticles significantly reduces cardiotoxicity, whilst prolonging the presence of the drug in the systemic circulation [5-8]. For these reasons long-circulating or stealth PEG-coated Liposomal Doxorubicin (PLD) was approved for clinical use (Caelyx ® in Europe and Doxil ® in the USA) [7]. Despite these promising aspects, Doxil did not substantially improve efficacy [6, 8]. Preclinical evidence suggests that slow and passive drug release from these stealth liposomes impedes their therapeutic efficacy [9]. Thermosensitive liposomes (TSL) combine the features on high drug loading efficiency and reduced toxicity due to liposomal drug encapsulation, with the possibility of triggered drug release around a tunable membrane phase transition temperature (T_m), typically ~40°C [10-12]. Incorporating Dox into stealth thermosensitive liposomes (Dox-TSL) enables a prolonged circulation half-life, and controlled localized Dox release from the nanocarrier upon HT [13-15]. However, the substantial premature leakage of Dox from lysolipid based TSL (Dox-LTSL) at physiological temperature remains an important issue [16-17]. Recently, we have reported on an optimized stealth TSL formulation for mild hyperthermia (HT) (40-42°C) induced content release [18]. After adopting the optimized stealth TSL formulation, we encapsulated Dox into these TSL.

Mild HT is routinely used in the clinic and is known to strongly improve the outcome of chemotherapy or radiotherapy, without significant side effects [19-20]. HT can improve the antitumor effect of some chemotherapeutic compounds (ie. Dox) by several mechanisms [21]. Increased perfusion, vascular permeability and interstitial microconvection cause increased drug levels and improved tissue oxygenation [22]. In addition, increased tumor cell sensitivity occurs upon mild HT as well as DNA repair inhibition [23-24]. Although reaching mild hyperthermic temperatures (40-43°C) uniformly within a tumor depends on the location of the tumor, and its perfusion, the development in technology and equipment nowadays allows for precise heating of a defined tissue volume up to 43°C, using external microwave or high intensity focused ultrasound [25-26].

The combination of Dox-TSL and local HT has the potential to achieve high concentrations of bioavailable Dox in heated tumors. Lysolipid-based Dox-LTSL was invented by Needham's group, and its temperature sensitivity, release mechanisms were reported [11]. Dox-LTSL is currently under thorough study in clinical trials [27, 16]. The approach is to systemically administer

long-circulating stealth Dox-LTSL, in combination with local mild HT at the tumor to trigger intravascular Dox release from the Dox-LTSL and subsequent diffusion of free Dox throughout the HT treated tumor tissue [28]. An essential requirement for this approach is a desirable TSL formulation, with minimum content leakage at physiological temperature in serum and maximum content release at 41-42°C. We have previously reported an optimized TSL formulation for content release [18]. In this study, we characterized Dox-TSL for *in vitro* stability and cytotoxicity, *in vitro* and *in vivo* Dox release kinetics and cellular uptake under mild HT by fluorescence microscopy and confocal microscopy. *In vivo* Dox release and delivery kinetics were quantified and subjected to computer modeling. We propose that the optimized Dox-TSL with prolonged circulation time at physiological temperature and triggered drug release at mild HT further improve the therapeutic efficacy of the combination approach. For this purpose, we compared the therapeutic efficacy of Dox-TSL with lysolipid based Dox-LTSL for intravascular Dox release upon local mild HT, on subcutaneous (s.c.) tumor growth control.

2. Materials and methods

2.1. Lipids and chemical reagents

The phospholipids 1,2-dipalmityol-*sn*-glycero-3-phosphocholine (DPPC), 1,2-distearoyl-*sn*-glycero-3-phosphocholine (DSPC), 1,2-distearoyl-*sn*-glycero-3-phosphoethanolamine-*N*-PEG_{2000} (DSPE-PEG_{2000}) were provided by Lipoid (Ludwigshafen, Germany). Monostearoylphosphatidylcholine (MSPC) was purchased from Avanti Polar Lipid Inc. Dox was purchased from Pharmachemie. Other chemical reagents were obtained from Sigma Aldrich (Netherlands) unless otherwise specified.

2.2. Liposomes

TSL at 80 nm in diameter were composed of DPPC/DSPC/DSPE-PEG_{2000} in a molar ratio of 80:15:5. We prepared Dox-LTSL at 120 nm in diameter composed of DPPC/MSPC/DSPE-PEG_{2000} in a molar ratio of 85:10:5 for the comparison on the therapeutic efficacy study [29, 17]. Liposomes were prepared by lipid film hydration and extrusion method at 60°C (thermobarrel extruder, Northern Lipids, Vancouver, Canada) [30, 18]. Filters pore size at 80 – 200 nm were used for Dox-TSL, and 100 – 200 nm were used for Dox-LTSL. Size and polydispersity index (PDI) were determined by dynamic light scattering using a Zetasizer Nano ZS (Malvern Instruments, Worcestershire, UK). Loading of Dox into TSL and LTSL was performed according to a citrate-based pH-gradient Dox-loading method [31-32], with initial Dox/lipid ratio (mole/mole) at 0.15:1 for Dox-TSL and 0.05:1 for Dox-LTSL [17]. Briefly, across membrane 300 mM citrate pH 4 was inside and HN buffer (150 mM NaCl, 20 mM HEPES) pH 7.4 was outside. Mixture of TSL and Dox was incubated at 39°C for 10

minutes. Free Dox was removed from suspension by high speed centrifuge (maximum radial distance 10.70 cm, 39,000 rpm, at 4°C for 1 hour). Dox-TSL and Dox-LTSL were stored in His buffer (150 mM NaCl, 20 mM histidine) pH 6.5 at -20°C, and used within two weeks. Lipid concentration was measured by phosphate assay [33]. Cryo-transmission electron microscopy (Cryo-TEM) images of Dox-TSL were captured by a Leo 912 Omega TEM microscope (Carl Zeiss NTS GmbH, Oberkochen, Germany) to visualize the encapsulated Dox inside of TSL [34-35]. Briefly, a thin liquid film placed on a microperforated copper grid was frozen in liquid ethane and prepared for imaging in a cooling chamber cooled with liquid nitrogen.

2.3. Cell lines and culture

Murine BFS-1 sarcoma was obtained from Ludwig-Maximilians University, Munich, Germany, human BLM melanoma was obtained from Nijmegen University, the Netherlands and Human Umbilical Vein Endothelial Cells (HUVEC) were isolated in-house. BFS-1 and BLM were routinely cultured in RPMI-1640 medium with 25mM Hepes with 2 mM L-glutamine with 10% fetal calf serum (FCS) (Lonza, Belgium), and HUVEC were routinely cultured in human fibronectine (Roche) coated flasks (Greiner Bio-One, the Netherlands) in DMEM with 4.5g/l glucose with 2 mM L-glutamine, human serum (Lonza, Belgium) (20%) and recombinant human basic fibroblast growth factor (Tebu-Bio) and human endothelial-SFM (InVitrogen).

2.4. In vitro Dox encapsulation, stability and release kinetics

Encapsulated Dox was determined after exposure of 20 μl of 5 mM [lipid] suspension of Dox-TSL to 180 μl of detergent (2% Triton X-100 in distilled H_2O) at 45°C for 30 minutes in a thermal-shaker (Eppendorf Thermomixer) at 1400 rpm to measure maximal Dox fluorescence by spectrofluorometry (Ex. 482 nm/Em. 594 nm, Ex slit 10 nm/Em slit 5 nm) (Hitachi F-4500 Fluorescence Spectrophotometer). After incubation, samples were diluted in 10 mM Tris/NaCl 0.9% at pH 8.0 at 1:50 (v/v) and measured by spectrofluorometry, as positive controls (I_∞). Samples in the replacement of detergent to 180 μl of pure FCS at 37°C for 1 hour were measured as Dox-TSL leakage ($I_{leakage}$). Samples in 180 μl of FCS mixed at room temperature were measured as negative controls (I_0). All samples were adjusted to contain identical amount of FCS. Dox encapsulation efficiency was determined as Dox/lipid = [Dox]/[lipid] [18]. Stability (%) = $100 - (I_{leakage} - I_0)/(I_\infty - I_0) \times 100$.

For *in vitro* temperature-dependent Dox release, 20 μl of 5 mM [lipid] Dox-TSL suspension in HN buffer 7.4 was added to pre-heated 180 μl of FCS and incubated for 5 minutes at desired temperatures (ranging from 37 to 45°C) in a thermal-shaker at 300 rpm. After incubation, samples were diluted in 10 mM Tris/NaCl 0.9% at pH 8.0 at 1:50 (v/v) and measured by spectrofluorometry. For

in vitro time-dependent Dox release, 20 μl of 5 mM [lipid] Dox-TSL suspension in HN buffer 7.4 was added to pre-heated 3 ml of FCS and incubated for 1 hour at 42°C under stirring, and monitored online by spectrofluorometry. After 1 hour incubation, 20 μl of 10% Triton X-100 was added to obtain maximum Dox release which was used as positive control. Samples mixed at room temperature (20°C) were measured as negative controls. Dox-TSL encapsulation, stability and release kinetics were compared to Dox-LTSL [15], a lysolipid based formulation which is currently in clinical trials.

2.5. In vitro Dox-TSL cytotoxicity

BFS-1, BLM and HUVEC were seeded in 96-well flat bottom plates (2,000 cell/well for BFS-1 and BLM, 6,000 cell/well for HUVEC), and recovered overnight. Dox-TSL and Dox were diluted in serum-free medium (at various concentrations) and filtrated through 0.45 μm filters before use. After adding Dox-TSL and Dox to the cells, the 96-well plates were immediately placed in a water bath at HT (42°C) (plates were vacuum sealed to be waterproof) or in an incubator at normothermia (NT) (37°C) for 1 hour. The validity of the experimental setup was confirmed by comparing cell survival at 72 hours post-HT to post-NT. The water bath set at 42.5°C took 10 minutes to heat medium to 42°C in the 96-well plates, and an electronic thermometer probe was applied to measure medium temperature. After incubation at desired temperatures, cells were washed three times with serum-free medium, and incubated in fresh medium at 37°C for 72 hours. Cytotoxicity was tested using a colorimetric XTT assay for cell viability as described by the manufacturer [36]. IC50s (50% cell inhibition) were calculated by interpolation.

2.6. In vitro cellular Dox uptake

BLM and HUVEC were seeded in rings (4 cm in diameter) on glass pre-coated with fibronectin (37°C for 30 minutes) (50,000 cell/ring for BLM, 25,000 cell/ring for HUVEC), and recovered overnight. HUVEC tended to detach under HT conditions, thus low amount of HUVEC was seeded to ease HUVEC attachment during the experiments. Hoechst was added to medium without phenol red (1:100 in rings) and incubated at 37°C for 30 minutes, to allow visualization of nuclei. Medium was then refreshed with Dox-TSL suspension (50 μM Dox) in serum -free medium without phenol red. Cells were incubated at 37°C (control) or 42°C (HT) for 1 hour (it took 10 minutes to reach medium temperature of 42°C). Images (40-fold magnification) of bright field and channels for Hoechst (binding to DNA) and Dox were taken pre-HT, every 10 minutes during HT up to 1 hour under Zeiss microscope 100M (40x oil lens) with a Hamamatsu camera. Cells without the addition of Dox-TSL were experimented as controls at 42 and 37°C.

2.7. Animal models and in vivo tumor models

C57BL/6 and NMRI *nu/nu* mice were purchased from Charles River and housed at 20-22°C, humidity of 50-60%, and 12 hour light-dark cycles. Sterile rodent food and acidified vitamin C-fortified water were given *ad libitum*. Eight-week old mice at weight of 20-25 g were used. Mice with constitutive vascular endothelial cell expression of an eNOS-Tag-GFP fusion protein were developed by Dr. R. de Crom and R. van Haperen, Department of Cell Biology, Erasmus MC, Rotterdam, the Netherlands, bred in-house and used for window chamber intravital microscopy studies when appropriate. All animal studies were done in accordance to protocols approved by the committee on Animal Research of Erasmus MC, Rotterdam, the Netherlands.

Murine BFS-1 sarcoma and human BLM melanoma cells were routinely cultured as described above. Tumor cells (10^6) were injected subcutaneously in flanks of mice, and bulk tumors of 1 cm in diameter were used for transplantation. A small viable tumor piece (~1 mm^3) of murine BFS-1 sarcoma was removed from the bulk tumor and transplanted in the fascia of a dorsal skin flap placed in a window chamber in mice [18]. For *in vivo* efficacy study, a tumor piece (~3 mm^3) of human BLM melanoma was transplanted subcutaneously in the hind leg of NMRI *nu/nu* mice. After tumor transplantation, mice carrying window chambers were housed individually at 30°C and 60% humidity. Mice were used for experiments, when tumors reached ~5 mm in diameter in dorsal skin flap window chamber models and s.c. models.

2.8. In vivo Dox release

In vivo Dox release kinetics was studied by intravital fluorescence microscopy. Mice were anesthetized with isofluorane (Nicholas Piramal, London, UK) and placed on a thermal mattress at 37°C during experiments. An external circular resistive heating coil was attached to the glass at the back side of the window chamber to provide homogenous local HT [18]. Thermocouples (point-welded thin manganese and constantan wires from Thessco®, Amsterdam) were imbedded in window chambers to monitor tissue temperature online. Dox-TSL (7 mg/kg) was injected intravenously through the tail vein. Regions of interest were selected by confocal microscopy (Zeiss LSM 510 META). Background images were captured before liposome administration. Amplifier offsets for both GFP and Dox were adjusted to intensity 0 when the lasers were off for initial image calibration. Initial images were taken, and then heating was started within 20 minutes post-administration. Window chamber tissues were heated up to 42°C in ~10 minutes and remained for 1 hour, followed by resting without HT (temperature decreased down to 30°C in ~15 minutes). Dox release was monitored online by a Helium-Neon laser (543 nm), and GFP-expressing endothelial cells were visualized by an argon laser (488 nm). Fluorescent channels (GFP: BP 505-550, Dox: LP 585, Plan-Neofluar 10x/0.3

lens) were recorded in 40 μm thin single images and 120 μm thick Z-stack before and after HT. Intermittent images were taken every 8 seconds during heating, HT at 42°C. Images with higher magnifications (Plan-Neofluar 20x/0.5 lens, scan zoom 2.0) were taken at the end of the experiments to capture Dox uptake in nuclei. Images of 512x512 pixels were analyzed with LSM image software (Zeiss, Germany). Dox intensity was quantified as fluorescence intensity (AU) (area unit) by Image J (Wayne Rasband, National Institutes of Health, USA).

2.9. Quantitative image analysis

In vivo Dox release upon local mild HT was quantified by image processing methods in software Matlab and MeVisLab. Motion compensation was performed by geometrical transformation between images in each time series. Intravascular regions were identified by GFP-tag endothelial lining. Vessel distance maps were then generated by Euclidean distance transfer [37], and average Dox fluorescence intensity calculated depending on distance to closest vessel, up to 27.5 μm [38]. Dox penetration during HT was visualized by surface plots.

2.10. Therapeutic efficacy and tumor growth control

NMRI *nu/nu* mice were transplanted with s.c. human BLM melanoma in their right hind legs. Upon reaching tumor size of 5 mm in diameter, mice were anesthetized, and the right tumor bearing hind legs were covered in aquasonic ultrasound gel (Parker Laboratories, Inc.) to ensure efficient heat transfer to the tumor surface. Surrounding tissues and muscles were protected by a syringe. The hind legs were maintained inside of the syringes and fixed onto a rack to ensure a steady position in a water bath during the HT treatment. When tumor temperature reached 42°C, Dox-TSL and Dox-LTSL in PBS suspension were administered at 3 mg/kg through a tail vein. The tumor temperature was maintained at 42°C for 1 hour. Mice with Dox-TSL and Dox-LTSL administration under NT, and with PBS administration under HT or NT were used as control groups. Mice were then released back to their cages. Tumor size was measured on the day of experiments, and every other day after experiments. When tumor size reached 2 cm^3 (Height x Width x Depth x 0.4), mice were euthanized, otherwise mice were euthanized on day 26 post-treatment. Tumor size related euthanization was used as measure for survival.

2.11. Statistics

All *in vitro* data are represented as mean ± standard error of the mean (SEM) of experiments in triplicates, and analyzed by paired Mann-Whitney test (p-value ≤ 0.05). *In vivo* results are analyzed by Kruskal Wallis for multiple

groups.

3. Results

3.1. In vitro characterization of liposomes

In vitro Dox-TSL size, size distribution, stability, temperature-dependent and time-dependent Dox release kinetics were determined (Table 1). Size and homogeneity of the TSL population were confirmed by Cryo-TEM (Fig. 1A) [35]. Dox was present in the liposome interior in a crystallized form as demonstrated by the electron dense fibrous appearance inside TSL. These Dox-TSL were stable during storage at -20°C for up to 5 weeks with Dox retention in TSL > 80% (data not shown). In the temperature-dependent release assay, Dox-TSL released their content with increasing temperature, starting at 39°C. Over 80% of Dox was released at the optimal temperature for this formulation at 42°C in 5 minutes in the presence of 90% FCS (Fig. 1B) [18]. By contrast, LTSL already released significant quantity of their Dox in 5 minutes at 37°C in 90% of serum and reached maximal release temperature at 40-41°C.

Table. 1. Liposome characterization.

	Size (nm)	PDI	Dox/lipid (mole/mole)	Stability (%) at 37°C in 90% FCS in 1 hour*	Release at 42°C in 99% FCS (%)	
					1 minute	1 hour*
Dox-TSL	86±1	0,03±0,01	0,13±0,01	66±1	75±14	99±1
Dox-LTSL	127±5	0,04±0,02	0,05±0,01	49±10	99±1	99±1

*Nonparametric Mann-Whitney test, p value ≤ 0.05. Data are represented as mean ± standard error of the mean (SEM), N=3.

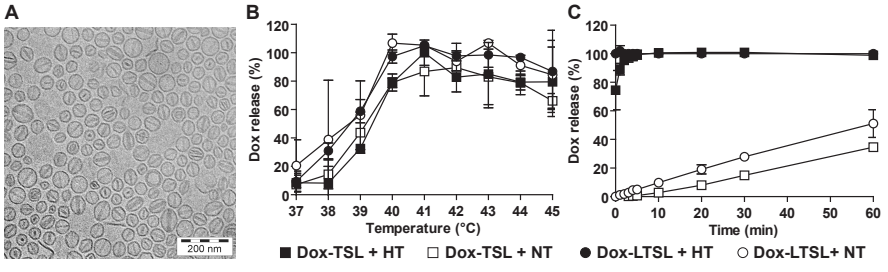

Fig. 1. Cryo-TEM image of Dox-TSL (A). Bar, 200 nm. Temperature-dependent Dox release from TSL and LTSL during 5 minutes incubation in serum at different temperatures (B). Dox-TSL in 50% FCS (□), Dox-TSL in 90% FCS (■), Dox-LTSL in 50% FCS (⭘), Dox-LTSL in 90% FCS (●). Time-dependent Dox release from Dox-TSL and Dox-LTSL during 1 hour incubation at 37°C and 42°C in 99% FCS (C). Dox-TSL at 37°C (□), Dox-TSL at 42°C (■), Dox-LTSL at 37°C (⭘), Dox-LTSL at 42°C (●). N=3.

At the optimal Dox-TSL release temperature 42°C, we followed release rate in time. Dox-TSL released virtually all its Dox in 5 minutes in the presence of 99.3% FCS (Fig. 1C). *In vitro* stability characterization revealed Dox-TSL to be more stable at 37°C in the presence of serum than LTSL, which released significantly more Dox under these physiological conditions (Table 1). Yet Dox-TSL displayed fast Dox release at mild HT.

3.2. In vitro cytotoxicity

The cytotoxicity of Dox-TSL was tested under short-term (1 hour) mild HT (42°C) and NT (37°C) conditions toward murine BFS-1 sarcoma, human BLM melanoma cell lines, and HUVEC. The cytotoxicity of Dox-TSL under HT was equivalent to free Dox under HT in both murine BFS-1 sarcoma and human BLM melanoma cell lines (Table 2, Fig. 2B,C). Dox-TSL showed a 60-fold and 80-fold decrease in IC_{50} upon HT compared to NT against murine BFS-1 sarcoma and human BLM melanoma cell lines (Table 2). Free Dox under HT caused a 4-fold reduction on IC_{50} compared to NT in both tumor cell lines (Table 2). In view of possible delivery of Dox to tumor vascular endothelial cells we also investigated *in vitro* Dox delivery to proliferating endothelial cells (HUVEC). For HUVEC, HT also caused a decrease in the IC_{50} of Dox-TSL (10-fold reduction compared to NT) (Table 2). However, HUVEC, in contrast to both BLM and BFS-1 tumor cell lines displayed similar Dox chemosensitivity regardless of HT or NT (Fig. 2C and Table 2).

Table. 2. IC_{50} (μM) of Dox-TSL in comparison to Dox.

	HT			NT		
	BLM	BFS-1	HUVEC	BLM	BFS-1	HUVEC
Dox-TSL	0.09±0.03	0.30±0.22	2.50±1.02	7.90±0.91	5.31±0.01	26.10±11.40
Dox	0.25±0.02	0.17±0.26	4.01±0.77	0.98±0.09	0.75±0.13	3.12±0.68

Data are represented as mean ± SEM. N=3.

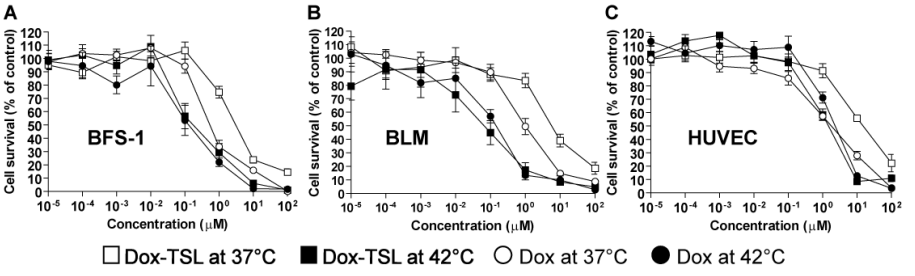

Fig. 2. *In vitro* cytotoxicity of Dox-TSL against murine BFS-1 sarcoma (A), human BLM melanoma (B) cell lines and HUVEC (C). Dox-TSL at 37°C (□), Dox-TSL at 42°C (■), Dox at 37°C (○), and Dox at 42°C (●).Data are represented as mean ± SEM. N=3.

3.3. In vitro Dox uptake in nuclei

Upon exposure of human BLM melanoma cells and HUVEC to Dox-TSL under HT (42°C) and NT (37°C) for 1 hour, cellular uptake of Dox was monitored online. Nuclear co-localization of Dox and Hoechst was observed (Fig. 3). Under HT, nuclear uptake of Dox was visualized when BLM melanoma cells were maintained at 42°C for 10 minutes, and Dox intensity in nuclei continuously increased. In 30 minutes under HT, almost all Dox released from Dox-TSL in the medium had been taken up by nuclei. Nuclear uptake of Dox from Dox-TSL was much less and slower under NT (Fig. 3). By the end of 1 hour NT, nuclear update of Dox from Dox-TSL was less than that observed at 30 minutes HT in both human BLM melanoma cells and HUVEC.

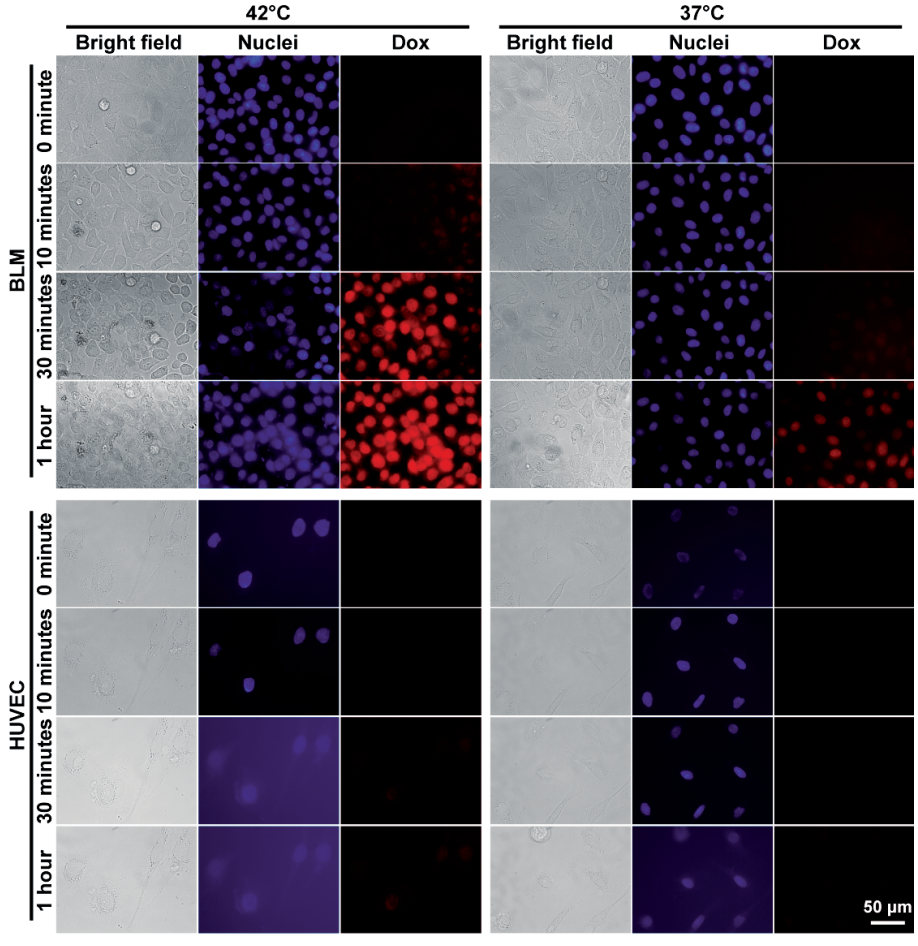

Fig. 3. *In vitro* cellular Dox uptake by human BLM melanoma cell line and HUVEC upon incubation with Dox-TSL at HT and NT. Bar, 50 μm.

3.4. In vivo Dox release from Dox-TSL under local mild HT

In vivo Dox release from TSL was observed by intravital fluorescence microscopy on dorsal skin flap window chamber models in mice implanted with murine BFS-1 sarcoma. In agreement with *in vitro* stability data (Fig. 1) Dox-TSL were stable at 37°C in circulation with minimal Dox fluorescence detected (Fig. 4A). Dox-TSL started to slowly release Dox intravascularly, when the temperature in the tumor reached 40°C (Fig. 4A). Massive Dox release occurred when the

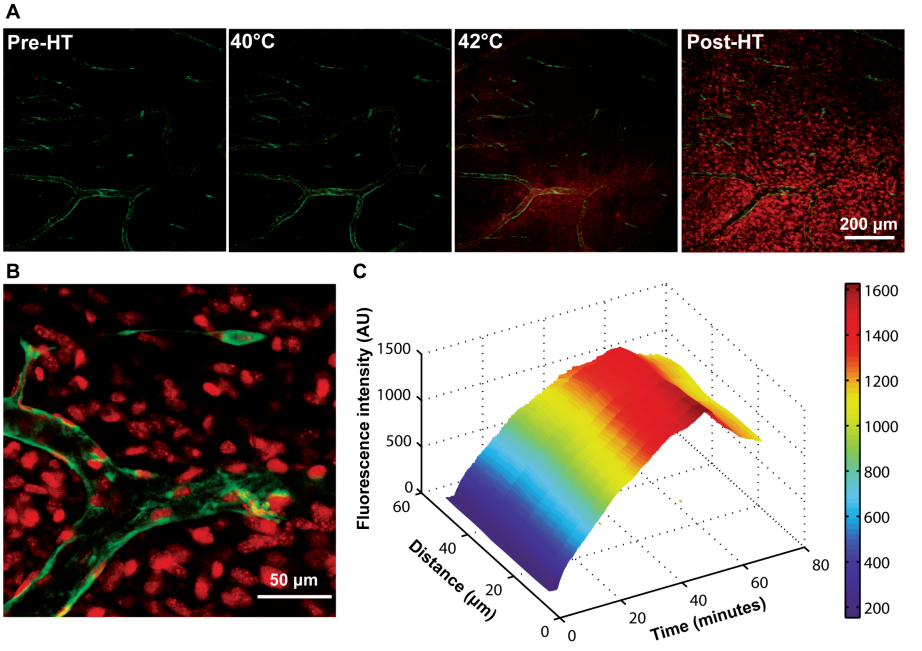

Fig. 4. *In vivo* Dox release from Dox-TSL in murine BFS-1 sarcoma (A), and subsequent cellular uptake by murine BFS-1 sarcoma cells and endothelial cells (B). Images are presented as merged GFP endothelial cells (green) and Dox (red) fluorescence. Bar in A, 200 μm. Bar in B, 50 μm. Quantitative Dox intensity and penetration depth during mild HT, tumor tissue temperature reached 42°C by 20 minutes (C).

temperature was reaching 42°C (Fig. 4A). It took 2 minutes to increase from 40 to 42°C. Dox from circulating Dox-TSL was continuously delivered to tumor tissue upon Dox-TSL passage through the heated tumor vasculature. Released Dox rapidly penetrated tumor tissue and was internalized quickly by tumor cells and vascular endothelial cells accumulating at high concentrations in their nuclei (Fig. 4B). Upon HT, a boost of intravascular Dox release caused a major initial homogeneous Dox delivery throughout the tumor tissue. Dox quickly diffused and penetrated further into the interstitial space up to at least 50 μm away from the tumor vasculature (Fig. 4C and Supplemental Video 1). After 30 minutes HT, intravascular Dox intensity started to decrease, as circulating Dox-TSL had emptied their contents and Dox concentrated in nuclei (Fig. 4C). Moreover, the stable Dox intensity also indicates a continuous Dox delivery to extravascular extracellular space (EES) during HT, as a supply for subsequent cellular uptake. The Dox concentration in cellular nuclei continued to increase during HT (Supplemental Video 1). *In vivo* Dox release demonstrated efficient local mild HT controlled intravascular Dox release from Dox-TSL and rapid intracellular accumulation.

Correlations of time, Dox concentration and penetration depth were demonstrated in a mathematical model (Fig. 4C). Homogeneous Dox intensity increased to maximal of over 8-fold compare to initial Dox intensity (200 AU) during heating period with tissue temperature of 42°C (1400 AU). Steady increase in fluorescence up to HT at 42°C for 30 minutes, after which a decrease was observed. This indicated liposomes were emptied and Dox intensity became heterogeneous throughout the tumor tissue as soon as cellular uptake of Dox became dominant and remained stable afterwards (Supplemental Video 1).

3.5. Tumor growth control

Treatments of systemic Dox-TSL and Dox-LTSL in combination with local mild HT at tumors were compared for tumor growth control in human BLM melanoma xenografts. Dox-TSL showed overall better tumor growth control than Dox-LTSL over a time course of 26 days after a single treatment of intravascularly triggered Dox release by local mild HT (Fig. 5A,B). Mice after the treatment of Dox-TSL and mild HT had tumor growth delay of ~16 days, while mice after the treatment of Dox-LTSL and mild HT had tumor growth delay of 8 days. By Day 26, 6 out of 9 mice survived with end tumor size <11x15x10 mm^3 after treatment of Dox-TSL and local mild HT; while only 2 out of 9 mice survived with end tumor size of ~13x16x12 mm^3 after treatment of Dox-LTSL and local mild HT. In sham group, all of 9 mice had to be euthanized because of large tumor size. Intravascular release of Dox from Dox-TSL showed improved survival of mice bearing s.c. human BLM melanoma up to 26 days after a single treatment (Fig. 5C).

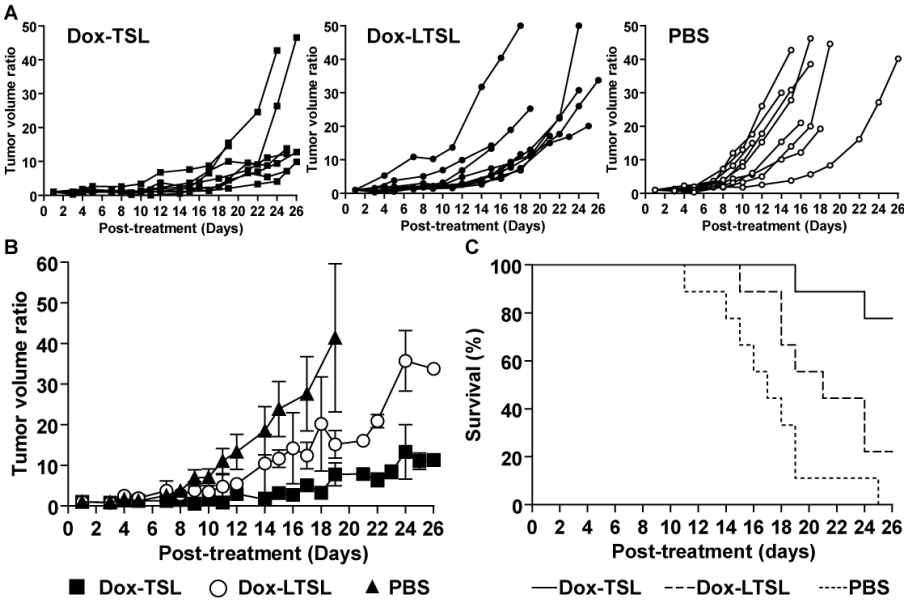

Fig. 5. Tumor growth control of Dox-TSL and Dox-LTSL (A, B). Dox-TSL with HT (■), Dox-LTSL with HT (◘), PBS with NT (▲). Data are represented as mean ± SEM. N=4. Compare of survival after a single treatment (C). Dox-TSL with HT (–), Dox-LTSL with HT (- -), PBS with NT (····). N=9.

4. Discussion

Dox-LTSL have been studied in combination with local HT at tumor sites [11] to induce intravascular drug release-mediated control of tumor growth and are currently in clinical trials [27, 16, 28]. Lysolipid-based Dox-LTSL are known to release significant quantities of Dox at physiological temperatures in serum and thus have a fast plasma clearance upon administration [32, 16, 39-40]. Inspired by these prior promising results, we aimed to further improve TSL-mediated drug delivery by establishing a more stable formulation. We omitted the lysolipid and made use of an optimal DSPE-PEG_{2000} density to prolong drug retention at physiological temperature in circulation with peak rate at 42°C [18]. These Dox-TSL were significantly smaller (80 nm) than LTSL (120 nm) [29, 17], to further promote rapid release at their T_m [41].

Dox can relatively rapidly pass cellular membranes followed by strong binding to DNA in cellular nuclei. Because of the increased perfusion, vascular permeability and microconvection in the EES induced by HT, after release, Dox distributed homogeneously into tumor tissue at distances up to 50 μm away from tumor feeding blood vessels (Fig. 4). In addition, Dox delivery continued to increase during the course of the HT treatment, due to new drug-filled Dox-TSL being available in circulating and arriving in the heated tumor

tissue. Due to the continuous supply of drug-loaded TSL, Dox delivered by TSL will penetrate deeper into EES than administration of free Dox, which is rapidly cleared from circulation [7]. Importantly, we observed nuclear Dox uptake *in vivo* in tumor cells as well as in tumor vascular endothelial cells (Fig. 4B). Thus, intratumoral Dox release from Dox-TSL causes a dual targeting of both intratumoral endothelial cells and adjacent tumor cells. We were able to demonstrate that *in vitro* exposure of HUVEC to Dox in free form and Dox-TSL in combination with mild HT causes significant intracellular Dox delivery and concomitant cytotoxicity, at levels similar to those observed in tumor cells.

For local mild HT induced intravascular drug release approach, lysolipid-free Dox-TSL with a prolonged stability at physiological temperature, are expected to provide significantly higher dose of bioavailable Dox at tumor sites. Dox-TSL showed a prolonged tumor growth control and improved survival by 4-fold over Dox-LTSL (78% v.s. 22%). Our cytotoxicity results indicated that murine BFS-1 sarcoma and human BLM melanoma cell lines had a lower IC_{50} than HUVEC upon combining HT and Dox, in contrast to incubations with Dox, but without HT. This finding suggests cancer cells are more prone to thermal stress than normal cells, which leads to cell sensitization towards a chemotherapeutic compound [42-44]. HT is known to sensitize tumor cells through enhancing drug uptake, initiating cellular stress responses [45] and by inhibiting DNA repair [24]. Apparently normal endothelial cells do not show such sensitization to Dox treatment. Future studies will be focused on the exact contribution of cytotoxicity done to both cell types to the overall anti-tumor activity, for instance by making use of cell-specific targeted triggered drug delivery approaches [46-48].

Intravascular drug release leads to a concentration gradient from the vessels into the tissue, which means perivascular regions normally receive a higher dose of chemotherapy than hypoxic and necrotic regions. Smart application of mild HT with thermosensitive nanocarriers for chemotherapeutic drug delivery has the potency to strongly improve drug levels also in tissues further away from functional vessels due to HT-mediated enhancement of tumor perfusion, vascular permeability and interstitial fluid flow. Combining these benefits of HT with optimal thermosensitive nanocarriers that demonstrate high levels of nanoparticle extravasation [49-50] and penetration into tumor tissues [50], HT triggered drug release bears the potential to significantly improve tumor drug delivery.

5. Conclusion

Our study provides a detailed *in vitro* and *in vivo* study toward an optimized nano-sized Dox-TSL formulation, in which several critical aspects for stability and triggered drug delivery were combined. This resulted in Dox-TSL with high drug loading efficiency, stability at physiological temperature in

circulation, and fast drug release potential under local mild HT. These Dox-TSL showed improved tumor growth control and overall survival compared to Dox-LTSL through an intravascular drug release upon local mild HT. The combination of the optimized Dox-TSL and local mild HT resulting in drug delivery to both tumor and tumor vascular endothelial cells may thus lead to clinically more efficacious advanced drug delivery systems.

Acknowledgements

This study is funded by Stichting Vanderes, Stichting Fondsen, SEHK. We thank Halil Ozkal, Debby Schipper, Csilla Scholten and Thomas Soullié at Erasmus Medical Center, Rotterdam for technical support, Sabine Barnert at Institute of Pharmaceutical Sciences, Albert-Ludwigs University, Freiburg, Germany for Cryo-TEM imaging.

Supplemental Video 1.
In vivo Dox-TSL release kinetics under mild HT in murine BFS-1 sarcoma.

References

[1] P.K. Singal, N. Iliskovic, Doxorubicin-induced cardiomyopathy, N. Engl. J. Med., 339 (1998) 900-905.
[2] D.J. Slamon, B. Leyland-Jones, S. Shak, H. Fuchs, V. Paton, A. Bajamonde, T. Fleming, W. Eiermann, J. Wolter, M. Pegram, J. Baselga, L. Norton, Use of chemotherapy plus a monoclonal antibody against HER2 for metastatic breast cancer that overexpresses HER2, N. Engl. J. Med., 344 (2001) 783-792.
[3] T.M. Allen, P.R. Cullis, Drug delivery systems: entering the mainstream, Science, 303 (2004) 1818-1822.
[4] G.A. Koning, G.C. Krijger, Targeted multifunctional lipid-based nanocarriers for image-guided drug delivery., Anticancer Agents Med Chem, 7 (2007) 425-440.
[5] D.W. Northfelt, B.J. Dezube, J.A. Thommes, B.J. Miller, M.A. Fischl, A. Friedman-Kien, L.D. Kaplan, C. Du Mond, R.D. Mamelok, D.H. Henry, Pegylated-liposomal doxorubicin versus doxorubicin, bleomycin, and vincristine in the treatment of AIDS-related Kaposi's sarcoma: Results of a randomized phase III clinical trial, Journal of Clinical Oncology, 16 (1998) 2445-2451.
[6] I. Judson, J.A. Radford, M. Harris, J.Y. Blay, Q. van Hoesel, A. le Cesne, A.T. van Oosterom, M.J. Clemons, C. Kamby, C. Hermans, J. Whittaker, E.D. di Paola, J. Verweij, S. Nielsen, Randomised phase II trial of pegylated liposomal doxorubicin (DOXIL (R)/CAELYX (R)) versus doxorubicin in the treatment of advanced or metastatic soft tissue sarcoma: a study by the EORTC Soft Tissue and Bone Sarcoma Group, European Journal of Cancer, 37 (2001) 870-877.
[7] A. Gabizon, H. Shmeeda, Y. Barenholz, Pharmacokinetics of pegylated liposomal doxorubicin - Review of animal and human studies, Clin Pharmacokinet, 42 (2003) 419-436.
[8] M.E.R. O'Brien, N. Wigler, M. Inbar, R. Rosso, E. Grischke, A. Santoro, R. Catane, D.G. Kieback, P. Tomczak, S.P. Ackland, F. Orlandi, L. Mellars, L. Alland, C. Tendler, C.B.C.S. Grp, Reduced cardiotoxicity and comparable efficacy in a phase III trial of pegylated liposomal doxorubicin HCl (CAELYX (TM)/Doxil (R)) versus conventional doxorubicin for first-line treatment of metastatic breast cancer, Annals of Oncology, 15 (2004) 440-449.
[9] A.L.B. Seynhaeve, S. Hoving, D. Schipper, C.E. Vermeulen, G.A. de Wiel-Ambagtsheer, S.T. van Tiel, A.M.M. Eggermont, T.L.M. ten Hagen, Tumor necrosis factor alpha mediates homogeneous distribution of liposomes in murine melanoma that contributes to a better tumor response, Cancer Research, 67 (2007) 9455-9462.
[10] W.J. Yatvin MB, Dennis WH, Blumenthal R, Design of liposomes for enhanced local release of drugs by hyperthermia, Science, 202 (1978) 1290-1293.
[11] D. Needham, G. Anyarambhatla, G. Kong, M.W. Dewhirst, A new temperature-sensitive liposome for use with mild hyperthermia: Characterization and testing in a human tumor xenograft model, Cancer

Research, 60 (2000) 1197-1201.
[12] L.H. Lindner, M.E. Eichhorn, H. Eibl, N. Teichert, M. Schmitt-Sody, R.D. Issels, M. Dellian, Novel temperature-sensitive liposomes with prolonged circulation time, Clinical Cancer Research, 10 (2004) 2168-2178.
[13] Q. Chen, S. Tong, M.W. Dewhirst, F. Yuan, Targeting tumor microvessels using doxorubicin encapsulated in a novel thermosensitive liposome, Molecular Cancer Therapeutics, 3 (2004) 1311-1317.
[14] A.A. Secord, E.L. Jones, C.A. Hahn, W.P. Petros, D. Yu, L.J. Havrilesky, J.T. Soper, A. Berchuck, I. Spasojevic, D.L. Clarke-Pearson, L.R. Prosnitz, M.W. Dewhirst, Phase I/II trial of intravenous Doxil (R) and whole abdomen hyperthermia in patients with refractory ovarian cancer, International Journal of Hyperthermia, 21 (2005) 333-347.
[15] P.S. Yarmolenko, Y. Zhao, C. Landon, I. Spasojevic, F. Yuan, D. Needham, B.L. Viglianti, M.W. Dewhirst, Comparative effects of thermosensitive doxorubicin-containing liposomes and hyperthermia in human and murine tumours, Int J Hyperthermia, 26 (2010) 485-498.
[16] R.T. Poon, N. Borys, Lyso-thermosensitive liposomal doxorubicin: a novel approach to enhance efficacy of thermal ablation of liver cancer, Expert Opin Pharmacother, 10 (2009) 333-343.
[17] A.H. Negussie, P.S. Yarmolenko, A. Partanen, A. Ranjan, G. Jacobs, D. Woods, H. Bryant, D. Thomasson, M.W. Dewhirst, B.J. Wood, M.R. Dreher, Formulation and characterisation of magnetic resonance imageable thermally sensitive liposomes for use with magnetic resonance-guided high intensity focused ultrasound, Int J Hyperthermia, 27 (2011) 140-155.
[18] L. Li, T.L. ten Hagen, D. Schipper, T.M. Wijnberg, G.C. van Rhoon, A.M. Eggermont, L.H. Lindner, G.A. Koning, Triggered content release from optimized stealth thermosensitive liposomes using mild hyperthermia, J Control Release, 143 (2010) 274-279.
[19] J. van der Zee, D.G. Gonzalez, G.C. van Rhoon, J.D.P. van Dijk, W.L.J. van Putten, A.A.M. Hart, G. Dutch Deep Hyperthermia, Comparison of radiotherapy alone with radiotherapy plus hyperthermia in locally advanced pelvic tumours: a prospective, randomised, multicentre trial, Lancet, 355 (2000) 1119-1125.
[20] R.D. Issels, L.H. Lindner, J. Verweij, P. Wust, P. Reichardt, B.C. Schem, S. Abdel-Rahman, S. Daugaard, C. Salat, C.M. Wendtner, Z. Vujaskovic, R. Wessalowski, K.W. Jauch, H.R. Durr, F. Ploner, A. Baur-Melnyk, U. Mansmann, W. Hiddemann, J.Y. Blay, P. Hohenberger, E.-S.E. European Org, Neo-adjuvant chemotherapy alone or with regional hyperthermia for localised high-risk soft-tissue sarcoma: a randomised phase 3 multicentre study, Lancet Oncology, 11 (2010) 561-570.
[21] W.C. Dewey, Arrhenius relationships from the molecule and cell to the clinic, International Journal of Hyperthermia, 10 (1994) 457-483.
[22] C.W. Song, Effect of local hyperthermia on blood flow and microenvironment: a review, Cancer Res, 44 (1984) 4721s-4730s.
[23] G.A. Koning, A.M.M. Eggermont, L.H. Lindner, T.L.M. ten Hagen,

Hyperthermia and Thermosensitive Liposomes for Improved Delivery of Chemotherapeutic Drugs to Solid Tumors, Pharmaceutical Research, 27 (2010) 1750-1754.
[24] P.M. Krawczyk, B. Eppink, J. Essers, J. Stap, H. Rodermond, H. Odijk, A. Zelensky, C. van Bree, L.J. Stalpers, M.R. Buist, T. Soullie, J. Rens, H.J. Verhagen, M.J. O'Connor, N.A. Franken, T.L. Ten Hagen, R. Kanaar, J.A. Aten, Mild hyperthermia inhibits homologous recombination, induces BRCA2 degradation, and sensitizes cancer cells to poly (ADP-ribose) polymerase-1 inhibition, Proc Natl Acad Sci U S A, 108 (2011) 9851-9856.
[25] M.M. Paulides, J.F. Bakker, E. Neufeld, J. Van der Zee, P.P. Jansen, P.C. Levendag, G.C. Van Rhoon, The HYPERcollar: A novel applicator for hyperthermia in the head and neck, International Journal of Hyperthermia, 23 (2007) 567-576.
[26] M. de Smet, E. Heijman, S. Langereis, N.M. Hijnen, H. Grull, Magnetic resonance imaging of high intensity focused ultrasound mediated drug delivery from temperature-sensitive liposomes: An in vivo proof-of-concept study, Journal of Controlled Release, 150 (2011) 102-110.
[27] M.L. Hauck, S.M. Larue, W.P. Petros, J.M. Poulson, D.H. Yu, I. Spasojevic, A.F. Pruitt, A. Klein, B. Case, D.E. Thrall, D. Needham, M.W. Dewhirst, Phase I trial of doxorubicin-containing low temperature sensitive liposomes in spontaneous canine tumors, Clinical Cancer Research, 12 (2006) 4004-4010.
[28] A.A. Manzoor, L.H. Lindner, C.D. Landon, J.-Y. Park, A.J. Simnick, M.R. Dreher, S. Das, G. Hanna, W. Park, A. Chilkoti, G.A. Koning, T.L.M. ten Hagen, D. Needham, M.W. Dewhirst, Overcoming limitations in nanoparticle drug delivery: triggered, intravascular release to improve drug penetration into tumors, Cancer Research, 72 (2012) 5566-5575.
[29] J.K. Mills, D. Needham, The materials engineering of temperature-sensitive liposomes, Methods Enzymol, 387 (2004) 82-113.
[30] D.D. Lasic, Preparation of liposomes, in: D.D. Lasic (Ed.) Liposomes from physics to applications, Elsevier Science, Amsterdam, 1993, pp. 63-107.
[31] L.D. Mayer, M.B. Bally, P.R. Cullis, Uptake of adriamycin into large unilamellar vesicles in response to a pH gradient, Biochim Biophys Acta, 857 (1986) 123-126.
[32] M. Hossann, M. Wiggenhorn, A. Schwerdt, K. Wachholz, N. Teichert, H. Eibl, R.D. Issels, L.H. Lindner, In vitro stability and content release properties of phosphatidylglyceroglycerol containing thermosensitive liposomes, Biochim.Biophys.Acta, 1768 (2007) 2491-2499.
[33] F.S. Rouser G, Yamamoto A., Two dimensional then layer chromatographic separation of polar lipids and determination of phospholipids by phosphorus analysis of spots., Lipids, 5 (1970) 494-496.
[34] X. Li, D.J. Hirsh, D. Cabral-Lilly, A. Zirkel, S.M. Gruner, A.S. Janoff, W.R. Perkins, Doxorubicin physical state in solution and inside liposomes loaded via a pH gradient, Biochim Biophys Acta, 1415 (1998) 23-40.
[35] M. Almgren, K. Edwards, G. Karlsson, Cryo transmission electron microscopy of liposomes and related structures, Colloids and Surfaces

a-Physicochemical and Engineering Aspects, 174 (2000) 3-21.
[36] N.W. Roehm, G.H. Rodgers, S.M. Hatfield, A.L. Glasebrook, An improved Colorimetric assay for cell-proliferation and viability utilizing the tetrazolium salt XTT, Journal of Immunological Methods, 142 (1991) 257-265.
[37] M.R. Dreher, W.G. Liu, C.R. Michelich, M.W. Dewhirst, F. Yuan, A. Chilkoti, Tumor vascular permeability, accumulation, and penetration of macromolecular drug carriers, J Natl Cancer I, 98 (2006) 335-344.
[38] A. Gasselhuber, M.R. Dreher, A. Partanen, P.S. Yarmolenko, D. Woods, B.J. Wood, D. Haemmerich, Targeted drug delivery by high intensity focused ultrasound mediated hyperthermia combined with temperature-sensitive liposomes: Computational modelling and preliminary in vivo validation, International Journal of Hyperthermia, 28 (2012) 337-348.
[39] B. Banno, L.M. Ickenstein, G.N. Chiu, M.B. Bally, J. Thewalt, E. Brief, E.K. Wasan, The functional roles of poly(ethylene glycol)-lipid and lysolipid in the drug retention and release from lysolipid-containing thermosensitive liposomes in vitro and in vivo, J Pharm Sci, 99 (2010) 2295-2308.
[40] W.T. Al-Jamal, Z.S. Al-Ahmady, K. Kostarelos, Pharmacokinetics & tissue distribution of temperature-sensitive liposomal doxorubicin in tumor-bearing mice triggered with mild hyperthermia, Biomaterials, 33 (2012) 4608-4617.
[41] M. Hossann, T. Wang, M. Wiggenhorn, R. Schmidt, A. Zengerle, G. Winter, H. Eibl, M. Peller, M. Reiser, R.D. Issels, L.H. Lindner, Size of thermosensitive liposomes influences content release, J Control Release, 147 (2010) 436-443.
[42] D.A. Averill, C. Su, Sensitization to the cytotoxicity of adriamycin by verapamil and heat in multidrug-resistant Chinese hamster ovary cells, Radiat Res, 151 (1999) 694-702.
[43] M. Hermisson, M. Weller, Hyperthermia enhanced chemosensitivity of human malignant glioma cells, Anticancer Res, 20 (2000) 1819-1823.
[44] G.P. Raaphorst, D.P. Yang, The evaluation of thermal cisplatin sensitization in normal and XP human cells using mild hyperthermia at 40 and 41 degrees C, Anticancer Res, 25 (2005) 2649-2653.
[45] H.H. Kampinga, Cell biological effects of hyperthermia alone or combined with radiation or drugs: a short introduction to newcomers in the field, Int J Hyperthermia, 22 (2006) 191-196.
[46] R.M. Schiffelers, G.A. Koning, T.L. ten Hagen, M.H. Fens, A.J. Schraa, A.P. Janssen, R.J. Kok, G. Molema, G. Storm, Anti-tumor efficacy of tumor vasculature-targeted liposomal doxorubicin, J Control Release, 91 (2003) 115-122.
[47] A.H. Negussie, J.L. Miller, G. Reddy, S.K. Drake, B.J. Wood, M.R. Dreher, Synthesis and in vitro evaluation of cyclic NGR peptide targeted thermally sensitive liposome, J Control Release, 143 (2010) 265-273.
[48] B.M. Dicheva, T.L. Hagen, L. Li, D. Schipper, A.L. Seynhaeve, G.C. Rhoon, A.M. Eggermont, L.H. Lindner, G.A. Koning, Cationic Thermosensitive Liposomes: A Novel Dual Targeted Heat-Triggered Drug Delivery Approach for Endothelial and Tumor Cells, Nano Lett, (2012). ePub ahead of print DOI: 10/1021/nl3014154.

Chapter 5

A novel two-step approach for advanced liposomal chemotherapy in combination with local mild hyperthermia

Li Li, Timo L.M. ten Hagen, Thomas Soullié, Csilla Scholten, Ann L.B. Seynhaeve, Alexander M.M. Eggermont, Gerben A. Koning

5

Submitted.

Chapter 6

The effect of heat cycling on intratumoral liposome accumulation and triggered drug release

Li Li, Timo L.M. ten Hagen, Martin Hossann, Thomas Soullié, Gerard C. van Rhoon, Alexander M.M. Eggermont, Gerben A. Koning

6

In preparation.

Chapter 7

Discussion

Nanocarriers

Nanoparticles can deliver a plethora of compounds such as chemotherapeutic drugs, contrast agents, genetic materials for both clinical diagnostics and treatment [1-3]. Multidisciplinary studies include the fields of material engineering, chemistry, genetics, proteomics, etc. [4-6]. In view of nanoparticle-mediated delivery of anticancer drugs, numerous new developments are being reported, e.g. on the incorporation of doxorubicin (Dox) into various nanoparticles for cancer treatment [7-11]. In this thesis, Dox is employed as the chemotherapeutic agent for the treatment of solid tumors. Liposomes of ~100 nm in diameter are chosen as nanoparticles for drug encapsulation and triggered release. An external stimulus of mild HT is applied to manipulate tumor microenvironment for improved liposomal drug delivery and triggered drug release from the liposomal nanocarrier.

DSPE-PEG$_{2000}$ in liposomes

Incorporation of DSPE-PEG$_{2000}$ in the liposome membrane affects membrane integrity and permeability, however the presence of PEG at the liposomal surface through a phospholipid bilayer anchor, is necessary for stealth liposomes with favourable pharmacokinetics [12-17]. More, DSPE-PEG$_{2000}$ prevents liposome aggregation in plasma [18]. In this thesis, classic temperature sensitive phospholipids 1,2-dipalmityol-*sn*-glycero-3-phosphocholine (DPPC) and 1,2-distearoyl-*sn*-glycero-3-phosphocholine (DSPC) are adopted to guarantee an active content release of thermosensitive liposomes (TSL) upon mild HT [19]. The fine-tuning of DSPE-PEG$_{2000}$ concentration for TSL generates essential features for both stability and release. TSL with optimized 5 mol% of DSPE-PEG$_{2000}$ showed significant higher content retention in serum at physiological temperature than TSL with higher DSPE-PEG$_{2000}$ concentrations, whereas content release of TSL with DSPE-PEG2000 densities lower than 5 mol% were only suboptimal. In Chapter 2, an optimal DSPE-PEG$_{2000}$ concentration was defined for the first time, for the use of TSL in combination with mild HT for triggered content release [20]. DSPE-PEG$_{2000}$ grafted on membrane surface causes steric repulsion between opposing polymers [21]. DSPE-PEG$_{2000}$ can form interdigitated mushroom, mushroom or brush regimes, depending on the density of grafting sites and DSPE-PEG$_{2000}$ polymer size [22]. DSPE-PEG$_{2000}$ from 1 to 4 mol% increases mushroom regime, while DSPE-PEG$_{2000}$ from 4 to 5 mol% drives mushroom-to-brush transition. Thus, the mix of regimes present during T_m in this optimized formulation is expected to ease content release. When DSPE-PEG$_{2000}$ further increases from 5 to 10 mol%, rigid brush regime grafted on the inner surface of lipid membrane occupies space of the aqueous core, reducing content encapsulation in our TSL. A dramatic decrease in content encapsulation was also observed in another TSL formulation (involving novel lipid 1,2-dipalmitoyl-*sn*-glycoero-3-phosphoglyceroglycerol) with 10 mol% DSPE-PEG$_{2000}$ by Hossann et al. [23-24]. In addition, Kenworthy

et al. found no further increase of liposome circulation time, when PEG-lipid concentration was more than 10 mol% [21]. They and others stated that higher concentrations of DSPE-PEG_{2000} or DSPE-PEG_{5000} would promote the formation of micelles and destabilization of liposomes [17]. It is likely that the micelle forming tendency of PEG-DSPE also could explain the increasing instability of our TSL formulation at PEG density of 6 mol% and higher. On the other hand, the heterogeneous DSPE-PEG_{2000} regimes around 5 mol% seems to stabilize the grain boundaries in DPPC/DSPC bilayers optimally, enhancing content retention at physiological temperature and release upon reaching T_m. In comparison, lysolipids are thought to also localize at the grain boundaries and cause porous defects upon reaching T_m, yet lysolipid presence also causes significant leakage of contents at physiological temperature. In an attempt to further stabilize lysolipid-based TSL (LTSL) the DSPE-PEG_{2000} concentration was also increased from previous 3.8 mol% to recent 5.2 mol% [25-26]. The combination of lysolipids and DSPE-PEG_{2000} can be replaced by single-chain pegylated Brij surfactants, and these Brij-TSL display a similar stability and release kinetics to lysolipid-based TSL [27-28]. The selection of Brij surfactants is based on their unique structure, which resembles single-chain lysolipids and DSPE-PEG_{2000}. Therefore, the loss of Dox from Dox-LTSL at 37°C was also resembled in Dox-Brij-TSL for the same reason. Lysolipids and Brij have the tendency to dissociate from the lipid membrane, causing Dox leakage [29-30, 27]. Although Brij surfactants are interesting alternatives to lysolipids and DSPE-PEG_{2000}, the pK of neither Dox-LTSL nor Dox-Brij-TSL is desirable for intravascular drug release, for which high concentration of liposomal drugs in circulation is required. In Chapter 4, *in vitro* studies present that Dox-TSL (DPPC/DSPC/DSPE-PEG_{2000} in molar ratio of 85:10:5) have significantly more Dox retention at 37°C in serum than Dox-LTSL (DPPC/MSPC/DSPE-PEG_{2000} in molar ratio of 85:10:5). An *in vivo* therapeutic efficacy study also presents that mice treated with Dox-TSL have longer tumor suppression and improved survival compared to Dox-LTSL, when applied in combination with local mild HT for intravascular drug release (Chapter 4). These results are likely to be explained by improved drug retention in circulation. However, pK study is required to prove the speculation. A balance between release rate at mild HT and stability at physiological temperature may better serve intravascular drug release. A Dox-TSL formulation with slower Dox release rate at mild HT of 42°C and high Dox retention at 37°C is designed for interstitial drug release in a two-step mild HT approach (Chapter 5). The optimal DSPE-PEG_{2000} concentration also benefits other non-temperature sensitive liposome formulations on drug loading efficiency, pK, and shelf-life.

TSL formulations for intravascular and interstitial drug release

Two TSL formulations are designed in this thesis, DPPC/DSPC/DSPE-PEG_{2000} in molar ratios of 80:15:5 and 55:40:5 (Chapter 2, 4 and 5). These fast and slow drug release formulations differ in stability and release kinetics at mild HT,

in order to suit treatment planning for intravascular and interstitial drug delivery [31]. Local mild HT at tumors to trigger drug release from circulating TSL is defined as intravascular release [25-26]. In this setting, intratumoral drug uptake relies on diffusion of drug after release, while redistribution of drug through circulation leads to systemic toxicity. In case of Dox-LTSL, inefficient Dox retention at 37°C in circulation also contributes to systemic toxicity. Local mild HT at tumors to trigger drug release from TSL in the extravascular extracellular space (EES) is defined as interstitial release. Intratumoral drug concentration highly depends on TSL extravasation and penetration in the interstitial space. The first, fast releasing, TSL (Dox-fTSL) formulation features a T_m at 43°C with rapid drug release at 42°C, which is desirable for intravascular content release from TSL upon mild HT (Chapter 4). However, different from the lysolipid-based TSL, which have a fast drug plasma clearance upon administration because of substantial Dox leakage at physiological temperature, Dox-fTSL improve content retention at physiological temperature (Chapter 4) [24, 32, 30, 33]. The second, slow releasing, TSL formulation (Dox-sTSL) with increased DSPC incorporation features a T_m at 45°C, resulting in significantly lowered content leakage of Dox-fTSL at 37°C, while still actively releasing their contents at 42°C, yet over a prolonged period of up to one hour (Chapter 5). Dox-sTSL is preferred for extravascular content release, which excessively relies on intratumoral liposome accumulation through liposome extravasation and penetration across tumor vasculature (Chapter 5).

Intravascular drug release approach

For intravascular drug release, Dox-fTSL is administered systemically followed by mild HT locally applied at tumors to trigger Dox release (Chapter 4). *In vitro* Dox-fTSL releases over 90% of its Dox within 5 minutes at 42°C, and *in vivo* circulating Dox-fTSL releases all Dox within 30 minutes at 42°C as evidenced by intravital confocal microscopy (Chapter 4). Thus, for the purpose of triggering Dox release, a thermal dose of 42°C for 30 minutes would be sufficient. However, local mild HT at tumors also increases the blood flow and interstitial fluid flow, which facilitates the intratumoral delivery of Dox-fTSL (Chapter 3) [34]. In addition these processes after Dox release from Dox-fTSL, favor the penetration of Dox throughout the tumor, which was demonstrated to increase up to 30 minutes during 1 hour mild HT treatment (Chapter 4). On the one hand, increased blood flow brings Dox-fTSL into heated tumors for drug release. On the other hand, increased blood flow may counteract the intratumoral drug accumulation by circulating drugs to redistribute in the rest of the body. It only takes about 20 seconds if not less for Dox-fTSL and Dox-LTSL in circulation to pass through heated tumors [35]. Therefore, ultra-fast drug release from TSL upon mild HT is crucial to meet the needs of intratumoral-intravascular drug release. In terms of encapsulated drugs, chemotherapeutic compounds with high cellular binding affinity are preferred

to ensure sufficient intratumoral drug uptake, minimizing drug washout. In Chapter 4, mild HT plus Dox-LTSL suppresses tumor growth of s.c. human BLM melanoma in mice for 8 days, while mild HT plus Dox-fTSL doubles tumor growth suppression to 16 days. More, mild HT plus Dox-fTSL triples survival of mice bearing s.c. human BLM melanoma by mild HT plus Dox-LTSL. Mild HT at 42°C also sensitizes *in vitro* tumor cell lines (murine BFS-1 sarcoma and human BLM melanoma) towards Dox-TSL, and speeds up the nuclear uptake of Dox in human BLM melanoma cell line and human umbilical vein endothelial cells (HUVEC) (Chapter 4). Heat stress causes cellular protein denaturation. Moreover, nuclear compartment is most sensitive for protein aggregation, which may contribute to cell death upon heat stress [36-39]. Some studies imply that chemotherapy combination with mild HT shows better cell killing. Comparing Dox-TSL and Dox-LTSL, the higher intratumoral chemodose leads to greater inhibition of cell proliferation, tumor suppression and better survival. In general, mild HT for 1 hour offers more advantages than mild HT for 30 minutes. Apart from duration, hyperthermic temperatures are just as important. Mild HT at 39°C can generally induce content release of most TSL with T_m around mild HT. Nevertheless, in many cases, TSL content release at 39°C is considered premature leakage, which shall be prevented if possible. Dox-fTSL has lesser leakage than Dox-LTSL at 39°C and significantly more Dox retention at 37°C, yet comparable release at 41-42°C (Chapter 4) [26]. Mild HT at 41-42°C is feasible in clinical application, however, it is highly dependent on tumor size, location and perfusion. Mild HT above 43°C can cause irreversible vascular damage, and is also difficult to reach in the clinic because of acute local discomfort on patients' disease sites. Therefore, TSL design with an aim for rapid release at mild HT of 41-42°C in combination with high stability at physiological temperature has optimal potential for successful clinical application.

Interstitial drug release approach

Interstitial drug release relies on intratumoral liposomal drug accumulation. Mild HT at tumors induces hyperpermeable tumor vasculature for liposomal drug extravasation and penetration into the EES (Chapter 3) [40-41]. The minimal thermal dose of 41°C for 30 minutes is sufficient to alter tumor vasculature permeability in four most common murine and xenograft tumor models. Mild HT of 41°C for 1 hour temporarily elevates tumor vasculature permeability for 8 hours post-HT, allowing liposomal drugs to escape from circulation and penetrate at least 27.5 μm into the interstitial space (Chapter 3). The observed duration of permeable tumor vasculature is significantly longer than that observed by Kong et al., who also mainly observed perivascular liposome accumulation and no deep tissue penetration [40-41]. Upon mild HT, intratumoral liposomal drug accumulation is heterogeneous, because of heterogeneous tumor vasculature permeability and perfusion. The temporarily elevated blood flow, insterstitial fluid flow and pressure changes during mild

HT are driving forces for liposomal drug deep penetration in the EES. The complexity of the EES depends on tumor type, size and structure of the specific interstitial matrix. Mild HT can have greater influence on the interstitial fluid flow, when the matrix structure is scattered. The level of interstitial liposomal drug accumulation is also determined by the size of liposomes. Chauhan et al. reported that decreasing interstitial fluid flow hindered the delivery of nanoparticles at 125 nm in diameter, however improved the delivery of nanoparticles at 12 nm in diameter [42]. This approach of tumor vasculature normalization by blocking vascular endothelial growth factor (VEGF) receptor-2, reduced pore size on vessel walls, increased steric and hydrodynamic hindrances, therefore limits liposome size for intratumoral accumulation. In contrast, we observed that mild HT enlarges the gaps between endothelial cells up to 10 μm to maximize extravascular localization of liposomes. This approach of tumor vasculature abnormalization is applicable to a broad spectrum of nanoparticles. For interstitial drug release, intratumoral accumulation of liposomal drugs rather than the actual drug release determines the therapeutic efficacy (Chapter 5). Two-step mild HT approach delivers drugs into tumors by firstly inducing hyperpermeable tumor vasculature for liposomal drug extravasation and penetration into the EES and secondly releasing drugs from TSL to induce their bioavailability. Long-circulating slow content releasing TSL are most adequate for two-step mild HT approach. Extravascularly accumulated Dox-sTSL slowly releases Dox upon mild HT at 42°C for 1 hour, comparably extravascular, non thermosensitive PLD (Doxil) also passively releases Dox over time through degradation or tumor cell internalization [43]. Tumor growth control and survival indicate that PLD in combination with two-step approach is as effective as Dox-sTSL in combination with two-step approach. The long-circulating nature of PLD and the first step of mild HT that induced hyperpermeable tumor vasculature both enable a maximal intratumoral PLD accumulation. These results confirm the importance of such an intratumoral liposomal drug accumulation process. As a matter of fact, mild HT to induce permeable tumor vasculature suits most nanocarriers if not all, for intratumoral drug delivery.

Intravascular vs. interstitial drug release

Comparing intravascular and interstitial drug release upon mild HT, TSL formulations with stable drug retention at physiological temperature are required for both approaches. For intravascular drug release, rapid drug release and precise heating of tumor volume are equally important for therapeutic efficacy [26]. However, for interstitial drug release, neither rapid drug release nor precise heating of tumor volume is essential for therapeutic efficacy (Chapter 5). This is because tumor vasculature responds significantly and becomes permeable upon mild HT, while normal vasculature remains intact (Chapter 3). This innate feature of tumor vasculature allows combination of TSL with regional mild HT when precise heating of tumor volume is not

feasible. After the first step of mild HT, systemic liposomal drugs of all kinds have the opportunity to gradually extravasate through permeable tumor vasculature and localize in tumors. Subsequent drug release and uptake by cells are much less time-restricted than with intravascular drug release. When mild HT is applied as the first step of mild HT, interstitial drug release is expected to be beneficial for advanced stages of cancer with multiple metastatic sites. Upon accumulation of liposomal drugs at metastatic sites, drug delivery depends on slow passive release or active triggered release. In case of mild HT triggered drug release from TSL, imaging guided drug release is feasible for clinical practice.

Heat cycling

Heat cycling is to alternate heat on and off moments. Considering the current technologies on mild HT, microwave applicators can provide continuous heat for a prolonged period. Newly developing high intensity focused ultrasound (HIFU) applications for mild HT generates heat with focused beams at a small volume, and scans through a defined region at high speed to elevate its local temperature. At a HIFU focused volume, the heat is on, after which the heat of that volume will be off until the next round of scanning arrives. The interval between two heat-on moments in HIFU is short for small tumors, and therefore is considered to provide continuous mild HT, but the interval will be longer when treating larger tumors in a multi focal approach. In this thesis, an external resistive electric heating coil is adopted to provide homogeneous mild HT at dorsal skin flap window chamber tissues. This applicator needs ~10 minutes to reach tissue temperature of 41-42°C, therefore heat cycling is scheduled to remain at 42°C for 1 or 5 minutes to balance the ratio of on-off moments, (Chapter 6). On-off heat alternations cause transient blood flow, interstitial fluid flow and pressure changes, in turn augment intratumoral liposomal drug delivery. Besides the fact that on-off heat alternations trigger content release from TSL during heat-on moments.

When mild HT is applied at a highly perfused tumor or regions of a tumor, local excessive heat is constantly removed from perfused regions through circulation also causing heat cycling effects. The study on heat cycling demonstrates that heat on and off stresses tumor vasculature to become permeable for liposome extravasation and interstitial penetration, and triggers content release from TSL. The concept of heat cycling brings an alternative to advanced liposomal drug delivery to solid tumors.

Conclusion

The overall goal of the thesis is to present the use of TSL and mild HT for advanced liposomal chemotherapy to solid tumors. TSL formulation is optimized regarding DSPE-PEG_{2000} concentration. Dox encapsulation is

customized for the specified TSL formulations. Tumor vasculature response to thermal stress is evaluated among multiple tumor models. Thermal doses of mild HT to induce permeable tumor vasculature and to trigger content release from the TSL are determined. Mild HT is applied in different formats for optimal intravascular or interstitial drug release. A single conventional mild HT, two-step mild HT and heat cycling can tailor treatment planning, according to tumor type, size, location and perfusion. An optimal treatment planning of mild HT and systemic liposomal chemotherapy can be assigned to a multitude of solid tumors. Additionally, nanocarriers from many other categories besides TSL can benefit from intratumoral accumulation and subsequent interstitial release. Taking the advantage of tumor microenvironment manipulation by mild HT, nanocarriers can be further optimized for various purposes. Future studies involve imaging-guided drug delivery and release, specific targeting on elevated protein expression, cellular membrane binding and internalization, synergy of two and more nanocarrier populations. The effect of mild HT on tumor microenvironment needs to be vastly explored. The combination and optimization of the use of nanocarriers and mild HT will meet the needs to improve clinical anticancer treatment outcome.

References:

[1] Q.A. Pankhurst, J. Connolly, S.K. Jones, J. Dobson, Applications of magnetic nanoparticles in biomedicine, Journal of Physics D-Applied Physics, 36 (2003) R167-R181.
[2] R.P. Choudhury, V. Fuster, Z.A. Fayad, Molecular, cellular and functional imaging of atherothrombosis, Nature Reviews Drug Discovery, 3 (2004) 913-925.
[3] X. Michalet, F.F. Pinaud, L.A. Bentolila, J.M. Tsay, S. Doose, J.J. Li, G. Sundaresan, A.M. Wu, S.S. Gambhir, S. Weiss, Quantum dots for live cells, in vivo imaging, and diagnostics, Science, 307 (2005) 538-544.
[4] A.N. Shipway, E. Katz, I. Willner, Nanoparticle arrays on surfaces for electronic, optical, and sensor applications, Chemphyschem, 1 (2000) 18-52.
[5] C. Loo, A. Lowery, N.J. Halas, J. West, R. Drezek, Immunotargeted nanoshells for integrated cancer imaging and therapy, Nano Letters, 5 (2005) 709-711.
[6] M. Lundqvist, J. Stigler, G. Elia, I. Lynch, T. Cedervall, K.A. Dawson, Nanoparticle size and surface properties determine the protein corona with possible implications for biological impacts, Proceedings of the National Academy of Sciences of the United States of America, 105 (2008) 14265-14270.
[7] L. Minati, V. Antonini, S. Torrengo, M. Dalla Serra, M. Boustta, X. Leclercq, C. Migliaresi, M. Vert, G. Speranza, Sustained in vitro release and cell uptake of doxorubicin adsorbed onto gold nanoparticles and covered by a polyelectrolyte complex layer, International Journal of Pharmaceutics, 438 (2012) 45-52.
[8] S. Mitra, B. Subia, P. Patra, S. Chandra, N. Debnath, S. Das, R. Banerjee, S.C. Kundu, P. Pramanik, A. Goswami, Porous ZnO nanorod for targeted delivery of doxorubicin: in vitro and in vivo response for therapeutic applications, Journal of Materials Chemistry, 22 (2012) 24145-24154.
[9] L. Sun, X.F. Ma, C.M. Dong, B.S. Zhu, X.Y. Zhu, NIR-Responsive and Lectin-Binding Doxorubicin-Loaded Nanomedicine from Janus-Type Dendritic PAMAM Amphiphiles, Biomacromolecules, 13 (2012) 3581-3591.
[10] Z.H. Wang, Y. Yu, W.B. Dai, J.K. Lu, J.R. Cui, H.N. Wu, L. Yuan, H. Zhang, X.Q. Wang, J.C. Wang, X. Zhang, Q. Zhan, The use of a tumor metastasis targeting peptide to deliver doxorubicin-containing liposomes to highly metastatic cancer, Biomaterials, 33 (2012) 8451-8460.
[11] T. Xing, X.Z. Yang, F. Wang, B. Lai, L.F. Yan, Synthesis of polypeptide conjugated with near infrared fluorescence probe and doxorubicin for pH-responsive and image-guided drug delivery, Journal of Materials Chemistry, 22 (2012) 22290-22300.
[12] T.M. Allen, C. Hansen, F. Martin, C. Redemann, A. Yauyoung, Liposomes Containing Synthetic Lipid Derivatives of Poly(Ethylene Glycol) Show Prolonged Circulation Half-Lives Invivo, Biochimica Et Biophysica Acta, 1066 (1991) 29-36.

[13] D. Papahadjopoulos, T.M. Allen, A. Gabizon, E. Mayhew, K. Matthay, S.K. Huang, K.D. Lee, M.C. Woodle, D.D. Lasic, C. Redemann, F.J. Martin, Sterically Stabilized Liposomes - Improvements in Pharmacokinetics and Antitumor Therapeutic Efficacy, Proceedings of the National Academy of Sciences of the United States of America, 88 (1991) 11460-11464.
[14] K. Edwards, M. Johnsson, G. Karlsson, M. Silvander, Effect of polyethyleneglycol-phospholipids on aggregate structure in preparations of small unilamellar liposomes, Biophys J, 73 (1997) 258-266.
[15] M. Johnsson, K. Edwards, Liposomes, disks, and spherical micelles: aggregate structure in mixtures of gel phase phosphatidylcholines and poly(ethylene glycol)-phospholipids, Biophys J, 85 (2003) 3839-3847.
[16] N. Dos Santos, C. Allen, A.M. Doppen, M. Anantha, K.A. Cox, R.C. Gallagher, G. Karlsson, K. Edwards, G. Kenner, L. Samuels, M.S. Webb, M.B. Bally, Influence of poly(ethylene glycol) grafting density and polymer length on liposomes: relating plasma circulation lifetimes to protein binding, Biochim Biophys Acta, 1768 (2007) 1367-1377.
[17] M.C. Sandstrom, E. Johansson, K. Edwards, Influence of preparation path on the formation of discs and threadlike micelles in DSPE-PEG(2000)/lipid systems, Biophys Chem, 132 (2008) 97-103.
[18] H. Yoshioka, Surface Modification of Hemoglobin-Containing Liposomes with Polyethylene-Glycol Prevents Liposome Aggregation in Blood-Plasma, Biomaterials, 12 (1991) 861-864.
[19] W.J. Yatvin MB, Dennis WH, Blumenthal R, Design of liposomes for enhanced local release of drugs by hyperthermia, Science, 202 (1978) 1290-1293.
[20] L. Li, T.L. ten Hagen, D. Schipper, T.M. Wijnberg, G.C. van Rhoon, A.M. Eggermont, L.H. Lindner, G.A. Koning, Triggered content release from optimized stealth thermosensitive liposomes using mild hyperthermia, J Control Release, 143 (2010) 274-279.
[21] A.K. Kenworthy, S.A. Simon, T.J. McIntosh, Structure and Phase-Behavior of Lipid Suspensions Containing Phospholipids with Covalently Attached Poly(Ethylene Glycol), Biophysical Journal, 68 (1995) 1903-1920.
[22] P.G. deGennes, Polymers at an interface: a simplified view., Adv. Colloid Interface Sci. , 27 (1987) 189-209.
[23] L.H. Lindner, M.E. Eichhorn, H. Eibl, N. Teichert, M. Schmitt-Sody, R.D. Issels, M. Dellian, Novel temperature-sensitive liposomes with prolonged circulation time, Clinical Cancer Research, 10 (2004) 2168-2178.
[24] M. Hossann, M. Wiggenhorn, A. Schwerdt, K. Wachholz, N. Teichert, H. Eibl, R.D. Issels, L.H. Lindner, In vitro stability and content release properties of phosphatidylglyceroglycerol containing thermosensitive liposomes, Biochim.Biophys.Acta, 1768 (2007) 2491-2499.
[25] P.S. Yarmolenko, Y. Zhao, C. Landon, I. Spasojevic, F. Yuan, D. Needham, B.L. Viglianti, M.W. Dewhirst, Comparative effects of thermosensitive doxorubicin-containing liposomes and hyperthermia in human and murine tumours, Int J Hyperthermia, 26 (2010) 485-498.

[26] A.A. Manzoor, L.H. Lindner, C.D. Landon, J.-Y. Park, A.J. Simnick, M.R. Dreher, S. Das, G. Hanna, W. Park, A. Chilkoti, G.A. Koning, T.L.M. ten Hagen, D. Needham, M.W. Dewhirst, Overcoming limitations in nanoparticle drug delivery: triggered, intravascular release to improve drug penetration into tumors, Cancer Research, (2012).
[27] T. Tagami, M.J. Ernsting, S.D. Li, Efficient tumor regression by a single and low dose treatment with a novel and enhanced formulation of thermosensitive liposomal doxorubicin, Journal of Controlled Release, 152 (2011) 303-309.
[28] T. Tagami, M.J. Ernsting, S.D. Li, Optimization of a novel and improved thermosensitive liposome formulated with DPPC and a Brij surfactant using a robust in vitro system, Journal of Controlled Release, 154 (2011) 290-297.
[29] M.C. Sandstrom, L.M. Ickenstein, L.D. Mayer, K. Edwards, Effects of lipid segregation and lysolipid dissociation on drug release from thermosensitive liposomes, Journal of Controlled Release, 107 (2005) 131-142.
[30] B. Banno, L.M. Ickenstein, G.N. Chiu, M.B. Bally, J. Thewalt, E. Brief, E.K. Wasan, The functional roles of poly(ethylene glycol)-lipid and lysolipid in the drug retention and release from lysolipid-containing thermosensitive liposomes in vitro and in vivo, J Pharm Sci, 99 (2010) 2295-2308.
[31] D. Needham, M.W. Dewhirst, The development and testing of a new temperature-sensitive drug delivery system for the treatment of solid tumors, Advanced Drug Delivery Reviews, 53 (2001) 285-305.
[32] R.T. Poon, N. Borys, Lyso-thermosensitive liposomal doxorubicin: a novel approach to enhance efficacy of thermal ablation of liver cancer, Expert Opin Pharmacother, 10 (2009) 333-343.
[33] W.T. Al-Jamal, Z.S. Al-Ahmady, K. Kostarelos, Pharmacokinetics & tissue distribution of temperature-sensitive liposomal doxorubicin in tumor-bearing mice triggered with mild hyperthermia, Biomaterials, 33 (2012) 4608-4617.
[34] C.W. Song, Effect of local hyperthermia on blood flow and microenvironment: a review, Cancer Res, 44 (1984) 4721s-4730s.
[35] A.A. Manzoor, L.H. Lindner, C.D. Landon, J.Y. Park, A.J. Simnick, M.R. Dreher, S. Das, G. Hanna, W. Park, A. Chilkoti, G.A. Koning, T.L.M. ten Hagen, D. Needham, M.W. Dewhirst, Overcoming Limitations in Nanoparticle Drug Delivery: Triggered, Intravascular Release to Improve Drug Penetration into Tumors, Cancer Research, 72 (2012) 5566-5575.
[36] H.H. Kampinga, N. Turkeluygur, J.L.R. Roti, A.W.T. Konings, The relationship of increased nuclear-protein contnent induced by hyperthermia to killing of HeLa S3 cells, Radiation Research, 117 (1989) 511-522.
[37] A.A. Michels, V.T. Nguyen, A.W. Konings, H.H. Kampinga, O. Bensaude, Thermostability of a nuclear-targeted luciferase expressed in mammalian-cells-destabilizing influence of the intranuclear microenvironment, European Journal of Biochemistry, 234 (1995) 382-389.
[38] J.R. Lepock, H.E. Frey, M.L. Heynen, G.A. Senisterra, R.L. Warters, The nuclear matrix is a thermolabile cellular structure, Cell Stress & Chaperones, 6 (2001) 136-147.
[39] J.R. Lepock, Role of nuclear protein denaturation and aggregation in

thermal radiosensitization, International Journal of Hyperthermia, 20 (2004) 115-130.
[40] G. Kong, R.D. Braun, M.W. Dewhirst, Hyperthermia enables tumor-specific nanoparticle delivery: effect of particle size, Cancer Res, 60 (2000) 4440-4445.
[41] G. Kong, R.D. Braun, M.W. Dewhirst, Characterization of the effect of hyperthermia on nanoparticle extravasation from tumor vasculature, Cancer Res, 61 (2001) 3027-3032.
[42] V.P. Chauhan, T. Stylianopoulos, J.D. Martin, Z. Popovic, O. Chen, W.S. Kamoun, M.G. Bawendi, D. Fukumura, R.K. Jain, Normalization of tumour blood vessels improves the delivery of nanomedicines in a size-dependent manner, Nat Nanotechnol, 7 (2012) 383-388.
[43] A.L.B. Seynhaeve, S. Hoving, D. Schipper, C.E. Vermeulen, G.A. de Wiel-Ambagtsheer, S.T. van Tiel, A.M.M. Eggermont, T.L.M. ten Hagen, Tumor necrosis factor alpha mediates homogeneous distribution of liposomes in murine melanoma that contributes to a better tumor response, Cancer Research, 67 (2007) 9455-9462.

Summary

Liposomes are nano-sized drug carriers widely used to deliver chemotherapeutic compounds in cancer treatments. While prolonging drug retention in circulation and preventing certain toxic side-effects, liposomal drugs still need to overcome matters on specific accumulation in the tumor and controlled drug release. The aim of this thesis is to introduce local mild hyperthermia (HT) and thermosensitive liposomes (TSL) to liposomal chemotherapy, to improve therapeutic outcome.

Chapter 1 introduces in more detail the background of the study and gives an introduction to the several sections of the thesis and research topics. In **Chapter 2**, we describe a TSL formulation composed of classic temperature sensitive phospholipids, omitting the lyso-lecithin used in a clinically applied formulation for ultrafast release, but with an optimized poly(ethylene glycol) (PEG) surface concentration for stability at physiological temperature and fast release at mild HT (41-43°C). These optimized TSL ensure a prolonged content retention at physiological temperature when exposed to serum proteins, and also feature *in vitro* and *in vivo* rapid content release at mild HT. At present, two major drug delivery approaches using TSL and mild HT are being proposed. The first approach aims to use mild HT in a two-step approach to first manipulate tumor vasculature, promoting enhanced liposome extravasation, followed by a second mild HT to trigger drug release.

Chapter 3 investigates the first step in this approach; the effect of mild HT on tumor vasculature permeability for liposome extravasation and intratumoral penetration. Multiple thermal doses are compared for levels of liposome density in the extravascular extracellular space (EES), penetration depth in murine and xenograft tumor models. Mild HT induced heterogeneous intratumoral liposome accumulation in all tumor models. Liposomes extravasated through tumor vasculature and penetrated deep into the interstitial space following the HT enhanced interstitial fluid flow.

A second drug delivery approach is the intravascular drug release approach in which circulating TSL are triggered to rapidly release their contents upon their passage through tumor vasculature. This approach is demonstrated in **Chapter 4,** which focuses on *in vitro* and *in vivo* profiling of doxorubicin (Dox) encapsulated in optimized TSL. Dox-TSL *in vitro* stability and release kinetics in serum, and *in vivo* tumor growth control and survival after a single treatment of intravascular Dox release are compared to Dox encapsulated in lyso-lipid based TSL, which is currently in clinical trials. Optimized Dox-TSL further prolonged tumor growth control and improved survival than lyso-lipid based TSL when applied in combination with mild HT.

Chapter 5 proposes the novel two-step mild HT approach. The first-step local

mild HT is for inducing permeable tumor vasculature, after which liposomal drugs are systemically administered at physiological tumor temperature. Liposomal drugs are allowed to circulate for two hours, to gradually accumulate in the EES in tumors through permeable tumor vasculature. Then, the second-step local mild HT is applied to trigger interstitial Dox release from extravasated Dox-TSL. Tumor growth control and survival after the two-step mild HT approach is compared to intravascular release approach. The two-step mild HT approach was less effective compared to intravascular release approach. However, the two-step mild HT approach is an alternative to conventional mild HT, and may be more beneficial to large and deep seated tumors when regional mild HT is required.

Chapter 6 studies the effect of heat cycling on tumor vasculature permeability and content release kinetics of TSL. Heat cycling was used to mimic the clinical application of high intensity focused ultrasound (HIFU) based heating of large tumors. While HIFU, with a treatment focus of a few millimeters, is scanning through tumors, every fraction of a tumor is experiencing tissue heating and cooling alternately, resulting in a rather heterogeneous heat delivery. Through each heat cycle, contents are released from TSL and tumor vasculature accumulates heat stress affecting its permeability. The therapeutic efficacy of heat cycling is investigated and compared to continuous mild HT. Heat cycling induced hyperpermeable tumor vasculature for intratumoral liposomal drug accumulation, triggered intravascular Dox release from TSL, and effectively suppressed tumor growth, which was merely as sufficient as continuous mild HT.

Chapter 7 discusses the results of the studies in relation to the current status of mild HT mediated drug delivery using TSL and presents an outlook for future developments and possible further improvements of this triggered drug delivery approach.

Samenvatting

Liposomen zijn kleine vetbollen met een diameter van circa 100 nm en worden veel gebruikt als drager systeem voor chemotherapeutica in de behandeling van kanker. Hoewel insluiting van chemotherapeutica in liposomen de verblijftijd in de bloedbaan kan verlengen en bepaalde toxische bijwerkingen kan voorkomen, moeten de liposomen nog wel in hogere mate ophopen in tumoren en daar ook gecontroleerd hun inhoud vrijgeven. Het doel van het onderzoek beschreven in dit proefschrift is het gebruik van locale milde hyperthermie en thermosensitieve liposomen (TSL) om de therapeutische uitkomst van liposomale chemotherapie verder te verbeteren.

In hoofdstuk 1 wordt de achtergrond van de studie nader geïntroduceerd en wordt een introductie gegeven op de verschillende onderdelen en onderzoeksonderwerpen van de studie. In hoofdstuk 2, beschrijven we een TSL formulering bereid met veelgebruikte temperatuur-gevoelige fosfolipiden, waarin lyso-lecithine, die in een klinische toegepaste formulering wordt gebruikt voor ultrasnelle release, niet is opgenomen. Wel is van deze TSL de concentratie poly(ethyleen glycol) (PEG) op het liposoom oppervlak geoptimaliseerd om TSL stabiliteit bij fysiologische temperatuur te combineren met een snelle afgifte van de inhoud tijdens milde hyperthermie (41-43 °C). Deze geoptimaliseerde TSL waren in staat langdurig hun inhoud vast te houden bij fysiologische temperaturen in aanwezigheid van serumeiwitten en gaven snelle afgifte van hun inhoud tijdens milde hyperthermie. Er worden twee belangrijke methoden voorgesteld om geneesmiddelafgifte te verkrijgen met TSL in combinatie met milde hyperthermie. De eerste methode heeft als doel milde hyperthermie toe te passen in een twee-staps aanpak waarin de eerste hyperthermiebehandeling het tumorvaatbed manipuleert en daarmee accumulatie van liposomen in de tumor promoot, gevolgd door een tweede milde hyperthermiebehandeling die chemotherapie afgifte induceert.

Hoofdstuk 3 bestudeert de eerste stap van deze methode; het effect van milde hyperthermie op de permeabiliteit van tumorbloedvaten, op liposoomuittreding en verdere doordringing in het tumorweefsel. De effecten van verschillende temperatuurdoses op liposoomophoping en doordringingsdiepte in de tumor zijn vergeleken in verschillende muizen en humane (xenograft) tumor modellen. Milde hyperthermie induceerde heterogene intratumorale ophoping van liposomen in alle tumormodellen. Liposomen extravaseerden uit tumorbloedvaten en drongen ver het tumor interstitium binnen onder invloed van de door de hyperthermie toegenomen interstitiële vloeistofstroom.

De tweede methode voor geneesmiddelafgifte door middel van TSL en hyperthermie is de intravasculaire afgifte, waarbij circulerende TSL tijdens passage door tumorbloedvaten worden verwarmd en vervolgens snel locaal

in het tumorgebied hun inhoud afgeven. Deze methode is gedemonstreerd in hoofdstuk 4, wat zich richt op de *in vitro* en *in vivo* stabiliteit en afgiftekinetiek van doxorubicine (Dox) ingesloten in geoptimaliseerde TSL. Van deze Dox-TSL is *in vitro* de stabiliteit en afgiftekinetiek bepaald in serum en zijn *in vivo* de effecten op tumorgroei en overleving van tumordragende muizen na eenmalige behandeling vergeleken met een behandeling met Dox in lysolipide-gebaseerde TSL, een formulering die op dit moment in klinische studies wordt gebruikt. De geoptimaliseerde Dox-TSL waren in staat tumorgroei sterker te remmen en de overlevingsduur van tumordragende muizen te verlengen in vergelijking met de lysolipid-Dox-TSL behandeling, in combinatie met milde hyperthermie.

In hoofdstuk 5 wordt de twee-staps milde hyperthermie behandelingsmethode nader onderzocht. De eerste locale milde hyperthermie zal het tumorvasculatuur meer permeabel maken, waarna de liposomale chemotherapie systemisch wordt toegediend bij een fysiologische tumor temperatuur. Liposomen krijgen 2 uur de tijd voor circulatie en zullen in die periode geleidelijk ophopen in de tumor door de permeabele tumorbloedvaten. Vervolgens zal de tweede milde hyperthermie behandeling worden toegepast om in het tumor interstitium Dox afgifte te stimuleren van geëxtravaseerde liposomen. De effectiviteit van deze twee-staps milde hyperthermie methode op tumor groei en overleving van tumordragende muizen is vergeleken met die van de intravasculaire afgifte en bleek minder groot. Desalniettemin biedt de twee-staps methode een belangrijk alternatief die voordeel kan opleveren bij de behandeling van grote en diep gelegen tumoren die normaliter door middel van regionale milde hyperthermie worden behandeld.

Hoofdstuk 6 bestudeerd de effecten van warmtecycli op de permeabiliteit van tumorbloedvaten en afgifte van de inhoud van TSL. De toepassing van warmtecycli benadert de klinische toepassing van high intensity focused ultrasound (HIFU) voor de verwarming van grote tumoren. Wanneer tijdens een dergelijke HIFU behandeling de tumor wordt gescand met gericht hoog intens ultrageluid met een behandelingsfocus van slechts enkele millimeters, zullen de verschillende delen van de tumor afwisselende cycli van opwarming en afkoeling ondervinden, hetgeen leidt tot een heterogene temperatuursverdeling. Tijdens iedere warmteclycus zal inhoud van de TSL in dat gebied worden vrijgegeven en ondervindt het tumorvasculatuur warmte stress, hetgeen de vaatpermeabiliteit zal verhogen. De therapeutische werking van warmtecycli is onderzocht en vergeleken met de toepassing van continue milde hyperthermie. Toepassing van warmtecycli induceerde naast verhoogde tumorvaatpermeabiliteit en extravasatie van liposomen ook intravasculaire Dox afgifte uit TSL en was in staat om de tumorgroei effectief te onderdrukken in een vergelijkbare mate als bij de combinatie van continue milde hyperthermie en Dox-TSL.

In hoofdstuk 7 worden de resultaten van de studies bediscussieerd in verhouding tot de huidige status van milde hyperthermie-gemedieerde chemotherapie afgifte door TSL. Tevens presenteert dit hoofdstuk een vooruitzicht op toekomstige ontwikkelingen en mogelijke verdere verbeteringen van deze warmtegecontroleerde chemotherapie afgifte methode.

by Gerben A. Koning

Appendix

PhD Portfolio Summary
Curriculum Vitae
List of publications
Statement of appreciation
About the author

A

Erasmus MC
Universitair Medisch Centrum Rotterdam

PhD Portfolio Summary
Summary of PhD training and teaching activities

Name PhD student:	PhD period:
Li Li	27/02/2008 – 26/02/2013
Erasmus MC Department:	Promotor(s):
Surgery	Prof. A.M.M. Eggermont
Research School:	Supervisor:
Molecular Medicine	Dr. G.A. Koning

1. PhD training

	Year	ECTS
General academic skills		
- English Biomedical Writing and Communication	2008	2
- Photoshop and Illustrator CS5 Workshop for PhD-students and other researchers	2011	0.3
- Research management for PhD-students	2011	1
- Workshop Writing Successful Grant Proposals	2011	0.5
- Fire/Life Safety (Duke University)	2011	0.1
- Hazard Awareness for Animal Facilities (Duke University)	2011	0.1
- Ergonomics and Safety at DLAR and Other Animal Facilities (Duke University)	2011	0.1
Research skills		
- Basic Introduction Course on SPSS	2010	1
- Molecular Medicine	2010	0.7
- Short Introductory Course on Statistics & Survival Analysis for MD's	2010	0.5
- Laboratory Safety – General (Duke University)	2011	0.1
- Animal Handlers Part 1 – Regulations Impacting Animal Care and Use (Duke University)	2011	0.1
- Animal Handlers Part 2 – Veterinary Care (Duke University)	2011	0.1
- Animal Handlers Part 3 – Annual Refresher Training (Duke University)	2011	0.1
- Microscopic Image Analysis: From Theory to Practice	2011	0.8
In-depth courses		
- Animal Imaging Workshop by AMIE	2008	1.4
- Animal Experimentation Article 9	2008	3
- In Vivo Imaging "From Molecule to Organism"	2008	1.8
- Dox loading and characterization methods, Munich, Germany	2009	2
- Advanced Course "Molecular Immunology"	2010	3
- Basic and Translational Oncology	2010	1.8
- Mouse window models, Durham, USA	2011	2
- Advanced Drug Delivery & Drug Targeting	2011	1.8

Presentations		
- Imagination in Nijmegen, NL. "Triggered content release from optimized stealth thermosensitive liposomes using mild hyperthermia"	2009	1
- STM in Clearwater Beach, FL, USA. "A two-step approach for intratumoral drug delivery using optimized long-circulating thermosensitive liposomes and mild hyperthermia"	2010	1
- ESHO in Rotterdam, NL. "A two-step approach for intratumoral drug delivery using optimized long-circulating thermosensitive liposomes and mild hyperthermia"	2010	1
- KWF-Hyperthermia in Rotterdam, NL. "Two-step hyperthermia guided liposomal anticancer drug delivery"	2010	1
- Targeted Nanomedicine in Leiden, NL. "Hyperthermia induced intratumoral liposomal drug delivery and triggered release"	2010	1
- MUSC in Charleston, SC, USA. "Mild hyperthermia and thermosensitive liposomes to improve chemotherapy delivery to solid tumors"	2010	1
- Duke in Durham, NC, USA. "Mild hyperthermia induced liposomal drug delivery and triggered drug release in solid tumors"	2010	1
- STM in New Orleans, LA, USA. "Hyperthermia induced intratumoral liposomal drug delivery and triggered release"	2011	1
- KWF-Hyperthermia in Amsterdam, NL. "Launching the chemobombs for advanced drug delivery"	2011	1
- ESHO in Aarhus, Denmark. "Mild hyperthermia induced liposomal drug delivery and triggered drug release in solid tumors"	2011	1
- Molmed Day in Rotterdam, NL. "Launching the chemo bombs for advanced drug delivery to solid tumors"	2012	1
- STM in Portland, OR, USA. "Launching the chemo bombs for advanced drug delivery to solid tumors"	2012	1
International conferences		
- International Liposome Society – Liposome Advances, London, UK	2009	1
- Annual Meeting of the Society for Thermal Medicine, Clearwater Beach, FL, USA	2010	1
- 26th Annual Meeting of the European Society for Hyperthermic Oncology, Rotterdam, NL	2010	1
- Liposome Research Days, Vancouver, BC, Canada	2010	1
- Annual Meeting of the Society for Thermal Medicine, New Orleans, LA, USA	2011	1
- 27th Annual Meeting of the European Society for Hyperthermic Oncology, Aarhus, Denmark	2011	1
- Annual Meeting of the Society for Thermal Medicine, Portland, OR, USA	2012	1

Seminars and workshops		
- Mountain/Sea Liposome Workshop, Oberjoch, Germany	2008	1
- Lab science day	2008	0.2
- JNI oncology lectures	2008	1
- Surgery staff day	2008	0.2
- MolMed day	2009	0.2
- Lab science day	2009	0.2
- JNI oncology lectures	2009	1
- Mountain/Sea Liposome Workshop, Ameland, NL	2009	1
- Imagination, Nijmegen, NL	2009	0.2
- Surgery staff day	2009	0.2
- KWF Hyperthermia workshop, Rotterdam, NL	2009	0.2
- Molmed day	2010	0.2
- Lab science day	2010	0.2
- JNI oncology lectures	2010	0.2
- KWF Hyperthermia workshop, Rotterdam, NL	2010	0.2
- Molmed day	2011	0.2
- Lab science day	2011	0.2
- JNI oncology lectures	2011	0.2
- KWF Hyperthermia workshop, Amsterdam, NL	2011	0.2
- Molmed day	2012	0.2
2. Teaching activities		
	Year	**ECTS**
Supervising practicals and excursions		
- Liposome preparation and characterization, trainee Sylvia	2008	2
- Liposome preparation and characterization, trainee Halil	2009	2
- Liposome preparation and characterization, technician Halil	2010	2

Curriculum Vitae

Education:

27/02/2008 – 26/02/2013
PhD at Department of Surgery, Erasmus MC, Rotterdam, the Netherlands.
26/09/2005 – 13/09/2006
MSc in Biomedical Sciences at University of Bradford, Bradford, UK.
01/09/2000 – 25/06/2005
BSc in Medicine at Southern Medical University, Guangzhou, Guangdong, China.

Experience:

27/02/2008 – 26/02/2013
Junior Researcher at Erasmus MC, Rotterdam, the Netherlands.
01/02/2007 – 01/12/2007
Research Assistant at School of Pharmacy, University of Bradford, Bradford, UK.
11/02/2004 – 01/01/2005
Surgical Intern at Beijing Artillery General Hospital of P.R. China, Beijing, China.
15/02/2003 – 05/01/2004
Medical Intern at Guangzhou Military General Hospital of China, Guangzhou, China.

Major clinical skills:

Clinical diagnoses, radiological diagnoses, surgery, clinical treatment therapies, oriental-style therapies, etc..

Laboratory skills:

Dorsal skin flap window chamber and mammary window models, liposomes, cell culture, chemosensitivity assay, fluorescent spectrometry, intravital confocal microscopy, DNA thermal melting assay, etc..

Certificates:

Legal qualification as an animal experimentalist (Article 9).

Languages:

Chinese mandarin, native.
English, proficient.

Awards:

1. Nominatee for Chinese Government Award for Outstanding Self-Financed Students Abroad 2012.
2. New Investigator Award Winner at STM (Society for Thermal Medicine) in Portland, OR, in 2012.
3. Nominatee for Chinese Government Award for Outstanding Self-Financed Students Abroad 2011.
4. Student Award Winner for Biology at ESHO (European Society for Hyperthermic Oncology) in Aarhus, Denmark, in 2011.

Grants:

1. KWF (Dutch Cancer Society) travel grants 2011.

Visiting researcher:

1. 08/04/2011 – 26/04/2011, Prof. Mark Dewhirst's lab at Duke university, Durham, North Carolina, USA.
2. 27/06/2009 – 04/07/2009, Prof. Rolf Issels' lab at University Hospital Grosshadern, Ludwig-Maxililians University, Munich, Germany.

Lectures:

1. STM2012 in Portland, OR, USA, "Launching the chemo bombs for advanced drug delivery to solid tumors".
2. Molmed Day 2012, Rotterdam, NL, "Launching the chemo bombs for advanced drug delivery to solid tumors".
3. ESHO 2011 in Aarhus, Denmark, "Mild hyperthermia induced liposomal drug delivery and triggered drug release in solid tumors".
4. KWF-Hyperthermia on 11/11/2011 in Amsterdam, NL, "Launching the chemo bombs for advanced drug delivery".
5. STM 2011 in New Orleans, LA, USA, "Hyperthermia induced intratumoral liposomal drug delivery and triggered release".
6. Duke University in Durham, NC, USA, 19/04/2010. "Mild hyperthermia induced liposomal drug delivery and triggered drug release in solid tumors".
7. MUSC (Medical University of South Carolina) in Charleston, SC, USA, 11/04/2011, "Mild hyperthermia and thermosensitive liposomes to improve chemotherapy delivery to solid tumors".
8. Targeted Nanomedicine 2010 in Leiden, NL, "Hyperthermia induced intratumoral liposomal drug delivery and triggered release".
9. KWF-Hyperthermia 2010 in Rotterdam, NL, "Two-step hyperthermia guided liposomal anticancer drug delivery".
10. ESHO 2010 in Rotterdam, NL, "A two-step approach for intratumoral drug

delivery using optimized long-circulating thermosensitive liposomes and mild hyperthermia".
11. STM 2010 in Clearwater Beach, FL, USA, "A two-step approach for intratumoral drug delivery using optimized long-circulating thermosensitive liposomes and mild hyperthermia".
12. Imagination 2009 in Nijmegen, NL, "Triggered content release from optimized stealth thermosensitive liposomes using mild hyperthermia".
13. STM 2009 in Tucson, AZ, USA, "Triggered content release from optimized stealth thermosensitive liposomes using mild hyperthermia"

Chair:

1. Co-chair in Nanotechnology and Thermal Medicine session at STM 2012.
2. Co-chair in Thermosensitive nanomedicine session at ESHO 2010.

Memberships:

Student member of STM in 2009-2012.
Student member of ESHO in 2010-2012.
Associate member of AACR 2010-2013.
Junior Scholar in Training member of RRS in 2012.

List of publications:

1. **Li L**, ten Hagen TL, van Rhoon GC, Eggermont AM, Haemmerich D, Koning GA. The effect of heat cycling on tumor vasculature permeability for liposome extravasation and drug delivery. Journal of the National Cancer Institute, submitted. 2013.
2. **Li L**, ten Hagen TL, Eggermont AM, Koning GA. A novel two-step approach for advanced liposomal chemotherapy. Journal of Controlled Release, submitted. 2013.
3. **Li L**, ten Hagen TL, Hossann M, van Rhoon GC, Eggermont AM, Haemmerich D, Koning GA. Mild hyperthermia triggered Dox release from optimized stealth thermosensitive liposomes for intratumoral drug delivery. Journal of Controlled Release, in press. 2013.
4. **Li L**, ten Hagen TLM, Gasselhuber A, Yatvin J, van Rhoon GC, Eggermont AM, Haemmerich D, Koning GA. Improved intratumoral nanoparticle extravasation and penetration by mild hyperthermia. Journal of Controlled Release, in press. 2013. DOI: 10.1016/j.jconrel.2013.01.026.
5. Garelnabi EAE, Pletsas D, **Li L**, Kiakos K, Karodia N, Hartley JA, Phillips RM, Wheelhouse RT. A Strategy for Imidazotetrazine Prodrugs with Anti-cancer Activity Independent of MGMT and MMR. ACS Medicinal Chemistry Letters. 2012 3(12):965-8.
6. Dicheva B, ten Hagen TLM, **Li L**, Schipper D, Seynhaeve A, Rhoon G, Eggermont A, Lindner L, Koning GA. Cationic thermosensitive liposomes – a novel dual targeted heat-triggered drug delivery approach for endothelial and tumor cells. Nano Letters. Epub 2012 Jun 13.
7. Koning GA, **Li L**, ten Hagen TLM. Thermosensitive liposomes for the delivery of cancer therapeutics. Therapeutic Delivery. 2010 Nov 1(5):707-11.
8. **Li L**, ten Hagen TLM, Schipper D, Wijnberg TM, van Rhoon GC, Eggermont AM, Lindner LH, Koning GA. Triggered content release from optimized stealth thermosensitive liposomes using mild hyperthermia. Journal of Controlled Release. 2010 Apr 19;143(2):274-9.

Statement of appreciation

I would like to thank **Gerben**, **Timo** and **Lex** for offering me this great project and the best opportunities to grow during these five years. **Lex** gave me the freedom that a PhD student could only dream of, the understanding that one could ever wish for, and the salvation through my most difficult moments. I will always be very proud to brag about the **Prof. Eggermont** that I know of. Thank you, **Lex**, for being such a unique promoter of mine. For my research, **Timo** not only put bread no the table and a roof over my head, but also solved my day-to-day problems on-site and provided input and output when needed. Thank you, **Timo**, for being the Help on my PhD journey. I am convinced that I am not one of the easiest PhD students to supervise, being critical, demanding and all. Likewise, it was the most challenging and unforgettable experience of mine to work under the direct supervision of **Gerben**, who taught me that sometimes it was better to be agreeable than to be right. Thank you, **Gerben**, for transforming me from a naïve, ignorant and insecure pushover to an experienced, educated and confident stalwart.

I wish you could feel my appreciation to **Prof. Mark W. Dewhirst** from Duke University, USA, whose work I have been following for five years, and **Dr. Martin Hossann** from University Hospital of Munich, Germany, who contributed to my study on so many levels. Some people were with me on an earlier journey at University of Bradford, UK. **Dr. Steve M. Picksley** was the light that guided me through the MSc tunnel and the North Star that oriented my PhD direction. **Dr. Roger M. Phillips'** passion in science showed me what research was truly about. **Dr. Richard T. Wheelhouse** mentored me that preciseness and responsibility were the foundation that any study should be built on. It is my fortune to have met these wonderful scientists, supporting me excel in cancer research.

It was my pleasure to work with colleagues at Erasmus MC and international collaborators, in particular, **Mark Halberstadt**, whose dedication to my study meant a great deal to me. **Dr. Gert van Cappellen** brightened my vision in imaging. **Dr. Dieter Haemmerich**, **Dr. Lars H. Lindner** and **Prof. Gerard C. van Rhoon**, whose expertise I benefit from. It was a pleasant experience to work with knowledgable **Michiel Bolkestein**. To **Ann L.B. Seynhaeve** and other colleagues, whose names I cannot continue listing, I will always treasure the memory of your companionship.

It is a great perk to be a student member of **Society for Thermal Medicine (STM)** and **European Society for Hyperthermic Oncology (ESHO)**, where I got to meet legendary scientists and experts. It would be my only wish to become one among **Prof. David Needham**, **Dr. Robert J. Griffin**, **Dr. Erik Cressman** and so many other talented researchers.

Special thanks must go to **Dr. Gregory M. Palmer** for trusting me and offering me a terrific project. It is everything I hoped all my study over the years could ever lead to. Thank you for making my dream come true.

I shall thank my parents for believing in me and supporting me, my grandparents who taught me seemingly simplest things in life, which had however been life-changing. I mustn't forget my dearest Mietsie and Pepper, who bring tons of joy into my life.

"If I have seen further it is by standing on the shoulders of giants", said Isaac Newton.

A

About the author

Li Li was born early in the morning on Sunday 26th July 1981, probably the only time she ever gets up before sunrise, not to mention it was a Sunday. When she was ten, her grandfather was diagnosed with a thrombus in the brain stem and died in four days. After learning the fact that there was no doctor who would operate on him because of the disease location, she decided to become a surgeon herself to master the skills a surgeon should have. In 2000, she was selected as one of the only two females from Liaoning province, which ranks 14th in P.R. China with 43,746,323 inhabitants (2010), to study medicine at the First Military Medical University of P.R. China, in Guangzhou, Guangdong province.

When she was twenty, her grandmother, who had never smoked a single cigarette, was diagnosed with lung cancer and died in one hundred days. She realized how finite a clinician could offer to a cancer patient and how desperate it was to find a cure. Therefore, in 2005, she chose MSc in Biomedical Sciences at University of Bradford, UK and focused on cancer. From 2008 to 2013, she spent 5 years as a PhD student at Erasmus MC, Rotterdam, in the Netherlands to research on heat and nanomedicine related strategies for chemotherapy.

Since May 2013, she works in Prof. Dewhirst's lab at Duke University, Durham, NC, USA and dedicates herself to fight in the war against lung cancer.

Afterword

A thesis with an afterword is rare and to my knowledge unprecedented. When Li asked me to write an afterword I was surprised and honored, but not completely sure of what was expected from me. Why an afterword in a Thesis? Mostly a thesis is an overview of the candidates work, it described the why and how, shows achievements and chapters contain often published work. What would an afterword add?

Typically a Dutch thesis defense comes with a number of printed and colorfully covered little books, which do not only give the candidate an additional headache but also rips her of her last money. And for what? Mostly these theses disappear in drawers or are used to level computer screens, and if lucky they and up on a shelf. But reading a thesis; that is something else. In most cases the recipient of the unrecognized treasure flipped through it to check what had been published: how well did this one do. Or when more involved, went through the effort to read the acknowledgement, hoping to see his or her name or find out who is being thanked and why. Also the CV is popular: how did she get here, what did she do and most of all where is she going? Is it worth the effort I wonder?

But, looking back at the work presented here I recognize the duty I have here. Isn't a thesis, this thesis, a beautiful compilation of scientific work, yes showing indeed the persons work, but more so a line, a development, bringing the field forward. And when the proud owner of this thesis does makes the effort, and sit down, and read this thesis from start, through the progression made, till the goal which has been reached, scientific and personal growth will become apparent.

That is, I guess, my duty. To make you, proud owner of this thesis, read it. Sit down, go back to chapter 1, ignore for now the acknowledgement, or the so popular CV, and start reading. Because this work is a result of melting together numerous disciplines, builds on insight coming from all directions and shows how powerful and successful working together can be. Starting long time ago with isolated perfusions, liposomal formulations, triggered drug release, tumor manipulation, and recently hyperthermia a research line converged which is not only worth the reading but also worth the attention.
I am proud to deliver this afterword as I am proud of Li, of the work she conducted, of the results obtained and proud when realizing that where we came from developed so nicely. And I hope that you, the reader of this Afterword, will share my feelings.

by Timo L.M. ten Hagen